NuA4 and ecdysone impact cell cycle gene expression to regulate the proper timing of cell cycle exit in *Drosophila*

by

Kerry A. Flegel

A dissertation submitted in partial fulfillment
of the requirements for the degree of
Doctor of Philosophy
(Molecular, Cellular, and Developmental Biology)
in the University of Michigan
2016

Doctoral Committee:

Assistant Professor Laura Buttitta, Chair
Adjunct Assistant Professor Daniel A. Bochar
Professor Kenneth M. Cadigan
Associate Professor Gyorgyi Csankovszki

To my family.

ACKNOWLEDGMENTS

I would like to first thank my mentor, Laura, for taking a chance and accepting me as your first graduate student. It's been a great learning experience. I appreciate your scientific rigor and your help in becoming a better scientist, presenter, and writer. I will continue to use these skills, as well as the critical thinking skills that you have instilled in me, for years to come.

I would like to extend my gratitude to Gyorgyi, Ken, and Dan on my thesis committee for their support and scientific insight throughout the years. Not only did Ken and Gyorgyi give me valuable input from our committee meetings, but they also participated in the joint lab Gene Regulation meeting that helped to create a sense of community in our section of the department. I am glad for the Gene Regulation meeting because it gave me much needed practice in presenting while also maintaining my interest in the research being performed by neighboring labs. I am also grateful for the many meetings and presentation that our lab had with Cheng-Yu Lee's group because they helped me further develop as a scientist and critical thinker.

The Genetics Training Program (GTP) broadened my scientific horizons and encouraged my bioinformatics training that ended up being instrumental in reaching the major conclusion of my recent first author paper. I am thankful for GTP giving me many opportunities to improve as a critical thinker and presenter. I am also glad that being a GTP and Rackham Merit Fellow connected me with a diverse crowd and helped to fund my doctoral training.

During my scientific pursuits, I also enjoyed the opportunity to teach alongside Drs. Anuj Kumar, Timothy James, Andrzej Wierzbicki, Regina Baucom, and Megan Van Etten. Thank you for leading by example in your enthusiasm and helping me to become a better instructor.

In addition, I am thankful to Gyorgyi and Anuj for giving me the opportunity to do a rotation in their respective labs despite having no prior experience with either *Caenorhabditis elegans* or *Saccharomyces cerevisiae.* My exposure to the techniques and nomenclature in your respective fields have since aided in my understanding of many articles.

To Mary Carr and Diane Durfy who have helped make all the paperwork and changes in funding go smoothly throughout the years, thank you for always being there. It has been a huge relief to know that I could always count on you to help me fix a problem.

On a more personal note, I am eternally grateful for the continued support of my husband Adam. Thank you for sticking by me and making sure that I ate when I was otherwise distracted by writing. Furthermore, you and the cats have been great at tolerating my long work days and sometimes odd work hours.

I cannot express how deeply appreciative I am of my parents that are always there for me and have helped me in anyway that they could. The perseverance you instilled in me was instrumental for the completion of my doctoral training.

Thanks Amy, Abigail, Patrick, and Kendal for your visits, help, and being the goofballs that you are! I am also appreciative of my brothers that despite my infrequent visits, make me feel right at home by maintaining my position as their little sister with their jovial harassment. Phillip and Nancy, thank you for being awesome grandparents with whom we have a great time visiting and learning from. The faith you have in me has been an inspiration. Thanks Steve for visiting to lend us a hand or just to touch base, it is always great joking with you. I am also thankful to the rest of my family and in-laws for understanding our absence from many events over the years.

I would like to acknowledge my labmates that have become my friends. Rosaline (Dan), Yiqin, Shyama, and Ajai, I have enjoyed our discussions and learning alongside you. The mischief that we have gotten into has helped to balance the otherwise serious endeavor of scientific research. Thank you Chris for your willingness to help me with my bioinformatic pursuits and being a great friend. I am also grateful that you and Margarita have welcomed me into your home so I could get to know Aurora better (she is pretty awesome). Margarita, I have enjoyed having you as an honorary labmate during our dissertation sisterhood and really value your friendship and scientific input.

Finally, thanks to the Molecular, Cellular, and Developmental Biology Department at the University of Michigan for my doctoral training.

Now on to the next adventure!

TABLE of CONTENTS

DEDICATION ..... **ii**

ACKNOWLEDGMENTS ..... **iii**

LIST of FIGURES ..... **vii**

LIST of TABLES ..... **ix**

ABSTRACT ..... **x**

CHAPTER I
GENERAL INTRODUCTION **1**

The cell cycle 1
1.1 The regulation of Cyclins and Cdks 3
1.3 Cyclins and Cdks in G2/M regulation 6
1.4 Transcriptional control of the cell cycle 7
1.5 Cell cycle compensation 11
DNA damage response and the cell cycle 12
2.1 Cell cycle checkpoints 13
2.2 DNA damage response 14
Developmental control of cell cycle exit 18
3.1 Types of cell cycle exit 18
3.2 Establishing cell cycle exit 19
3.3 Gal4/UAS system 20
3.4 Screen to identify regulators of cell cycle exit 22
3.5 Nucleosome acetyltransferase of histone H4 complex (NuA4) 24
Drosophila melanogaster as a model system for cell cycle exit 25
4.1 Ecdysone steroid regulates *D. melanogaster* development and cell cycle exit 26
References **29**

CHAPTER II
The Tip60/NuA4 complex is required for proper cell cycle progression and the transition to a post-mitotic state in *Drosophila melanogaster* **37**

Abstract **37**
Introduction **38**
The transition from proliferation to a post-mitotic state in *Drosophila* 40
The NuA4 complex 40
Results **42**
Compromising NuA4 delays cell cycle exit 42
Compromising NuA4 does not alter the timing of terminal differentiation 44
Inhibition of NuA4 leads to ectopic cell cycle gene expression 45
Compromising NuA4 disrupts cell cycle progression 46
NuA4 inhibition deregulates cell cycle gene expression during active proliferation 48
The transcriptional response to Tip60 inhibition 50

NuA4 inhibition does not delay cell cycle exit through the p53-dependent DNA damage response 52
NuA4 inhibition does not delay cell cycle exit through altered E2F/DP function 53
Delaying the final G2-M transition impacts the proper repression of cell cycle genes at cell cycle exit 55
Promoting G2 progression when NuA4 is inhibited leads to aberrant mitoses and genetic instability 57
Discussion 58
The Tip60/NuA4 complex and cell cycle gene expression 59
The Tip60/NuA4 complex and DNA damage signaling 61
NuA4 and cancer 62
Materials and Methods 63
Acknowledgements 69
References 99

CHAPTER III
Ecdysone signaling induces two phases of cell cycle exit in *Drosophila* cells 105
Abstract 105
Introduction 106
Results 110
20-HE induces G2 phase cell cycle arrest 110
The Wee/Myt1 kinases are partially responsible for 20-HE induced G2 arrest 112
The 20-HE induced G2 arrest is reversible 113
20-HE removal leads to prolonged alterations in cell cycle dynamics 114
Cell cycle changes during wing metamorphosis are similar to those induced by pulsed 20-HE in cell culture. 115
A peak of Broad-Z1 expression is correlated with the G2 arrest in the wing. 118
Broad regulates the ecdysone-induced G2 cell cycle arrest in early pupal wings 119
Broad binds to the *stg* regulatory locus and overlaps with wing enhancers. 121
Discussion 122
The Ecdysone Receptor is a repressive complex in the wing 123
Gene expression changes during metamorphosis in the wing. 125
Tissue specific responses to ecdysone can mediate opposite effects on the cell cycle through the same target 126
Materials and Methods 127
Acknowledgements 130
References 147

CHAPTER IV
GENERAL DISCUSSION 153
NuA4 153
Development and ecdysone 159
References 160

LIST of FIGURES

Fig. 1.1 Canonical cell cycle 2

Fig. 1.2 Major cell cycle regulators 4

Fig. 1.3 Cell cycle phases of MMB and DREAM activity 10

Fig. 1.4 Oscillations of E2F and dREAM activity promote cell cycle progression 11

Fig. 1.5 Mechanism of H2AX/H2Av phosphorylation spreading from site of DNA damage . 16

Fig. 1.6 Conserved DNA damage response 18

Fig. 1.7 Gal4/UAS system spatially and temporally regulates transgene expression in *Drosophila* 21

Fig. 1.8 Development of the *Drosophila* wing 23

Fig. 1.9 Pulses of ecdysone coincide with major events in *Drosophila* development 27

Fig. 2.1. NuA4 inhibition delays cell cycle exit 70

Fig. 2.1a. Compromising NuA4 delays the timing of the final cell cycle 72

Fig. 2.2. NuA4 is essential for proper cell cycle gene repression at cell cycle exit 74

Fig. 2.2a. NuA4 inhibition does not delay terminal differentiation 75

Fig. 2.3. Compromising NuA4 disrupts cell cycle progression 76

Fig. 2.3a. NuA4 is needed for proper proliferation 78

Fig. 2.4. NuA4 inhibition deregulates cell cycle gene expression during active proliferation 80

Fig. 2.4a. Loss of NuA4 function alters expression of specific cell cycle genes 82

Fig. 2.5. NuA4 inhibition delays cell cycle exit independent of the p53-dependent DNA damage response (DDR) 83

Fig. 2.5a. NuA4 inhibition delays cell cycle exit and slows the cell cycle independent of several DDR components 84

Fig. 2.6. NuA4 affects cell cycle exit independent of DP function 86

Fig. 2.6a. NuA4 and DREAM genetically and physically interact 87

Fig. 2.7. Prolonging the final G2 delays cell cycle exit, de-represses cell cycle genes and causes ectopic neurons at the posterior wing margin 88

Fig. 2.7a. Slowing the final cell cycle does not delay cell cycle exit 89

Fig. 2.8. Accelerating G2-M when NuA4 is inhibited leads to severe mitotic defects 90
Fig. 3.1 Kc cell response to 20-HE involves a Wee/Myt-dependent cell cycle arrest in G2.131
Fig. 3.1a. 133
Fig. 3.2 20-HE induced arrest is reversible and leads to prolonged alterations in cell cycle dynamics 135
Fig. 3.2a. 137
Fig. 3.3 Cell cycle changes during wing metamorphosis. 139
Fig. 3.3a. 141
Fig. 3.4 G2 arrest in the prepupal wing coincides with a peak of Broad Z1 expression. 142
Fig. 3.4a. Complete GO term analysis for the RNA-seq timecourse data shown in Fig. 3.3 B. 143
Fig. 3.5 The prepupal wing G2 arrest is partially dependent upon Broad regulation of String. 144
Fig. 3.6 Broad binds to the *stg* regulatory locus and overlaps with wing enhancers. 146
Fig. 3.7 A model for how the temporal dynamics of Ecdysone signaling induce two phases of cell cycle arrest in *Drosophila* wings 147

LIST of TABLES

Table 2.1. RNAi lines for core NuA4 subunits 91
Table 2.1a. Genes induced by *Tip60^{DN}* and the DNA damage response 92
Table 2.2a. Genes induced by *Tip60^{DN}*, DREAM, and the DNA damage response 95
Table 2.3a. Genes regulated by *Tip60^{DN}* that are also targets of DREAM 96
Table 2.4a. Primer sequences for NuA4 dsRNA synthesis 99

ABSTRACT

During development, cell proliferation must be tightly controlled to ensure proper tissue and organ morphogenesis. During organogenesis, many cells undergo a process called terminal differentiation, where cells acquire their final fates and begin to perform essential physiological functions. Terminal differentiation is often accompanied by a transition to a non-dividing state, called cell cycle exit. As development proceeds, many cells exit the cell cycle, and most cells in mature organisms remain in a non-dividing, post-mitotic state. Despite its prevalence, how cells transition from a proliferative to a post-mitotic state is induced and maintained is not fully understood. In this thesis, I examine two aspects of cell cycle regulation that are essential for the proper transition of *Drosophila* epithelial cells from a proliferative to a post-mitotic state during development. In part 1, I describe a novel, critical role for the NuA4 chromatin remodeling and histone exchange complex in promoting the proper timing of cell cycle exit *in vivo*. Unlike other chromatin binding factors that repress cell cycle genes, NuA4 does not directly inhibit cell proliferation but instead suppresses a previously unknown intrinsic DNA damage response that occurs during late S-phase. My work revealed that suppression of this endogenous DNA damage response is required *in vivo* to properly coordinate S and G2 cell cycle progression with differentiation and cell cycle gene expression during tissue development.

In part 2, I examine how steroid hormone signaling plays a central role in coordinating the timing of cell cycle exit. Pulses of the steroid hormone ecdysone trigger a cascade of gene expression changes required to coordinate cell maturation with differentiation and cell cycle exit

during metamorphosis in holometabolous insects. Ecdysone signaling is most similar to vertebrate retinoic acid signaling, which also acts as an essential modulator of cell differentiation and cell cycle exit during development in many cell types. Yet, it remained unknown how ecdysone signaling impinges upon the cell cycle machinery to coordinate differentiation with cell cycle exit. Here, I reveal that ecdysone signaling in the *Drosophila* wing indirectly regulates the expression of a key cell cycle gene. My work shows that ecdysone signaling strongly induces a transcription factor, Broad, which in turn represses the expression of an essential mitosis promoting gene, the cdc25c phosphatase, to cause a temporary G2-phase cell cycle arrest. After the ecdysone pulse, as Broad expression declines the cdc25c phosphatase becomes re-expressed, which in turn promotes rapid mitotic entry that leads to a synchronized final cell cycle and subsequent cell cycle exit in the wing. In this manner, a pulse of the steroid hormone ecdysone synchronizes the final cell cycle in the *Drosophila* wing, while acting on other direct and indirect targets to promote the expression of genes involved in wing terminal differentiation.

Altogether, my work has revealed two essential signaling pathways that impact cell cycle gene expression and cell cycle progression to properly coordinate cell cycle exit with terminal differentiation during development.

CHAPTER I

GENERAL INTRODUCTION

As multicellular organisms develop, cell growth and division must be tightly orchestrated for proper tissue and organ morphogenesis. By a process called terminal differentiation, cells mature into their final fates during organogenesis and begin to perform essential physiological functions. Terminally differentiated cells often stop proliferating by transitioning to a non-dividing, post-mitotic state called G0 in a process termed cell cycle exit. Many cells exit the cell cycle as development proceeds, with most cells in mature organisms remaining in a non-dividing, post-mitotic state. Despite its prevalence, how the transition from a proliferative to a post-mitotic state is induced and maintained is not fully understood. To understand how cells stop proliferating, we must first consider the regulators that promote the cell cycle in actively proliferating cells.

The cell cycle

The canonical cell cycle can be artificially divided into these sequential phases: Gap1 (G1), DNA synthesis (S), Gap2 (G2), and Mitosis (M) (Fig. 1.1). During G1 cells grow, carry out differentiation associated physiological functions and respond to mitogenic factors. In late G1 they also license DNA replication origins by recruiting factors to the chromatin in preparation for DNA synthesis. Cells replicate their genome during S phase, as well as synthesize histones and duplicate centrioles. Cells continue to prepare for mitosis by accumulating the necessary proteins during G2. During mitosis, cells condense their genome into chromosomes (early prophase), break down the nuclear envelope (end of prophase), use the

mitotic spindles to centrally align chromosomes along the metaphase plate (metaphase), then they break the links between the sister chromatids of each chromosome so they can pulled to opposite poles of the spindle (anaphase). Once at opposing poles, nuclear envelopes re-form around the newly segregated chromosomes, which then de-condense (telophase). A cleavage furrow forms between the newly formed nuclei thereby contracting the plasma membrane and separating the nuclei into two daughter cells (cytokinesis). After mitosis, cells can either continue proliferating by initiating another cell cycle, or they can permanently stop proliferating and enter a non-cycling, post-mitotic state called cell cycle exit (Cooper, 2000). The transition to the post-mitotic state is accompanied by changes in gene expression, including increased expression of cell fate-specific factors and decreased expression of cell cycle-promoting genes (O'Keefe et al., 2012).

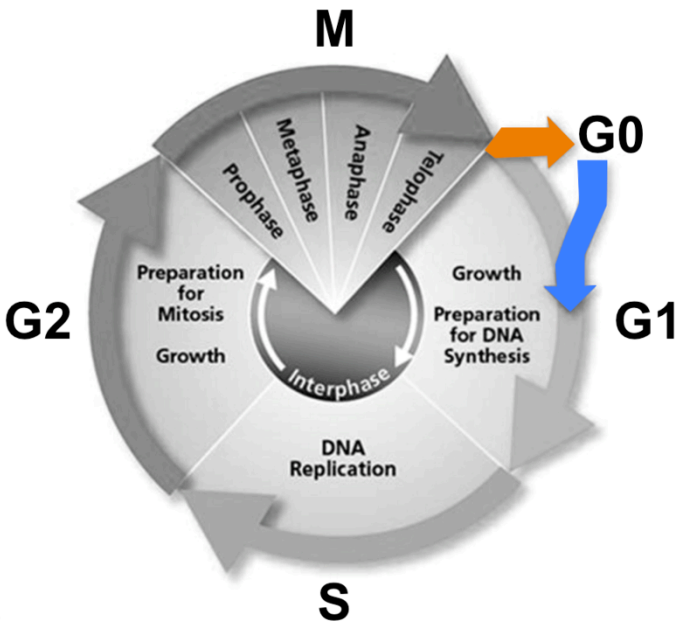

Fig. 1.1 Canonical cell cycle (Resources, n.d.). Cells proliferate via the conserved cell cycle that can be broken into the sequential phases: Gap1 (G1), DNA synthesis (S), Gap2 (G2), and Mitosis (M) to produce two identical daughter cells. After mitosis, cells can exit the cell cycle (G0) permanently, as occurs in most instances of exit associated with terminal differentiation or senescence (orange arrow), or become quiescent which is easily reversible (blue arrow).

1.1 The regulation of Cyclins and Cdks

Transitions through cell cycle phases are controlled by the activities of Cyclin/Cyclin dependent kinase (Cdk) complexes that phosphorylate hundreds of targets to trigger and coordinate the cellular changes that occur throughout the cell cycle. As the name implies, these kinase complexes are only active when the Cyclin subunit is bound. Thus, regulation of Cyclins at both the transcriptional and protein levels are critical for controlling cell cycle dynamics. Cyclin protein levels oscillate during the cell cycle in such a way that they are high during the phase(s) that they need to bind to their Cdk partner and promote cell cycle progression (Fig. 1.2). Generally, Cyclin proteins impact cell cycle progression by binding to and causing a conformational change in the Cdk that allows for activating phosphorylation of the Cdk T-loop (performed by a Cdk-activating kinase, CAK) and removal of other inhibitory phosphates on the Cdk. A Cyc/Cdk pair's activity can also be regulated by the allosteric binding of cyclin-dependent kinase inhibitor proteins (CKIs), such as the Cip/Kip type p21 (called Dacapo in flies) which impede the catalytic activity of the Cdk (Sherr & Roberts, 1999). In mammals there is an additional family of CKIs (inhibitors of Cdk4, INK4 type) that can also block activity of the G1 Cyc/Cdk by binding with Cdk4/6 to impede their association with CycD (Vidal & Koff, 2000). Once Cyc/Cdk pairs are active, they phosphorylate numerous cell cycle proteins to trigger cascades of events including the initiation of DNA replication, centrosome duplication, and the mitotic reorganization of the tubulin cytoskeleton (Mazumder et al., 2004, Errico et al., 2010).

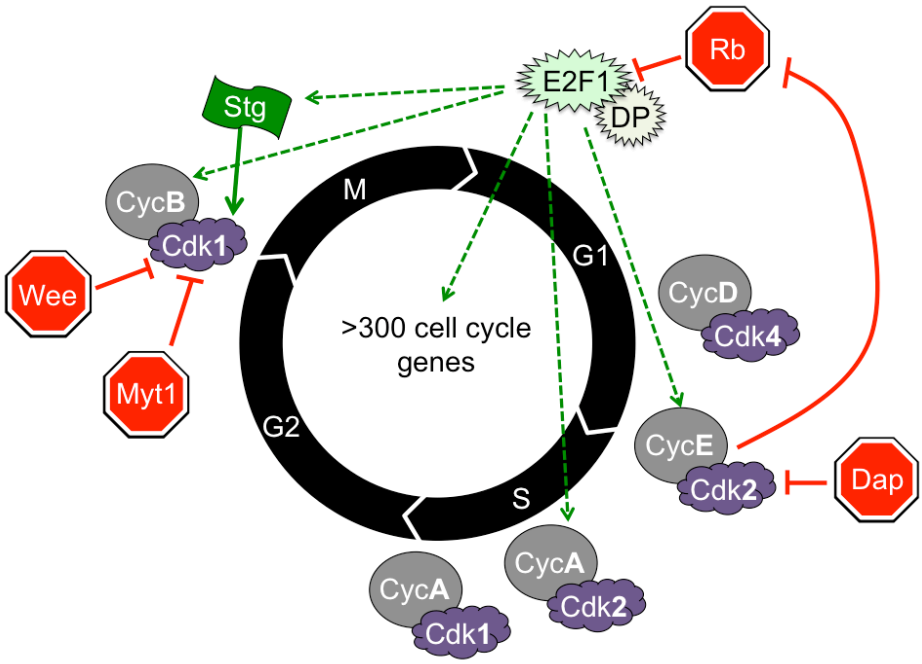

Fig. 1.2 Major cell cycle regulators. The activity of cyclin-dependent kinases (Cdk) are dependent upon their binding to Cyclins (Cyc). Cell cycle timing of Cyc/Cdk function is roughly shown by their placement. Though not shown here, phosphorylation of the Cdk T-loop (by the Cdk7 CAK) is required for Cdk activity and also stabilizes its interaction with Cyc. Dotted arrows show transcriptional effects, solid lines indicate the result of protein-protein interactions or post-translational modifications.

1.2 Cyclins and Cdks in G1/S regulation

The transition from G1 to S phase is regulated by the activities of the well conserved CycD/Cdk and CycE/Cdk pairs. CycD protein levels increase as cells grow in response to mitogenic EGF/Ras signaling during the G1 phase of the cell cycle (Roovers & Assoian, 2000). Active CycD/Cdk4 (as well as Cdk6 in mammals) complexes initiate a series of events to promote DNA synthesis (S phase). In early G1, CycD/Cdk complexes mono-phosphorylate the tumor suppressor pocket-protein Retinoblastoma (Rb) or Rb family members that bind and repress the transcription factor E2F/DP complex (Narasimha et al., 2014). The E2F/DP complex transcriptionally regulates the expression of hundreds of cell cycle genes, with increases in transcription-promoting E2F/DP complexes able to accelerate the cell cycle whereas decreases

slow the cell cycle (Neufeld et al., 1998). As CycD protein levels accumulate in mammals, the increasing amount of CycD/Cdk complexes can sequester CKIs from binding to and inhibiting CycE/Cdk2 complexes (Sherr & McCormick, 2002). In flies however, CycD/Cdk4 does not detectably sequester the CKI, Dacapo (Meyer et al., 2000). The conserved CUL4 E3 ubiquitin ligase instead promotes degradation of Dacapo during G1, which enables CycE/Cdk2 complexes to be active and promote the G1/S transition (Higa et al., 2006). Attainment of a critical threshold of CycE/Cdk2 activity causes hyper-phosphorylation of E2F/DP-associated Rb, which releases E2F/DP from Rb-mediated repression to in turn promote the transcription of *cycE* and *cdk2* in addition to several hundred other genes with critical roles in the cell cycle (described in detail later). Active CycE/Cdk2 complexes further phosphorylate Rb to cause its complete dissociation from the E2F1/DP complex, allowing full E2F1/DP activity (Foster et al., 2010). This signaling mechanism acts as a positive feedback loop between E2F1/DP and CycE/Cdk activities, where increased expression of *cycE* is promoted by E2F1/DP, and CycE/Cdk2 activity promotes E2F1/DP activity by phosphorylation of Rb. This feedback loop forms the basis of a bi-stable switch, which rapidly promotes progression from G1 into S phase once cells have committed to the cell cycle, by coordinating E2F activity with the triggering of DNA replication licensing through additional targets of CycE/Cdk2, such as Cdc6 and Cdc45 (Fisher, 2011). E2F1 and CycE proteins are respectively degraded during S phase via action of conserved E3 ubiquitin ligase complexes of the Cullin-Ring-Ligase ($CRL4^{cdt2}$) and Skp1-Cullin-F-box (SCF^{fbw7}) families (Marti et al., 1999, Campanero & Flemington, 1997, Hériché et al., 2003, Davidson & Duronio, 2012). Upon reaching a critical threshold of CycE/Cdk2 activity, CycE/Cdk2 autophosphorylates CycE to promote SCF^{fbw7} binding and proteosomal degradation of CycE (Knoblich et al., 1994, Clurman et al., 1996, Koepp et al., 2001, Welcker et al., 2003).

Also during S phase SCF^{skp2} causes degradation of the replication licensing machinery, ensuring that aberrant relicensing of the replication does not occur during the remainder of the cell cycle (Rossi et al., 2013).

1.3 Cyclins and Cdks in G2/M regulation

During S phase, the Cyc/Cdk complexes whose activities are needed for the G2/M transition also begin to accumulate. In mammals the CAK, Cdk7, catalyzes the activating T-loop phosphorylation of the free form of Cdk2 to preferentially stabilize Cdk2 (over Cdk1) binding to the accumulating CycA during early S phase, with CycA/Cdk1 complexes consequently forming during late S/G2 (Fisher, 2012). Active CycA/Cdk2 complexes phosphorylate and activate the Myb and FOXM1 transcription factors that promote *cycB* expression in G2 (described in more detail later). Flies however, have no known homolog of FOXM1 and there is no evidence of CycA/Cdk2 complexes, just CycA/Cdk1 (Knoblich et al., 1994, Sadasivam & DeCaprio, 2013). Although CycB/Cdk1 form a complex in G2, CycB concentration in the nucleus is below the threshold required to trigger entry into mitosis and Cdk1 activities are restrained by inhibitory phosphorylations catalyzed by the Wee (pY15) and Myt1 kinases (Cdk1 pY15 and pT14) (Lindqvist et al., 2009, Ayeni et al., 2014). Upon centrosome maturation, CycB/Cdk1 complexes are recruited to the centrosome where the polo-like kinase 1 (PLK1) is localized and whose activity promotes nuclear accumulation of the Cdc25c phosphatase, String. String removes inhibitory phosphorylations from cyclin-bound Cdk1, thereby promoting CycB/Cdk1 and CycA/Cdk1 activity that acts as a bi-stable switch to amplify CycB/Cdk1 activity and cause mitotic entry. This switch is the result of a feedback loop where active CycB/Cdk1 complexes

phosphorylate Wee, Myt1, and String, to further activate String but repress Wee and Myt1 with the help of PLK1 (Lindqvist et al., 2009).

For the completion of anaphase, CycA, CycB, and other mitotic promoting factors must be degraded. These proteins are marked for degradation at the metaphase-anaphase transition by an E3 ubiquitin ligase complex called the anaphase promoting complex/cyclosome (APC/C) (Grosskortenhaus & Sprenger, 2002). For cells to continue proliferating, high levels of APC/C activity must persist into the G1 phase of the cell cycle so the pre-replication complexes (pre-RCs) needed for DNA licensing can form (Fisher, 2011). RCA1 (*regulator of CycA*) inhibits APC/C activity after pre-RC formation, which allows the re-accumulation of Cyclins needed to form the Cyc/Cdk complexes whose activities initiate the next round of DNA replication (Zielke et al., 2006). Consequently, the levels of APC/C activity are not only important for cell cycle progression but also the decision of cells to permanently stop proliferating and exit the cell cycle (Buttitta et al., 2010).

1.4 Transcriptional control of the cell cycle

A conserved eukaryotic transcriptional oscillator controls cell cycle gene expression in proliferating cells (Orlando et al., 2008, Oikonomou & Cross, 2010). The oscillation is dependent upon changes in the activity or protein levels of master cell cycle regulatory E2F/DP complexes. E2Fs are a highly conserved family of transcription factors that have only two members in flies (E2F1 and E2F2) that must individually bind with DP for activity (van den Heuvel & Dyson, 2008). The two *Drosophila melanogaster* members of the tumor suppressor retinoblastoma protein family (Rbf1 and Rbf2) (Harrington et al., 1998) bind to E2F/DP complexes to negatively regulate E2F/DP activity. *Drosophila* E2F1/DP acts as a transcriptional

activator when not associated with Rbf1, whereas E2F2/DP antagonizes E2F1/DP activity to transcriptionally repress target genes regardless of Rbf1 or Rbf2 binding. When Rbf1 associates with E2F1, it physically blocks the function of E2F1's transactivation domain and is thought to recruit histone deacetylases that compact chromatin and make E2F targets less accessible to the transcriptional machinery (Dimova & Dyson, 2005, Harbour & Dean, 2000). As previously mentioned, Rbf association with E2F/DP is regulated by a feedback loop in which CycE/Cdk2 directly phosphorylates Rbf to cause its dissociation from E2F/DP complexes, E2F1/DP activity in turn promotes the expression of *cyclins E, A,* and *B* (Wei Du, Xie, & Dyson, 1996, W Du & Pogoriler, 2006). In mammals, when members of the RB family (p130, p107) bind to E2F2/DP, they can also recruit other proteins to form the DREAM (Dimerization partner (DP), Rb-like, E2F, and multi-vulval class B (MuvB)) and Myb-MuvB (MMB) complexes. Many of these mammalian genes are conserved and regulate gene expression via a DREAM-like complex in *D. melanogaster* and *Caenorhabditis elegans* (Sadasivam & DeCaprio, 2013).

The MuvB genes were first discovered as loss-of-function mutants in *C. elegans* that in certain combinations caused the worms to develop multiple vulva-type (Muv) organs. Multiple vulvas form because mutants lose the ability to repress an epidermal growth factor (EGF)-RAS signaling cascade which should normally be restricted to the vulval precursor cells, not active in other epidermal cells (further away from the EGF producing anchor cell) (Hill & Sternberg, 1992, Fay & Yochem, 2007). To get a Muv phenotype, Muv mutants must simultaneously disrupt genes in at least two of the three gene classes termed the "synthetic multi-vulva (synMuv) classes" (Ceol et al., 2006). Class A genes affect EGF expression, class B encode homologs to Rb (LIN-35), E2F (EFL-1), DP (DPL-1) as well as genes of unknown function that are homologous to components of the DREAM complex described above (lin-52, lin-53, lin-54,

lin-37, lin-9), and class C encode components of the nucleosome acetyltransferase of histone H4 (NuA4) complex (Ceol & Horvitz, 2004). The orthologs of the MuvB class are conserved in mammals and flies (as shown in parenthesis); LIN9 (Myb-interacting protein 130 (Mip130)), LIN54 (Mip120), LIN37 (Mip40), LIN52 (Lin52), and RBBP4 (Caf1/p55) (Sadasivam & DeCaprio, 2013).

In mammals, the MuvB core binds with either Myb or Rb family members to form two distinct complexes (respectively MMB or DREAM) that act in opposing manner upon transcription (Fig. 1.3). The mammalian MMB complex promotes cell cycle gene transcription, particularly genes involved in G2/M progression and the maintenance of chromosomal stability during mitosis (Laoukili et al., 2005). This is due to the MuvB core complex associating with Myb during S phase, with Myb's transactivation domain then being phosphorylated by CycA/Cdk2 during G2 to increase its activity (Johnson et al., 1999). Before the phosphorylated Myb is targeted for degradation by the SCF^{Fbxw7} E3 ubiquitin ligase complex during G2 (Kanei-Ishii et al., 2008), it recruits the forkhead box protein M1 (FOXM1) to promoters of cell cycle genes. This increases expression of the *polo-like kinase protein 1* (*PLK1*) that phosphorylates G2/M promoting factors such as FOXM1, Cdc25c, and CycB to positively regulate their activity and also phosphorylate the G2/M negative regulator, Wee, to repress its function (Fu et al., 2008). FOXM1 remains bound to the MuvB core until its phosphorylation by PLK1 enables FOXM1 to be recognized and targeted for degradation by APC/C during mitosis (Park et al., 2008). Degradation of both Myb and FOXM1 leaves the MuvB core free to be bound by Rb family members so as to form the DREAM complex in mitosis and early G1. The DREAM complex represses the expression of many G2/M cell cycle genes as well as Myb and FoxM1 (Sadasivam & DeCaprio, 2013). MuvB core alternating between binding with Myb and FoxM1

(to form MMB) or Rb family members (to form DREAM) causes signaling cascades that drives cell cycle progression.

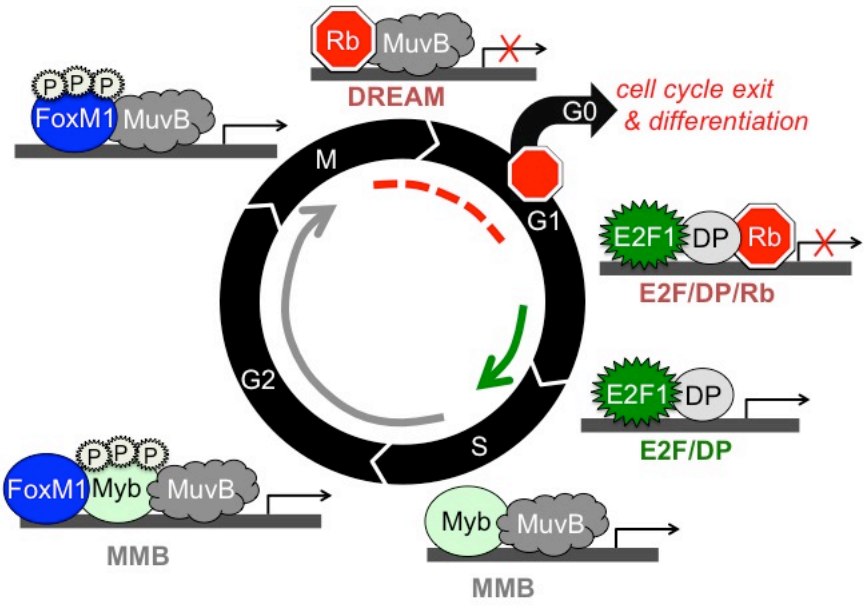

Fig. 1.3 Cell cycle phases of MMB and DREAM activity. The E2F1/DP transcription factor complex promotes cell cycle gene expression during G1/S when it is not bound by Rb or Rb family members. The MuvB core promotes cell cycle gene expression during S phase through part of mitosis when it is associated with Myb and/or FoxM1 (in mammals) transcription factors (MMB complex). Phosphorylation of Myb and FoxM1 increases their activity but also results in their degradation. The MuvB core associates with Rb family members to form the DREAM complex mid-mitosis into early G1, to repress the transcription of many cell cycle genes. Cell cycle genes are also repressed by the DREAM complex when cells exit the cell cycle into a state called G0 and terminally differentiate.

Flies however only have a single dREAM/MMB (*Drosophila* Rbf, E2F2, and Myb-MuvB) complex, and lack a clear FoxM1 homolog (Fig. 1.4). It is thought that in actively proliferating cells of *Drosophila*, E2F1/DP activator complexes form during G1 and G2, and Myb binds to MMB to promote cell cycle gene expression during G2 to M progression. Then after completion of the cell cycle, when Cyclin/Cdk activity is low, the repressive dREAM complex forms to repress cell cycle gene expression (Georlette et al., 2007, Wen et al., 2008,

Lewis et al., 2012, Lewis et al., 2004). In addition, dREAM/MMB has also been shown to repress a small number of specific differentiation-associated genes in a cell cycle independent manner, possibly acting constitutively at these sites throughout the cell cycle (Lee et al., 2010).

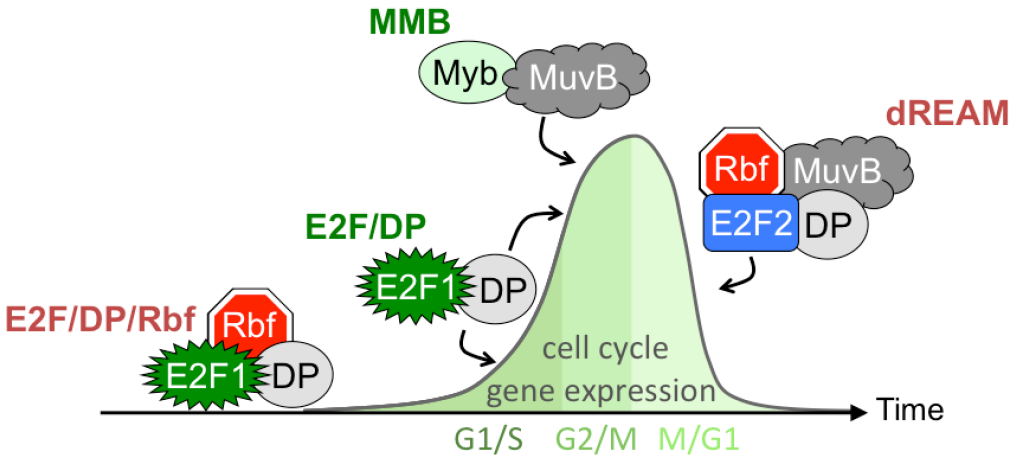

Fig. 1.4 Oscillations of E2F and dREAM activity promote cell cycle progression. When not bound by *Drosophila* Rbf, the E2F1/DP transcription factor complex promotes cell cycle gene expression to drive entry into and progression through the cell cycle. Cell cycle progression is further regulated by the Myb/MMB complex, which in cooperation with E2F1/DP promotes cell cycle gene expression. When Cyclin/Cdk2 activity is low, for example after mitosis, dREAM/MMB forms to repress the expression of cell cycle genes.

1.5 Cell cycle compensation

E2F1/DP activity promotes cell cycle progression during active proliferation by increasing the expression of critical cell cycle factors such as *cycE, cdc25c*, and *cycB* (Reis & Edgar, 2004). E2F1/DP activity is sufficient to control cell cycle speed, with high levels of E2F1 accelerating cell cycle progression and low levels of E2F1 slowing the cell cycle (Neufeld et al., 1998). Notably, E2F also "compensates" for the duration of each of the cell cycle phases to maintain the overall cell cycle timing. For example, if cells are temporarily arrested in G1 due to increased activity of the CKI Dacapo that represses CycE/Cdk2 activity, E2F1 protein levels become abnormally high due to the delayed entry into S-phase where E2F1/DP degradation occurs (Reis & Edgar, 2004, Shibutani et al., 2008). The increase in E2F1/DP activity causes an

increase in expression of *cycE* and the *cdc25c* (*string*) phosphatase. CycE eventually promotes G1/S progression, which is then rapidly followed by String activating CycB/Cdk1 to drive mitotic entry (Reis & Edgar, 2004). In this way, a slowing of G1/S progression results in a faster progression from G2/M that ultimately maintains the normal overall cell cycle length (Reis & Edgar, 2004). Similarly, slowed progression through G2/M also increases E2F1 protein levels through mechanisms that are still uniendtified, which then promotes increased expression of *string* and the G1/S rate-liming factor, *cycE*, resulting in a shortened subsequent G1/S transition (Reis & Edgar, 2004). Since delays in the cell cycle can alter the timing of the subsequent phases, we became interested in examining how temporary cell cycle arrests (such as those that occur in response to DNA damage) impact the cell cycle and the proper timing of cell cycle exit as tissues differentiate.

DNA damage response and the cell cycle

The DNA damage response (DDR) is a conserved cascade of protein activation that spreads the DNA damage signal throughout the nucleus and serves to prevent transmission of damaged genetic material to daughter cells (Song, 2005, Polo & Jackson, 2011). The type of damage (double-strand vs. single-strand DNA breaks) and the cell cycle stage at which the damage occurs result in activation of either distinct repair mechanisms or lead to programmed cell death. To repair damage, cells temporarily stop cell cycle progression by engaging a "checkpoint" and recruiting DNA repair proteins to the damage sites. Alternatively, excessive and irreparable DNA damage may induce the expression of apoptotic factors that cause cell death. Though both single- and double-strand DNA breaks can result in cell cycle arrests, my work has focused on the double-strand DNA break DDR pathway. This is because double-strand

DNA breaks in a parent cell can potentially lead to chromosomal aberrations being passed down to daughter cells, which increases the likelihood of oncogenic transformation of the daughter cells (Tang et al., 2012). In addition in proliferating cells, unrepaired singe strand breaks become double-strand breaks during the subsequent S-phase. It is therefore natural for this thesis to focus on double-strand DNA damage because it can impact our main topics of interest, cell cycle regulation and the decision to exit the cell cycle during differentiation in development.

2.1 Cell cycle checkpoints

Cells activate a checkpoint soon after encountering DNA double-strand breaks (DSBs) to provide the opportunity for the cells to repair the damage via homologous recombination (HR) or non-homologous end joining (NHEJ) (Vitale et al., 2011). Acquisition of damage during S phase activates an intra-S phase checkpoint to block DNA replication, and damage prior to mitosis activates a checkpoint at the G2-M transition to avoid improper chromosome segregation and mitotic catastrophe (Song, 2005). Checkpoint activation causes a temporary cell cycle arrest so the cell can attempt to repair the DNA damage. As long as cell cycle compensation is still operational, after the damage is repaired and the cell re-enters the cell cycle, the next phase transition would be expected to be accelerated and the overall cell cycle length of a population of cells would be largely preserved. Alternatively, extensive damage may require a prolonged arrest for complete repairs to be made, after which rapid progression through the next phases may be unable to rescue the overall cell cycle length.

If a cell perceives DNA damage prior to the M phase of its final cell cycle, a checkpoint is activated to arrest the cell in G2 and attempt to repair the damage. E2F1 is activated by DNA damage and drives the expression of many DNA repair genes (Polager et al., 2002, C. Stevens et

al., 2003). As the repairs are being made, the cell may also accumulate cell cycle-promoting factors that would have otherwise been used to accelerate its next G1/S transition (as described above). After repair of the DNA damage, the cell re-enters the cell cycle and completes its final mitosis at a later time than its wild type counterparts, thereby delaying that cell's exit from the cell cycle. This delayed mitosis can be easily mistaken to be the result of delayed cell cycle exit or extra divisions, unless live imaging is performed or the total number of cell doubling events is determined by lineage tracing.

2.2 DNA damage response

The DDR begins with the initial recognition of damaged DNA by the MRN complex, which rapidly associates with DSBs and soon thereafter recruits the ataxia telangiectasia mutated kinase (ATM) (Sun et al., 2009). The MRN complex is composed of the highly conserved Mre11 and Rad50 proteins and the lesser conserved Nbs1 protein, all of which preserve chromosomal integrity by functioning as the primary DSB detector (Ciapponi, Cenci, & Gatti, 2006). The mammalian acetyltransferase Tip60 performs a role in the initial steps of the DDR where it acetylates and activates the ATM kinase (Sun et al., 2005), however our studies of *Drosophila* Tip60 suggest this function is not conserved in flies (see discussion, chapter 2). ATM autophosphorylates to transition from an inactive dimer to an active monomer that proceeds to phosphorylate the Histone H2A variant near sites of DNA damage (called γH2AX in mammals or pH2Av in flies) (Sun et al., 2009). The initial site of γH2AX/pH2Av is recognized by MDC1 (mediator of DNA damage checkpoint 1) to facilitate the recruitment and retention of MRN complexes and ATM, which in turn leads to the phosphorylation of H2AX/H2Av at increasingly larger distances from the damage site (van Attikum & Gasser, 2009, Gontijo et al., 2003) (Fig.

1.5). The breast cancer associated gene 1 (BRCA1) represses transcription of the G2/M promoting *cyclinB* to contribute to cell cycle arrest while also promoting the transcription of certain DNA repair factors. In addition BRCA1 co-localizes with MRN complexes where it recruits DNA repair factors (MacLachlan et al., 2000, Deng, 2003). The spread of γH2AX around the site of damage also creates docking sites for the accumulation of additional DNA repair factors (Sun et al., 2007). Potentially hundreds of proteins other than H2AX/H2Av are also phosphorylated by ATM, including Chk2 and p53 (Sun et al., 2010). The Chk2 kinase is activated by ATM's activity and in turn phosphorylates Cdc25c (String in *Drosophila*) to trigger its nuclear export, which also contributes to a delay in cell cycle progression. Without nuclear Cdc25c the mitosis-promoting CycB/Cdk1complexes remain inactive to provide time for DNA repair in mammals (Pietenpol & Stewart, 2002). Chk2 and ATM activity also promote the activity of E2F1 to promote transcription of many DNA repair factors (Lin et al., 2001, Polager et al., 2002, Stevens et al., 2003, Stevens & La Thangue, 2004). After damage repair, the conserved chromatin remodeling complex Tip60/NuA4 quenches the DNA damage signal by acetylating γH2AX/pH2Av and using the helicase function of its p400 subunit (Domino in flies) to exchange it with an unmodified H2Av-H2B pair (Kusch et al., 2004).

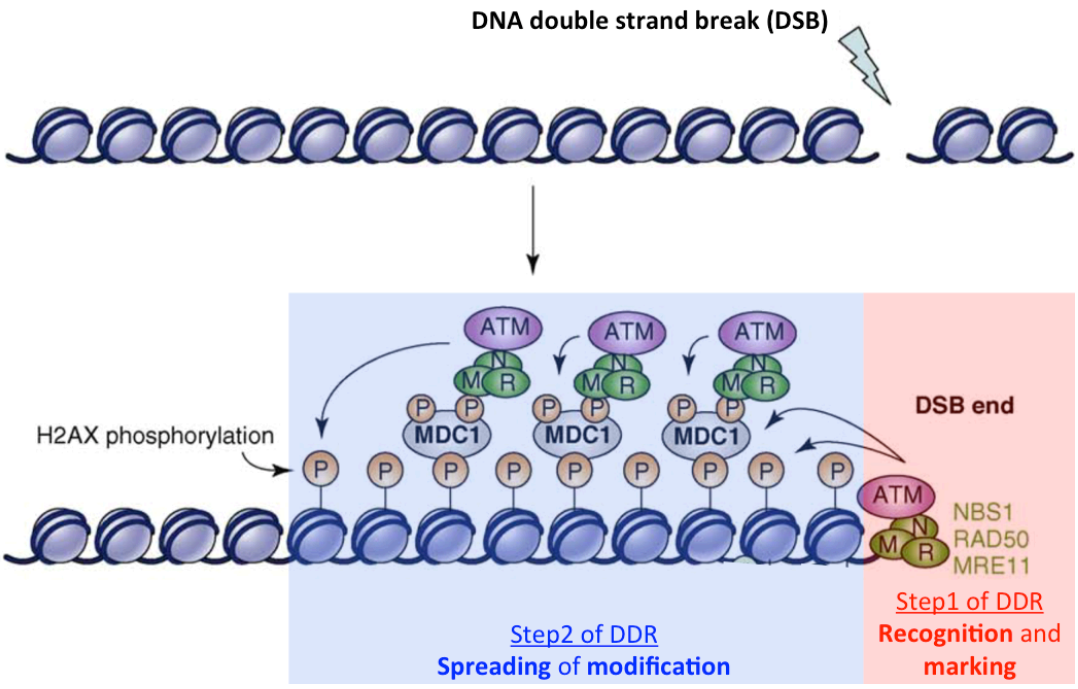

Fig. 1.5 Mechanism of H2AX/H2Av phosphorylation spreading from site of DNA damage (van Attikum & Gasser, 2009). DNA double-strand breaks are initially recognized by MDC1, which rapidly recruits the MRN complex (Mre11, Rad50, Nbs1) and the ATM kinase. ATM phosphorylates nearby H2A variants (H2AX/ H2Av), which in turn recruit more MDC1, MRN complexes, and ATM to phosphorylate H2A variants at increasing distance from the initial site.

Many of the components of the DDR are conserved in *Drosophila*, though some roles are slightly different that in mammals. Mei-41 (homolog of ATR) is the kinase that primarily controls the DDR checkpoint and DNA repair, whereas Tefu (homolog of ATM) is the predominant regulator of p53-dependent apoptosis and telomere stabilization (LaRocque et al., 2007). p53 is the conserved transcription factor that functions in both mammalian and fly DDRs and is most famous for being inactivated in >50% of human cancers (Momand et al., 1992, Freed-Pastor & Prives, 2012, Levine & Oren, 2009, Polager & Ginsberg, 2009). Upon DNA damage in mammals, p53 levels increase and either slow cell cycle progression by promoting *p21* expression (the CKI of the G1-S CyclinE/cdk2 pair) or induce programmed cell death by promoting the expression of apoptotic factors. In flies however, p53 protein levels do not

increase in response to DSB (Brodsky et al., 2004). Instead, p53 activity is increased by Chk2/MNK phosphorylation. Though *Drosophila* p53 is unable to slow G1-S progression (Ollmann et al., 2000, Brodsky et al., 2004), it has retained the ability to promote the expression of regulators of apoptosis, cell-cell signaling, and DNA repair (Fig. 1.6). It is thought that the decision to repair damage instead of performing a programmed cell death is controlled by the levels and duration of p53 activity, as well as the promoter-specificity of p53 at the time of damage. By post-translationally modifying p53 and/or by changing its' protein-protein interactions, signaling pathways (such as Ras) can affect whether p53 induces expression of pro-apoptotic or DNA repair genes (Riley et al.,, 2008). Despite mammalian Tip60 co-activating p53-target gene expression through its acetylation of nearby H4 histones (Tang, et al., 2006), and the acetylation of p53 itself impacting p53's promoter selectivity (Oren, 2003), we found that interaction between fly p53 and Tip60 was not needed for NuA4's role in cell cycle progression (Flegel et al., 2016). In chapter II, I describe how we instead found that a Tip60/NuA4 complex is needed to resolve endogenous DNA damage that occurs during normal proliferation, which otherwise induces a p53-independent DDR (Flegel et al., 2016). This slows cell cycle progression, and impacts the proper timing of cell cycle exit during development in the absence of proper Tip60/NuA4 function (Flegel et al., 2016). As previously mentioned, activation of the DDR during can cause a temporary cell cycle arrest that could delay cell cycle exit (section 2.1). Consistent with this we show that when Tip60/NuA4 function is compromised, discordant timing of E2F-target gene silencing and differentiation occurs. In this thesis, we examine how disruptions of the proper timing of the final cell cycle impact the timing of cell cycle exit, cell cycle gene repression, and terminal differentiation.

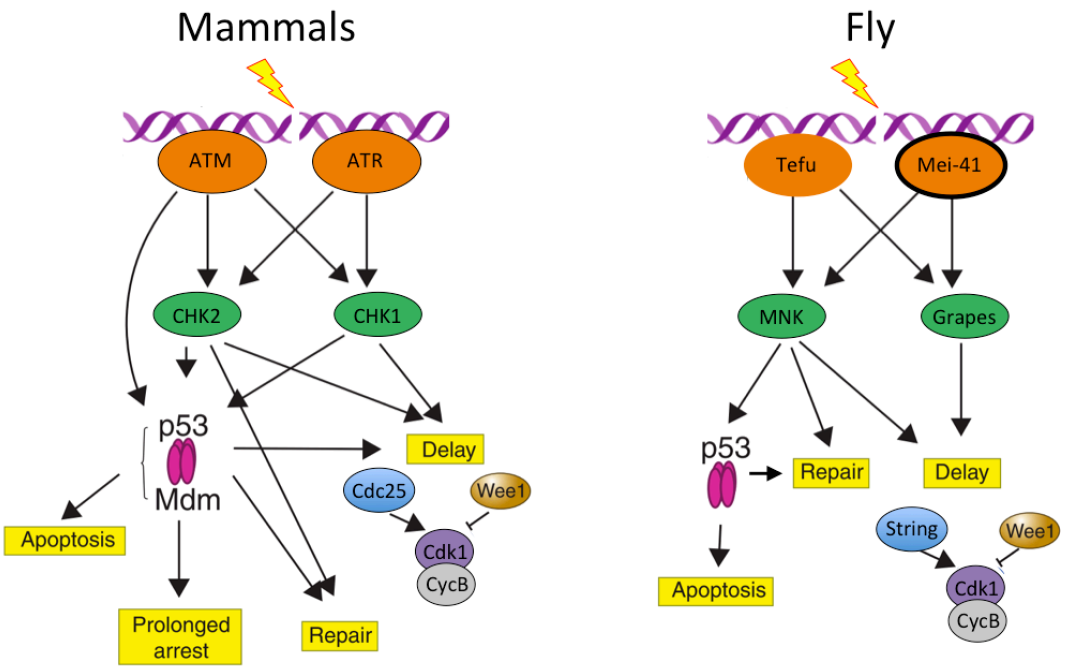

Fig. 1.6 Conserved DNA damage response Adapted from (Wahl & Carr, 2001). DNA double-strand breaks (DSBs) in mammals are detected by ATM, which acts predominantly through Chk2. ATR detects DNA single-strand breaks (SSBs) and acts predominantly through Chk1. In *Drosophila*, Mei-41/ATR primarily controls the DNA damage response (DDR) checkpoint and DNA repair, whereas Tefu/ATM is involved more in telomere stabilization and regulation of p53-dependent apoptosis (LaRocque et al., 2007).

Developmental control of cell cycle exit

3.1 Types of cell cycle exit

Cessation of proliferation and prolonged exit with a G1 or 2C DNA content are characteristics of quiescence, senescence, and cell cycle exit associated with terminal differentiation (Buttitta & Edgar, 2007). Though G0 has been used in the literature to refer to any of these distinct states of cell cycle exit, they differ in their causes and durations. Replicative senescence is one of several types of cellular senescence characterized as G1 arrested cells that have a distinct morphology, heterochromatin foci, and a characteristic gene expression profile (Narita et al., 2003, Zhang et al., 2005, Campisi, 2005, Narita & Lowe, 2005). Cellular senescence also includes age-associated replicative senescence that results from teleomere

shortening triggering a DNA damage response after many successive bouts of DNA replication (Schraml & Grillari, 2012, Bodnar et al., 1998). Another state of exit is known as quiescence when cells have stopped proliferating but can re-enter the cell cycle upon extrinsic signals from the environment. This includes cells in culture that are deprived of mitogens and quiescent adult mammalian stem cells that re-enter the cell cycle to maintain tissue homeostasis and respond to stresses such as wounding (Li & Bhatia, 2011). However, we focus on the developmentally regulated cell cycle exit associated with terminal differentiation, which is permanent in most cases and is the predominant cycling status in adult tissues. Cell cycle exit associated with terminal differentiation is defined as the transition to a non-proliferative and post-mitotic state where cells acquire their final cell fates to form functional tissues and organs. This is achieved by an intricate interplay of signaling cascades that is not yet fully understood.

3.2 Establishing cell cycle exit

Thus far several redundant mechanisms have been found to reinforce cell cycle exit associated with terminal differentiation, including transcriptional repression and increased degradation of cell cycle-promoting proteins. Endogenous transcriptional repression of cell cycle-promoting genes during cell cycle exit has been linked with increased expression of CKIs (such as Dacapo in flies) which repress CycE/Cdk2 activity (Baumgardt et al., 2014) and recruitment of Rb family members for formation of the DREAM/MMB complex to repress cell cycle genes (Blais & Dynlacht, 2007). Perturbations in the DREAM/MMB complex can shift cells from quiescence towards proliferation in mammalian tissue culture (Litovchick et al., 2007), but *in vivo* functions during terminal differentiation remain largely unknown (Forristal et al., 2014). Other transcription factors (yeast Stb3 and Xbp1) have also been found to promote

quiescence, specifically by recruiting chromatin remodelers, such as the histone deacetylase Rpd3, to promote chromatin closing and stable repression of cell cycle genes (McKnight et al., 2015). Rpd3 is critical for proper establishment of quiescence in yeast, yet it remains to be determined whether that translates to role in cell cycle exit associated with terminal differentiation in multicellular organisms.

To reinforce the developmentally regulated post-mitotic state, cells also have a double assurance mechanism through which they establish and maintain cell cycle exit (Buttitta et al., 2007). This mechanism makes post-mitotic cells refractory to increases individual complexes such as CycE/Cdk2 or E2F/DP, which normally positively regulate one another to promote cell cycle progression during active proliferation (Buttitta et al., 2007). This is achieved at least in part, by post-mitotic cells having increased activity of the anaphase promoting complex/cyclosome (APC/C), a ubquitin ligase complex whose activity promotes mitotic exit by triggering the degradation of major G2/M regulatory proteins including CycA, Geminin (Zielke et al., 2008), CycB, and the Cdc25c homolog, Stg (Grosskortenhaus & Sprenger, 2002). Consequently, for a cell to abrogate the double assurance mechanism of cell cycle exit, multiple cell cycle promoting complexes such as CycE/Cdk2 and E2F/DP would have to be expressed simultaneously at levels sufficient for CycE/Cdk2 to inhibit the high levels of APC/C activity during cell cycle exit (Buttittal et al. 2010).

3.3 Gal4/UAS system

Throughout this work we used the binary Gal4/UAS system to spatially and temporally drive transgene expression in specific fly tissues (Fig. 1.7). In this system adapted from yeast, Gal4 is a transcription activator that binds upstream activation sequences (UAS) to drive the

expression of downstream genes (Duffy, 2002). When transgenes encoding these are crossed into the same fly, the Gal4 can promote the expression of the sequence that lies immediately downstream of the UAS construct. For example, Gal4 controlled by a promoter for a gene that is normally expressed in the posterior of the wing (wing posterior - Gal4) mated to flies carrying a UAS construct controlling the expression of an RNA interference (RNAi) transgene and/or the marker, green fluorescent protein (GFP) will produce offspring that express the RNAi and/or GFP in the posterior of the wing blade. This system can be further modified by the inclusion of a temperature sensitive Gal80 ($Gal80^{TS}$) that binds Gal4 protein and inhibits gal4's activation of UASs. The $Gal80^{TS}$ is active at low (18°C) temperatures and therefore represses the Gal4 activity at the UAS. A shift to high temperatures (28°C) degrades the gal80, thereby releasing the gal4 to activate the UAS driven RNAi and/or GFP. Variations from the basic Gal4/UAS system are used throughout this work.

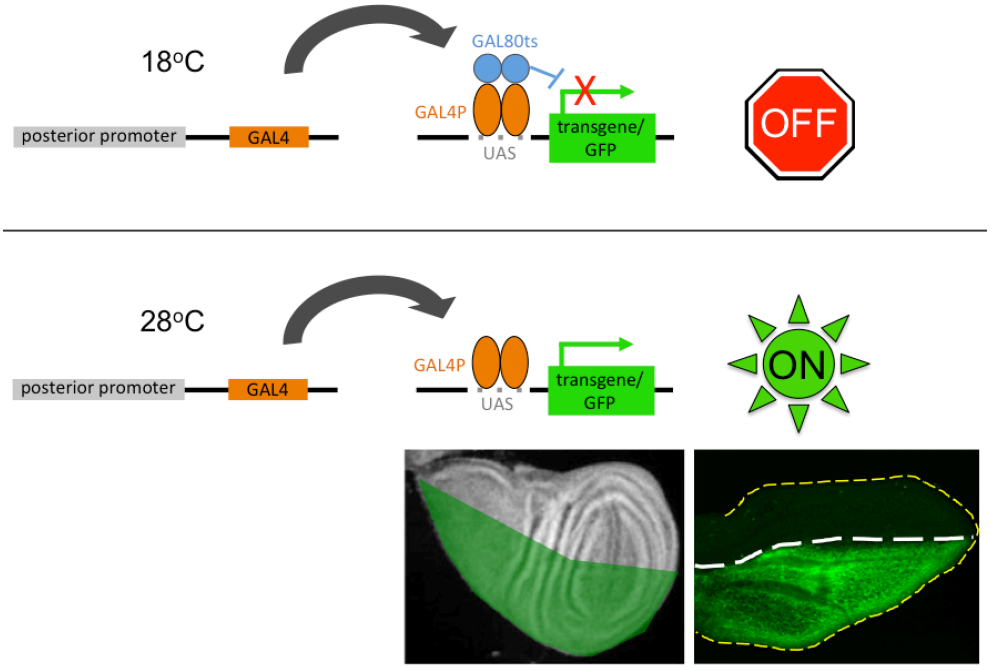

Fig. 1.7 Gal4/UAS system spatially and temporally regulates transgene expression in *Drosophila.* Flies with tissue-specific promoters driving Gal4 expression can be mated with flies possessing transgenes and fluorescent markers that are under control of the Gal4-responsive

upstream activating sequences (UAS), to produce progeny that have tissue-specific transgene expression. Adding an additional temperature sensitive Gal80 allows the transgene expression to be temporally restricted.

3.4 Screen to identify regulators of cell cycle exit

Twenty-four hours after the start of *Drosophila* metamorphosis, many tissues have become or are transitioning to a post-mitotic state associated with terminal differentiation (Fig. 1.8). As previously mentioned, when cells stop proliferating and terminally differentiate, E2F is thought to associate with dREAM to repress cell cycle genes. In the interest of identifying genes involved in the proper timing of cell cycle exit, a genetic screen for negative effectors of E2F transcriptional activity was performed. Approximately 2,000 RNAi lines from the TRiP collection (Ni et al., 2011) were screened for ectopic cell cycle activity in pupal eyes or wings at timepoints when these tissues are normally fully post-mitotic (Buttitta & Edgar, 2007).

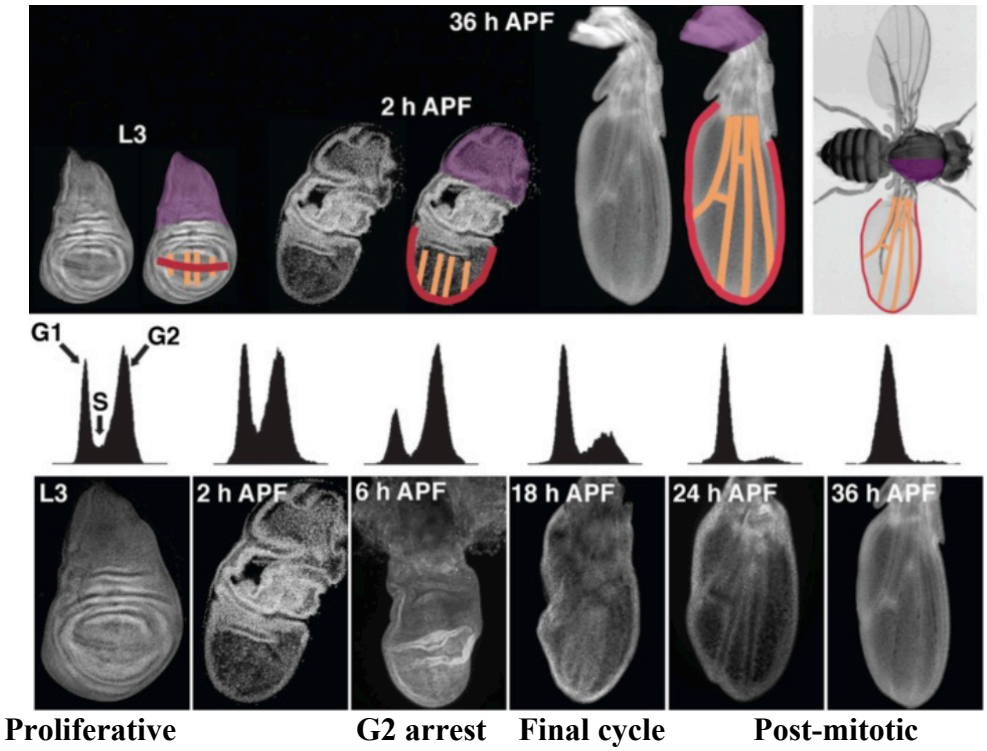

Fig. 1.8 Development of the *Drosophila* wing. The third larval instar (L3) wing disc evaginates during pupal metamorphosis to form the adult wing. Patterning of the vein (orange) and wing margin (red) allows changes in the gross morphological organization to be observed. During this process the cells that were once proliferating in the larval wing, now arrest in the G2 phase of the cell cycle 6h after pupa formation (APF). Release from this arrest causes cells to synchronously perform their final cell cycle. Most cells exit the final cell cycle with a G1 or 2C DNA content by 24h APF, and maintain their G1 DNA content throughout the rest of development as cells terminally differentiate.

The initial screen was performed by expressing the RNAi transgenes in the eye and assayed a PCNA-*white* reporter transgene previously described as a readout for E2F activity (Bandura et al., 2013). Since this reporter used the promoter of the E2F-responsive β-clamp DNA polymerase processivity factor, *Proliferating Cell Nuclear Antigen (PCNA),* increases in the reporter actually indicated de-repression of E2F activity but not necessarily effects on cell cycle exit. Therefore we performed a secondary dissection-based screen with selected RNAi lines in both the eye and wing, directly assessing the timing of cell cycle exit by monitoring the mitotic marker Ser-10-Phospho-Histone H3 (PH3). From this secondary screen, we identified

(and then went on to confirm) that inhibition of several components of the nucleosome acetyltransferase of histone H4 (Tip60/NuA4) complex delay cell cycle exit in eyes and wing and repress *Drosophila* E2F1 transcriptional activity during the transition to a post-mitotic state. The function of the NuA4 complex in cell cycle exit is described in more detail in chapter II.

3.5 Nucleosome acetyltransferase of histone H4 complex (NuA4)

NuA4 is a multi-subunit complex conserved from yeast to humans, best characterized as a H4 histone acetyltransferase (HAT) that opens chromatin to factors that regulate gene expression (Lu et al., 2009, Doyon et al., 2004). NuA4 has acetyltransferase, DNA helicase, histone reading, and histone exchange activities through which it plays an essential, conserved role in quenching the DNA damage signal (Lu et al., 2009, Doyon et al., 2004, Auger et al., 2008, Kusch et al., 2004). One of the earliest responses to DNA damage is the phosphorylation of H2A variants (H2AX known as H2Av in *Drosophila*) close to the damage site. Upon DNA repair, NuA4 quenches the damage signal by acetylating and replacing the modified variants with unmodified H2A variants (Auger et al., 2008, Kusch et al., 2004). NuA4 can also engage many transcription factors, including Myc, p53, NFκB, and E2F to turn on target gene expression in proliferating cells (Frank et al., 2003, Tang et al., 2006, Taubert et al., 2004). However, in specific contexts (such as embryonic stem cells) the NuA4 complex is an essential repressor (Fazzio et al., 2008) furthermore NuA4 can also promote the formation of closed chromatin in flies (Qi et al., 2006). NuA4 components were also found in *C. elegans* to genetically interact with the synMuvB components that are critical for both the activating and repressive transcriptional roles of dREAM/MMB (Ceol & Horvitz, 2004) suggesting a possible role in cell cycle regulation. In addition, RNAi of several NuA4 components in *Drosophila* cell culture de-

repressed an E2F1-responsive reporter and the NuA4 components were recruited to E2F1 targets in an E2F1-dependent manner, leading to the conclusion that NuA4 normally directly represses E2F1/DP targets (Lu et al., 2007). They also concluded that NuA4 components acted in parallel to the DREAM complex to repress E2F-target gene expression, because RNAi of a DREAM component (Rbf1) and a NuA4 component (Domino) synergistically increased the E2F1-responsive reporter (Lu et al., 2007). The combination of these roles within a cell may account for NuA4's paradoxical function as both a tumor suppressor and oncogene in the literature; but has unfortunately caused its positive vs. negative regulatory roles in cell cycle control to remain unresolved (Sapountzi, Logan, & Robson, 2006, Judes et al., 2015, Gorrini et al., 2007). Consistent with NuA4 normally promoting cell cycle progression, we found that compromising NuA4 delayed the timing of cell cycle exit in the fly wing and eye (see chapter II).

Drosophila melanogaster as a model system for cell cycle exit

Analysis of cell cycle regulation in mammals can be challenging due to the multiple, redundant factors involved in the process, often requiring double and triple mutants to be generated. By contrast, most cycle regulators are well conserved in *Drosophila melanogaster*, but with fewer paralogs facilitating genetic analysis of novel cell cycle regulatory pathways (Dimova & Dyson, 2005). We use Drosophila to study the cell cycle regulation that occurs as cells transition from a proliferating to a non-proliferating state during development, in a process coordinated with tissue differentiation called cell cycle exit.

4.1 Ecdysone steroid regulates *D melanogaster* development and cell cycle exit

In *Drosophila* many tissues transition from actively proliferating to a terminally differentiated, post-mitotic state during pupal metamorphosis (Fig. 1.8) . The onset of metamorphosis is controlled by an increased titer of the steroid hormone ecdysone, with subsequent developmental events naturally synchronized *in vivo* (Ashburner, 1989). This includes the final cell cycle in the *Drosophila* eye and wing that culminates with cells becoming post-mitotic 24 hours after pupa formation (APF) relatively synchronously (Tomlinson & Ready, 1987, O'Keefe et al., 2012, Schubiger & Palka, 1987, Milan et al., 1996) (Fig. 1.8).

The synchrony of the final cell cycle in the wing is a direct consequence of a temporary G2 arrest that occurs at 6 hours APF (O'Keefe et al., 2012). This and other pivotal points of *Drosophila* development are thought to be induced by the periodic secretion of the hormone ecdysone (Nijhout et al., 2014, Ou & King-Jones, 2013). Interestingly, ecdysone exposure in *Drosophila* tissue culture cells can also induce a cell cycle arrest in G2-phase (Echalier, 1997, Stevens et al., 1980), suggesting the mechanism through which ecdysone impacts the cell cycle may be similar in cell culture and fly wings. Steroid hormones play a central role in coordinating the timing of developmental events not only for the fly's transition from larva to pupa, but also the mammalian pre- to post-natal transitions and puberty. The ecdysone steroid hormone signaling explored here, is most similar to the vertebrate retinoic acid signaling pathway that also acts as a key modulator of cell differentiation in many cell types (Breitman et al., 1980). We are interested in how developmental cues such as these impinge upon cell cycle regulation and the decision of a cell to stop cycling and terminally differentiate into the tissues and organs that make up metazoans.

During *D. melanogaster* development, the steroid ecdysone is synthesized in the prothoracic gland after which peripheral tissues convert it into its active form of 20-hydroxyecdysone (20-HE). Upon dimerization with the nuclear ecdysone receptor (EcR) and the retinoid X receptor called Ultraspiracle in flies (USP) (Thomas et al., 1993), 20-HE induces tissue-specific cascades of gene expression that are synchronized across the whole animal to drive the coordinated events of metamorphosis (Emery et al.,1994). Though pulses of ecdysone occur several times during *Drosophila* development, it is not until the last larval instar (L3) and attainment of a critical weight that a large pulse of ecdysone triggers cessation of feeding after which a second, even larger pulse induces the molt to the pupa (Ou & King-Jones, 2013, Mirth et al., 2014) (Fig.1.9).

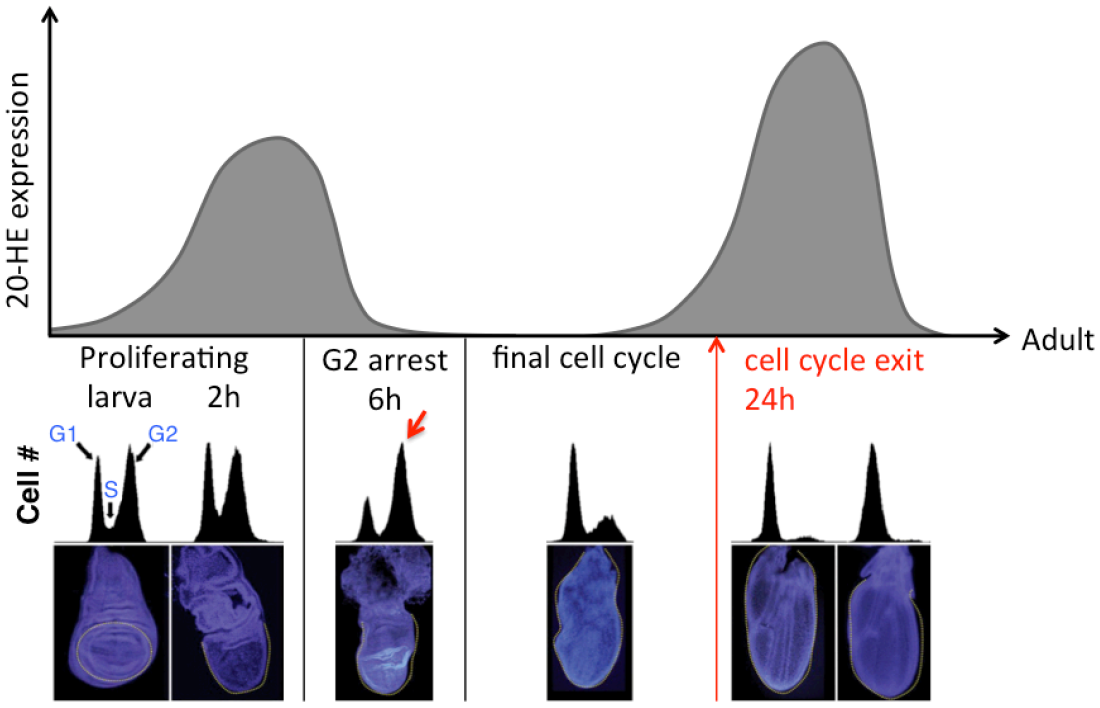

Fig. 1.9 Pulses of ecdysone coincide with major events in *Drosophila* development Adapted from O'Keefe et al., 2012 and Ou & King-Jones, 2013. A pulse of activated ecdysone (20-HE) promotes the larva to pupa transition called metamorphosis. The distribution of DNA content determined via flow cytometry (G1, S, G2) shows that the 20-HE pulse at the larva-pupa transition precedes a temporary arrest of cells in G2 (red arrow at 6h). This is followed by a large

peak of 20-HE that coincides with cell cycle exit and terminal differentiation. Time after puparium formation is indicated in hours (h).

The primary response to 20-HE is the induction of a small set of "early" transcriptional target genes that amplify the original signal by triggering the subsequent expression of many tissue-specific "late" genes. Different isoforms of early-response genes and the possible combinations therein also contribute to the tissue-specificity of ecdysone responses. The 20-HE early-response genes include members of the *broad (br)* locus which encodes 4 distinct proteins through alternative splicing. The Broad isoforms share a common N-terminus that is alternatively spliced with different combinations of C_2H_2 zinc finger pairs (termed Broad-Z1, Z2, Z3, Z4) through which Broad site-specifically binds DNA (Crossgrove et al., 1996). Although Broad protein is widely distributed in larva and prepupa (Emery et al., 1994, Huet et al., 1993), 20-HE responsive tissues differ in their relative abundance of each isoform and even these abundances can change throughout development to result in tissue-specific cascades of events (Bayer et al., 1996). A relationship between 20-HE, *broad* expression and cell cycle progression is supported by ectopic 20-HE signaling in the early pupal wing inducing *broad* expression (Schubiger & Truman, 2000) and naturally high levels of Broad coinciding with the temporary G2 arrest of the pupal wing (O'Keefe et al., 2012). These correlations led us to speculate that 20-HE pulses may impinge upon cell cycle progression through its regulation of Broad.

A large pulse of 20-HE induces pupal metamorphosis and expression of Broad, after which wing (O'Keefe et al., 2012, Fain & Stevens, 1982) and leg (Graves & Schubiger, 1982) cells rapidly accumulate in G2. Once released from this arrest, cells perform a final cell cycle before permanently exiting the cell cycle at the beginning of the largest pulse of 20-HE. In chapter III, we describe how a pulse of the steroid hormone ecdysone modulates the cell cycle

during metamorphosis to synchronize the final cell cycle, and therefore cell cycle exit, in the *Drosophila* wing.

Altogether, the work presented here examines the NuA4 and ecdysone signaling pathways and how they impact the transcriptional programs that normally maintain the proper developmental timing of cell cycle exit in the *Drosophila* eye and wing.

References

Ashburner, M. (1989). *Drosophila. A laboratory handbook.*

Auger, A., Galarneau, L., Altaf, M., Nourani, A., Doyon, Y., Utley, R. T., … Côté, J. (2008). Eaf1 is the platform for NuA4 molecular assembly that evolutionarily links chromatin acetylation to ATP-dependent exchange of histone H2A variants. *Molecular and Cellular Biology*, *28*(7), 2257–70.

Ayeni, J. O., Varadarajan, R., Mukherjee, O., Stuart, D. T., Sprenger, F., Srayko, M., & Campbell, S. D. (2014). Dual phosphorylation of cdk1 coordinates cell proliferation with key developmental processes in Drosophila. *Genetics*, *196*(1), 197–210.

Bandura, J. L., Jiang, H., Nickerson, D. W., & Edgar, B. A. (2013). The Molecular Chaperone Hsp90 Is Required for Cell Cycle Exit in Drosophila melanogaster, *9*(9).

Baumgardt, M., Karlsson, D., Salmani, B. Y., Bivik, C., MacDonald, R. B., Gunnar, E., & Thor, S. (2014). Global Programmed Switch in Neural Daughter Cell Proliferation Mode Triggered by a Temporal Gene Cascade. *Developmental Cell*, *30*(2), 192–208.

Bayer, C. A., Holley, B., & Fristrom, J. W. (1996). A Switch in Broad-ComplexZinc-Finger Isoform Expression Is Regulated Posttranscriptionally during the Metamorphosis of Drosophila Imaginal Discs. *Developmental Biology*, *177*(1), 1–14.

Blais, A., & Dynlacht, B. D. (2007). E2F-associated chromatin modifiers and cell cycle control. *Current Opinion in Cell Biology*, *19*(6), 658–662.

Bodnar, A. G., Ouellette, M., Frolkis, M., Holt, S. E., Chiu, C. P., Morin, G. B., … Wright, W. E. (1998). Extension of life-span by introduction of telomerase into normal human cells. *Science (New York, N.Y.)*, *279*(5349), 349–52.

Breitman, T. R., Selonick, S. E., & Collins, S. J. (1980). Induction of differentiation of the human promyelocytic leukemia cell line (HL-60) by retinoic acid. *Proceedings of the National Academy of Sciences of the United States of America*, *77*(5), 2936–40.

Brodsky, M. H., Weinert, B. T., Tsang, G., Rong, Y. S., Mcginnis, N. M., Golic, K. G., … Rubin, G. M. (2004). Drosophila melanogaster MNK / Chk2 and p53 Regulate Multiple DNA Repair and Apoptotic Pathways following DNA Damage, *24*(3), 1219–1231.

Buttitta, L. A., & Edgar, B. A. (2007). Mechanisms controlling cell cycle exit upon terminal differentiation. *Current Opinion in Cell Biology*, *19*(6), 697–704.

Buttitta, L. A., Katzaroff, A. J., & Edgar, B. a. (2010). A robust cell cycle control mechanism

limits E2F-induced proliferation of terminally differentiated cells in vivo. *The Journal of Cell Biology*, *189*(6), 981–96.
Buttitta, L. A., Katzaroff, A. J., Perez, C. L., de la Cruz, A., & Edgar, B. a. (2007). A double-assurance mechanism controls cell cycle exit upon terminal differentiation in Drosophila. *Developmental Cell*, *12*(4), 631–43.
Campanero, M. R., & Flemington, E. K. (1997). Regulation of E2F through ubiquitin-proteasome-dependent degradation: stabilization by the pRB tumor suppressor protein. *Proceedings of the National Academy of Sciences of the United States of America*, *94*(6), 2221–2226.
Campisi, J. (2005). Senescent cells, tumor suppression, and organismal aging: Good citizens, bad neighbors. *Cell*, *120*(4), 513–522.
Ceol, C. J., & Horvitz, H. R. (2004). A New Class of C . elegans synMuv Genes Implicates a Tip60 / NuA4-like HAT Complex as a Negative Regulator of Ras Signaling. *Developmental Cell*, *6*, 563–576.
Ceol, C. J., Stegmeier, F., Harrison, M. M., & Horvitz, H. R. (2006). Identification and classification of genes that act antagonistically to let-60 ras signaling in Caenorhabditis elegans vulval development. *Genetics*, *173*(2), 709–726.
Ciapponi, L., Cenci, G., & Gatti, M. (2006). The Drosophila nbs protein functions in multiple pathways for the maintenance of genome stability. *Genetics*, *173*(July), 1447–1454.
Clurman, B. E., Sheaff, R. J., Thress, K., Groudine, M., & Roberts, J. M. (1996). Turnover of cyclin E by the ubiquitin-proteasome pathway is regulated by cdk2 binding andcyclin phosphorylation. *Genes & Development*, *10*, 1979–1990.
Cooper, G. (2000). The Cell: A Molecular Approach. 2nd edition. Sunderland (MA): Sinauer Associates.
Crossgrove, K., Bayer, C. A., Fristrom, J. W., & Guild, G. M. (1996). The Drosophila Broad-Complex early gene directly regulates late gene transcription during the ecdysone-induced puffing cascade. *Developmental Biology*, *180*(2), 745–58.
Davidson, J. M., & Duronio, R. J. (2012). S Phase – Coupled E2f1 Destruction Ensures Homeostasis in Proliferating Tissues, *8*(8).
Deng, C.-X. (2003). Roles of BRCA1 in DNA damage repair: a link between development and cancer. *Human Molecular Genetics*, *12*(90001), 113R–123.
Dimova, D. K., & Dyson, N. J. (2005). The E2F transcriptional network: old acquaintances with new faces. *Oncogene*, *24*(17), 2810–2826.
Doyon, Y., Selleck, W., Lane, W. S., Tan, S., Côté, J., & Co, J. (2004). Structural and Functional Conservation of the NuA4 Histone Acetyltransferase Complex from Yeast to Humans. *Molecular and Cellular Biology*, 1884–1896. h
Du, W., & Pogoriler, J. (2006). Retinoblastoma family genes. *Oncogene*, *25*(38), 5190–5200.
Du, W., Xie, J., & Dyson, N. (1996). Ectopic expression of dE2F and dDP induces cell proliferation and death in the Drosophila eye, *15*(14), 3684–3692.
Duffy, J. B. (2002). GAL4 system in Drosophila: a fly geneticist's Swiss army knife. *Genesis (New York, N.Y. : 2000)*, *34*(1–2), 1–15.
Echalier, G. (1997). *Drosophila Cells in Culture*. *Drosophila Cells in Culture*. CHAP, New York: Academic Press.
Emery, I. F., Bedian, V., & Guild, G. M. (1994). Differential expression of Broad-Complex transcription factors may forecast tissue-specific developmental fates during Drosophila metamorphosis. *Development (Cambridge, England)*, *120*(11), 3275–87.

Errico, A., Deshmukh, K., Tanaka, Y., Pozniakovsky, A., & Hunt, T. (2010). Identification of substrates for cyclin dependent kinases. *Advances in Enzyme Regulation*, *50*(1), 375–399.
Fain, M. J., & Stevens, B. (1982). Alterations in the cell cycle of Drosophila imaginal disc cells precede metamorphosis. *Developmental Biology*, *92*(1), 247–258.
Fay, D. S., & Yochem, J. (2007). The SynMuv genes of Caenorhabditis elegans in vulval development and beyond David. *Dev Biol*, *306*(1), 1–9.
Fazzio, T. G., Huff, J. T., & Panning, B. (2008). An RNAi screen of chromatin proteins identifies Tip60-p400 as a regulator of embryonic stem cell identity. *Cell*, *134*(1), 162–74.
Fisher, D. (2011). Control of DNA Replication by Cyclin-Dependent Kinases in Development. In *Results and problems in cell differentiation* (Vol. 53, pp. 201–217).
Fisher, R. P. (2012). The CDK Network: Linking Cycles of Cell Division and Gene Expression. *Genes Cancer*, *3*(11–12), 731–738.
Flegel, K., Grushko, O., Bolin, K., Griggs, E., & Buttitta, L. (2016). Roles for the histone modifying and exchange complex NuA4 in cell cycle progression in Drosophila melanogaster. *Genetics*, *203*(3), 1265–1281.
Forristal, C., Henley, S. a, MacDonald, J. I., Bush, J. R., Ort, C., Passos, D. T., … Dick, F. a. (2014). Loss of the Mammalian DREAM Complex Deregulates Chondrocyte Proliferation. *Molecular and Cellular Biology*, *34*(12), 2221–2234.
Foster, D. A., Yellen, P., Xu, L., & Saqcena, M. (2010). Regulation of G1 Cell Cycle Progression: Distinguishing the Restriction Point from a Nutrient-Sensing Cell Growth Checkpoint(s). *Genes & Cancer*, *1*(11), 1124–31.
Frank, S. R., Parisi, T., Taubert, S., Fernandez, P., Fuchs, M., Chan, H.-M., … Amati, B. (2003). MYC recruits the TIP60 histone acetyltransferase complex to chromatin. *EMBO Reports*, *4*(6), 575–80.
Freed-Pastor, W. A., & Prives, C. (2012). Mutant p53 : one name , many proteins. *Genes & Development*, *26*, 1268–1286.
Fu, Z., Malureanu, L., Huang, J., Wang, W., Li, H., van Deursen, J. M., … Chen, J. (2008). Plk1-dependent phosphorylation of FoxM1 regulates a transcriptional programme required for mitotic progression. *Nature Cell Biology*, *10*(9), 1076–82.
Georlette, D., Ahn, S., MacAlpine, D. M., Cheung, E., Lewis, P. W., Beall, E. L., … Botchan, M. R. (2007). Genomic profiling and expression studies reveal both positive and negative activities for the Drosophila Myb MuvB/dREAM complex in proliferating cells. *Genes & Development*, *21*(22), 2880–96.
Gontijo, A., Green, C. M., & Almouzni, G. (2003). Repairing DNA damage in chromatin. *Biochimie*, *85*(11), 1133–1147.
Gorrini, C., Squatrito, M., Luise, C., Syed, N., Perna, D., Wark, L., … Amati, B. (2007). Tip60 is a haplo-insufficient tumour suppressor required for an oncogene-induced DNA damage response. *Nature*, *448*(7157), 1063–1067.
Graves, B. J., & Schubiger, G. (1982). Cell cycle changes during growth and differentiation of imaginal leg discs in Drosophila melanogaster. *Developmental Biology*, *93*(1), 104–110.
Grosskortenhaus, R., & Sprenger, F. (2002). Rca1 inhibits APC-Cdh1(Fzr) and is required to prevent cyclin degradation in G2. *Developmental Cell*, *2*(1), 29–40.
Harbour, J. W., & Dean, D. C. (2000). The Rb/E2F pathway: Expanding roles and emerging paradigms. *Genes and Development*, *14*(19), 2393–2409.
Harrington, E. a, Bruce, J. L., Harlow, E., & Dyson, N. (1998). pRB plays an essential role in cell cycle arrest induced by DNA damage. *Proceedings of the National Academy of*

Sciences of the United States of America, *95*(20), 11945–50.
Hériché, J.-K., Ang, D., Bier, E., & O'Farrell, P. H. (2003). Involvement of an SCFSlmb complex in timely elimination of E2F upon initiation of DNA replication in Drosophila. *BMC Genetics*, *4*, 9.
Higa, L. A., Yang, X., Zheng, J., Banks, D., Wu, M., Ghosh, P., … Zhang, H. (2006). Involvement of CUL4 Ubiquitin E3 Ligases in Regulating CDK Inhibitors Dacapo/p27 Kip1 and Cyclin E Degradation. *Cell Cycle*, *5*, 71–77.
Hill, R. J., & Sternberg, P. W. (1992). The gene lin-3 encodes an inductive signal for vulval development in C. elegans. *Nature*, *358*(6386), 470–6.
Huet, F., Ruiz, C., & Richards, G. (1993). Puffs and PCR: the in vivo dynamics of early gene expression during ecdysone responses in Drosophila. *Development (Cambridge, England)*, *118*(2), 613–27.
Johnson, T. K., Schweppe, R. E., Septer, J., & Lewis, R. E. (1999). Phosphorylation of B-Myb regulates its transactivation potential and DNA binding. *Journal of Biological Chemistry*, *274*(51), 36741–36749.
Judes, G., Rifaï, K., Ngollo, M., Daures, M., Bignon, Y.-J., Penault-Llorca, F., & Bernard-Gallon, D. (2015). A bivalent role of TIP60 histone acetyl transferase in human cancer. *Epigenomics*, *7*(8), 1351–63.
Kanei-Ishii, C., Nomura, T., Takagi, T., Watanabe, N., Nakayama, K. I., & Ishii, S. (2008). Fbxw7 acts as an E3 ubiquitin ligase that targets c-Myb for Nemo-like kinase (NLK)-induced degradation. *Journal of Biological Chemistry*, *283*(45), 30540–30548.
Knoblich, J. A., Sauer, K., Jones, L., Richardson, H., Saint, R., & Lehner, C. F. (1994). Cyclin E controls S phase progression and its down-regulation during Drosophila embryogenesis is required for the arrest of cell proliferation. *Cell*, *77*(1), 107–120.
Koepp, D. M., Schaefer, L. K., Ye, X., Keyomarsi, K., Chu, C., Harper, W., … Elledgel, S. J. (2001). Phosphorylation-Dependent Ubiquitination of Cyclin E by the SCF Fbw7 Ubiquitin Ligase. *Science*, *294*, 173–177.
Kusch, T., Florens, L., Macdonald, W. H., Swanson, S. K., Glaser, R. L., Yates, J. R., … Workman, J. L. (2004). Acetylation by Tip60 is required for selective histone variant exchange at DNA lesions. *Science (New York, N.Y.)*, *306*(5704), 2084–7.
Laoukili, J., Kooistra, M. R., Bras, A., Kauw, J., Kerkhoven, R. M., Morrison, A., … Medema, R. H. (2005). FoxM1 is required for execution of the mitotic programme and chromosome stability. *Nature Cell Biology*, *7*(2), 126–136.
LaRocque, J. R., Jaklevic, B., Tin, T. S., & Sekelsky, J. (2007). Drosophila ATR in double-strand break repair. *Genetics*, *175*(3), 1023–1033.
Lee, H., Ohno, K., Voskoboynik, Y., Ragusano, L., Martinez, A., & Dimova, D. K. (2010). Drosophila RB proteins repress differentiation-specific genes via two different mechanisms. *Molecular and Cellular Biology*, *30*(10), 2563–77.
Levine, A. J., & Oren, M. (2009). The first 30 years of p53: growing ever more complex. *Nature Reviews. Cancer*, *9*(10), 749–58.
Lewis, P. W., Beall, E. L., Fleischer, T. C., Georlette, D., Link, A. J., & Botchan, M. R. (2004). Identification of a Drosophila Myb-E2F2/RBF transcriptional repressor complex. *Genes & Development*, *18*(23), 2929–40.
Lewis, P. W., Sahoo, D., Geng, C., Bell, M., Lipsick, J. S., & Botchan, M. R. (2012). Drosophila lin-52 acts in opposition to repressive components of the Myb-MuvB/dREAM complex. *Molecular and Cellular Biology*, *32*(16), 3218–27.

Li, L., & Bhatia, R. (2011). Stem cell quiescence. *Clinical Cancer Research*, *17*(15), 4936–4941.
Lin, W., Lin, F., & Nevins, J. R. (2001). Selective induction of E2F1 in response to DNA damage , mediated by Selective induction of E2F1 in response to DNA damage , mediated by ATM-dependent phosphorylation, *53*, 1833–1844.
Lindqvist, A., Rodríguez-Bravo, V., & Medema, R. H. (2009). The decision to enter mitosis: feedback and redundancy in the mitotic entry network. *Journal of Cell Biology*, *185*(2), 193–202.
Litovchick, L., Sadasivam, S., Florens, L., Zhu, X., Swanson, S. K., Velmurugan, S., … DeCaprio, J. a. (2007). Evolutionarily Conserved Multisubunit RBL2/p130 and E2F4 Protein Complex Represses Human Cell Cycle-Dependent Genes in Quiescence. *Molecular Cell*, *26*(3), 539–551.
Lu, J., Ruhf, M.-L., Perrimon, N., & Leder, P. (2007). A genome-wide RNA interference screen identifies putative chromatin regulators essential for E2F repression. *Proceedings of the National Academy of Sciences of the United States of America*, *104*, 9381–9386.
Lu, P. Y. T., Lévesque, N., & Kobor, M. S. (2009). NuA4 and SWR1-C: two chromatin-modifying complexes with overlapping functions and components. *Biochemistry and Cell Biology = Biochimie et Biologie Cellulaire*, *87*(5), 799–815.
MacLachlan, T.K. Somasundaram, K., Sgagias, M., Shifman, Y., Muschel, R. J., Cowan, K. H., & B, E.-D. W. S. (2000). BRCA1 effects on the cell cycle and the DNA damage response are linked to altered gene expression. *Journal of Biological Chemistry*, *275*(4), 2777–2785.
Marti, a, Wirbelauer, C., Scheffner, M., & Krek, W. (1999). Interaction between ubiquitin-protein ligase SCFSKP2 and E2F-1 underlies the regulation of E2F-1 degradation. *Nature Cell Biology*, *1*(1), 14–19.
Mazumder, S., DuPree, E. L., & Almasan, a. (2004). A dual role of cyclin E in cell proliferation and apoptosis may provide a target for cancer therapy. *Current Cancer Drug Targets*, *4*(1), 65–75.
McKnight, J. N., Boerma, J. W., Breeden, L. L., & Tsukiyama, T. (2015). Global Promoter Targeting of a Conserved Lysine Deacetylase for Transcriptional Shutoff during Quiescence Entry. *Molecular Cell*, *59*(5), 732–743.
Meyer, C. a, Jacobs, H. W., Datar, S. a, Du, W., Edgar, B. a, & Lehner, C. F. (2000). Drosophila Cdk4 is required for normal growth and is dispensable for cell cycle progression. *The EMBO Journal*, *19*(17), 4533–4542.
Milan, M., Campuzano, S., & Garcia-Bellido, A. (1996). Cell cycling and patterned cell proliferation in the Drosophila wing during metamorphosis. *Developmental Biology*, *93*(October), 11687–11692.
Mirth, C. K., Tang, H. Y., Makohon-Moore, S. C., Salhadar, S., Gokhale, R. H., Warner, R. D., … Shingleton, A. W. (2014). Juvenile hormone regulates body size and perturbs insulin signaling in Drosophila. *Proceedings of the National Academy of Sciences of the United States of America*, *111*(19), 7018–23.
Momand, J., Zambetti, G. P., Olson, D. C., George, D., & Levine, A. J. (1992). The mdm-2 oncogene product forms a complex with the p53 protein and inhibits p53-mediated transactivation. *Cell*, *69*(7), 1237–1245.
Narasimha, A. M., Kaulich, M., Shapiro, G. S., Choi, Y. J., Sicinski, P., & Dowdy, S. F. (2014). Cyclin D activates the Rb tumor suppressor by mono- phosphorylation. *eLife*, *3*(e02872), 1–21.
Narita, M., & Lowe, S. W. (2005). Senescence comes of age. *Nat. Med.*, *11*(9), 920–922.

Narita, M., Nunez, S., Heard, E., Narita, M., Lin, A. W., Hearn, S. A., … Lowe, S. W. (2003). Rb-mediated heterochromatin formation and silencing of E2F target genes during cellular senescence. *Cell*, *113*(6), 703–716.

Neufeld, T. P., de la Cruz, a F., Johnston, L. a, & Edgar, B. a. (1998). Coordination of growth and cell division in the Drosophila wing. *Cell*, *93*(7), 1183–93. Retrieved from

Ni, J.-Q., Zhou, R., Czech, B., Liu, L.-P., Holderbaum, L., Yang-Zhou, D., … Perrimon, N. (2011). A genome-scale shRNA resource for transgenic RNAi in Drosophila. *Nature Methods*, *8*(5), 405–7.

Nijhout, H. F., Riddiford, L. M., Mirth, C., Shingleton, A. W., Suzuki, Y., & Callier, V. (2014). The developmental control of size in insects. *Wiley Interdisciplinary Reviews: Developmental Biology*, *3*(1), 113–134.

O'Keefe, D. D., Thomas, S. R., Bolin, K., Griggs, E., Edgar, B. a, & Buttitta, L. a. (2012). Combinatorial control of temporal gene expression in the Drosophila wing by enhancers and core promoters. *BMC Genomics*, *13*(1), 498.

Oikonomou, C., & Cross, F. R. (2010). Frequency control of cell cycle oscillators. *Current Opinion in Genetics & Development*, *20*(6), 605–12.

Ollmann, M., Young, L. M., Como, C. J. Di, Karim, F., Belvin, M., Robertson, S., … Buckbinder, I. (2000). Drosophila p53 Is a Structural and Functional Homolog of the Tumor Suppressor p53, *101*, 91–101.

Oren, M. (2003). Decision making by p53: life, death and cancer. *Cell Death Differ*, *10*(4), 431–442.

Orlando, D. A., Lin, C. Y., Bernard, A., Wang, J. Y., Socolar, J. E. S., Iversen, E. S., … Haase, S. B. (2008). Global control of cell-cycle transcription by coupled CDK and network oscillators. *Nature*, *453*(7197), 944–7.

Ou, Q., & King-Jones, K. (2013). *What Goes Up Must Come Down. Transcription Factors Have Their Say in Making Ecdysone Pulses*. *Current Topics in Developmental Biology* (1st ed., Vol. 103). Elsevier Inc.

Park, H. J., Costa, R. H., Lau, L. F., Tyner, A. L., & Raychaudhuri, P. (2008). Anaphase-promoting complex/cyclosome-CDH1-mediated proteolysis of the forkhead box M1 transcription factor is critical for regulated entry into S phase. *Molecular and Cellular Biology*, *28*(17), 5162–5171.

Pietenpol, J. ., & Stewart, Z. . (2002). Cell cycle checkpoint signaling: Cell cycle arrest versus apoptosis. *Toxicology*, *181–182*, 475–481.

Polager, S., & Ginsberg, D. (2009). p53 and E2f: partners in life and death. *Nature Reviews. Cancer*, *9*(10), 738–748.

Polager, S., Kalma, Y., Berkovich, E., & Ginsberg, D. (2002). E2Fs up-regulate expression of genes involved in DNA replication , DNA repair and mitosis. *Oncogene*, *21*(October 2001), 437–46.

Polo, S., & Jackson, S. (2011). Dynamics of DNA damage response proteins at DNA breaks: a focus on protein modifications. *Genes & Development*, *25*(5), 409–33.

Qi, D., Jin, H., Lilja, T., & Mannervik, M. (2006). Drosophila Reptin and other TIP60 complex components promote generation of silent chromatin. *Genetics*, *174*(1), 241–51.

Reis, T., & Edgar, B. A. (2004). Negative Regulation of dE2F1 by Cyclin-Dependent Kinases Controls Cell Cycle Timing, *117*, 253–264.

Resources, C.-D. L. (n.d.). Cell Cycle Analysis. Retrieved January 8, 2016, from http://www.pitt.edu/~super4/lecture/lec19281/004.htm

Riley, T., Sontag, E., Chen, P., & Levine, A. (2008). Transcriptional control of human p53-regulated genes. *Nature Reviews. Molecular Cell Biology*, *9*(5), 402–412.
Roovers, K., & Assoian, R. K. (2000). Integrating the MAP kinase signal into the G1 phase cell cycle machinery. *Bioessays*, *22*(9), 818–826.
Rossi, M., Duan, S., Jeong, Y. T., Horn, M., Saraf, A., Florens, L., … Pagano, M. (2013). Regulation of the CRL4Cdt2 ubiquitin ligase and Cell-Cycle exit by the SCFFbxo11 ubiquitin ligase. *Molecular Cell*, *49*(6), 1159–1166.
Sadasivam, S., & DeCaprio, J. a. (2013). The DREAM complex: master coordinator of cell cycle-dependent gene expression. *Nature Reviews. Cancer*, *13*(8), 585–95.
Sapountzi, V., Logan, I. R., & Robson, C. N. (2006). Cellular functions of TIP60. *The International Journal of Biochemistry & Cell Biology*, *38*(9), 1496–509.
Schraml, E., & Grillari, J. (2012). From cellular senescence to age-associated diseases: the miRNA connection. *Longevity & Healthspan*, *1*(1), 10.
Schubiger, M., & Palka, J. (1987). Changing spatial patterns of DNA replication in the developing wing of Drosophila. *Developmental Biology*, *123*(1), 145–153.
Schubiger, M., & Truman, J. W. (2000). The RXR ortholog USP suppresses early metamorphic processes in Drosophila in the absence of ecdysteroids. *Development (Cambridge, England)*, *127*, 1151–1159.
Sherr, C. J., & McCormick, F. (2002). The RB and p53 pathways in cancer. *Cancer Cell*, *2*(2), 103–112.
Sherr, C. J., & Roberts, J. M. (1999). CDK inhibitors: positive and negative regulators of G1-phase progression. *Genes & Development*, *13*(12), 1501–1512.
Shibutani, S. T., de la Cruz, A. F. A., Tran, V., Turbyfill III, W. J., Reis, T., Edgar, B. A., & Duronio, R. J. (2008). Intrinsic Negative Cell Cycle Regulation Provided by PIP Box- and Cul4 Cdt2-Mediated Destruction of E2f1 during S Phase. *Dev Cell*, *15*, 890–900.
Song, Y. (2005). Drosophila melanogaster: a model for the study of DNA damage checkpoint response. *Molecules and Cells*, *19*(2), 167–179.
Stevens, B., Alvarez, C. M., Bohman, R., & O'Connor, J. D. (1980). An ecdysteroid-induced alteration in the cell cycle of cultured Drosophila cells. *Cell*, *22*(3), 675–682.
Stevens, C., & La Thangue, N. B. (2004). The emerging role of E2F-1 in the DNA damage response and checkpoint control. *DNA Repair*, *3*(8–9), 1071–1079.
Stevens, C., Smith, L., & La Thangue, N. B. (2003). Chk2 activates E2F-1 in response to DNA damage. *Nature Cell Biology*, *5*(5), 401–409.
Sun, Y., Jiang, X., Chen, S., Fernandes, N., & Price, B. D. (2005). A role for the Tip60 histone acetyltransferase in the acetylation and activation of ATM. *Proceedings of the National Academy of Sciences of the United States of America*, *102*(37), 13182–13187.
Sun, Y., Jiang, X., & Price, B. D. (2010). Tip60: Connecting chromatin to DNA damage signaling. *Cell Cycle*, *9*(5), 930–936.
Sun, Y., Jiang, X., Xu, Y., Ayrapetov, M. K., Moreau, L. A., Whetstine, J. R., & Price, B. D. (2009). Histone H3 methylation links DNA damage detection to activation of the tumour suppressor Tip60. *Nature Cell Biology*, *11*(11), 1376–82.
Sun, Y., Xu, Y., Roy, K., & Price, B. D. (2007). DNA damage-induced acetylation of lysine 3016 of ATM activates ATM kinase activity. *Molecular and Cellular Biology*, *27*(24), 8502–9.
Tang, H. L., Tang, H. M., Mak, K. H., Hu, S., Wang, S. S., Wong, K. M., … Fung, M. C. (2012). Cell survival, DNA damage, and oncogenic transformation after a transient and reversible

apoptotic response. *Mol Biol Cell*, *23*(12), 2240–2252.
Tang, Y., Luo, J., Zhang, W., & Gu, W. (2006). Tip60-Dependent Acetylation of p53 Modulates the Decision between Cell-Cycle Arrest and Apoptosis. *Molecular Cell*, *24*(6), 827–839.
Taubert, S., Gorrini, C., Frank, S. R., Parisi, T., Fuchs, M., Chan, H.-M., … Amati, B. (2004). E2F-dependent histone acetylation and recruitment of the Tip60 acetyltransferase complex to chromatin in late G1. *Molecular and Cellular Biology*, *24*(10), 4546–4556.
Thomas, H. E., Stunnenberg, H. G., & Stewart, a F. (1993). Heterodimerization of the Drosophila ecdysone receptor with retinoid X receptor and ultraspiracle. *Nature*, *362*(6419), 471–475.
Tomlinson, A., & Ready, D. F. (1987). Neuronal differentiation in the Drosophila ommatidium. *Developmental Biology*, *120*(2), 366–376. JOUR.
van Attikum, H., & Gasser, S. M. (2009). Crosstalk between histone modifications during the DNA damage response. *Trends in Cell Biology*, *19*(5), 207–17.
van den Heuvel, S., & Dyson, N. J. (2008). Conserved functions of the pRB and E2F families. *Nature Reviews. Molecular Cell Biology*, *9*, 713–724.
Vidal, A., & Koff, A. (2000). Cell-cycle inhibitors: Three families united by a common cause. *Gene*, *247*(1–2), 1–15.
Vitale, I., Galluzzi, L., Castedo, M., & Kroemer, G. (2011). Mitotic catastrophe: a mechanism for avoiding genomic instability. *Nat Rev Mol Cell Biol*, *12*(6), 385–392.
Wahl, G. M., & Carr, a M. (2001). The evolution of diverse biological responses to DNA damage: insights from yeast and p53. *Nature Cell Biology*, *3*(12), E277-86.
Welcker, M., Singer, J., Loeb, K. R., Grim, J., Bloecher, A., Gurien-West, M., … Roberts, J. M. (2003). Multisite phosphorylation by Cdk2 and GSK3 controls cyclin E degradation. *Molecular Cell*, *12*, 381–392.
Wen, H., Andrejka, L., Ashton, J., Karess, R., & Lipsick, J. S. (2008). Epigenetic regulation of gene expression by Drosophila Myb and E2F2-RBF via the Myb-MuvB/dREAM complex. *Genes & Development*, *22*(5), 601–14.
Zhang, R., Poustovoitov, M. V., Ye, X., Santos, H. A., Chen, W., Daganzo, S. M., … Adams, P. D. (2005). Formation of macroH2A-containing senescence-associated heterochromatin foci and senescence driven by ASF1a and HIRA. *Developmental Cell*, *8*(1), 19–30.
Zielke, N., Querings, S., Grosskortenhaus, R., Reis, T., & Sprenger, F. (2006). Molecular dissection of the APC/C inhibitor Rca1 shows a novel F-box-dependent function. *EMBO Reports*, *7*(12), 1266–72.
Zielke, N., Querings, S., Rottig, C., Lehner, C., & Sprenger, F. (2008). The anaphase-promoting complex / cyclosome (APC / C) is required for rereplication control in endoreplication cycles. *Genes & Development*, *22*, 1690–1703.

CHAPTER II

The Tip60/NuA4 complex is required for proper cell cycle progression and the transition to a post-mitotic state in *Drosophila melanogaster*

Portions of this chapter have been published as:

Flegel, K., Grushko, O., Bolin, K., Griggs, E. & Buttitta, L. Roles for the histone modifying and exchange complex NuA4 in cell cycle progression in Drosophila melanogaster. *Genetics* **203,** 1265–1281 (2016).

Author Contributions: O. Grushko performed the experiments in Fig. 2.5a panels K-M.

K. Bolin and E. Griggs assisted with clone counts in Fig. 2.3 panel B.

Abstract

Robust and synchronous repression of E2F-dependent gene expression is critical to the proper oscillation of cell cycle gene expression in proliferating cells, as well as the proper timing of cell cycle exit when cells transition to a post-mitotic state. Previously NuA4 was suggested to act as a barrier to proliferation in *Drosophila* by repressing E2F-dependent gene expression. Here we show that NuA4 activity is required for the proper timing of a developmentally controlled cell cycle exit and the proper repression of cell cycle genes during the transition to the post-mitotic state *in vivo*. However, the delay of cell cycle exit caused by compromising NuA4 is not due to additional proliferation or effects on E2F activity. Instead NuA4 inhibition results in slowed cell cycle progression through late S and G2 phases due to aberrant activation of an intrinsic p53-

independent DNA damage response. A reduction in NuA4 function ultimately produces a paradoxical cell cycle gene expression program, where certain cell cycle genes become de-repressed in cells that are delayed during the G2 phase of the final cell cycle. Bypassing the G2 delay when NuA4 is inhibited leads to abnormal mitoses, genetic instability and results in severe tissue defects. NuA4 physically and genetically interacts with components of the E2F complex termed DREAM/MMB, and modulates a DREAM/MMB-dependent ectopic neuron phenotype in the posterior wing margin. However, this effect is also likely due to the cell cycle delay, as simply reducing Cdk1 is sufficient to generate a similar phenotype. Our work reveals that the major requirement for NuA4 in the cell cycle *in vivo* is to suppress an endogenous DNA damage response, which is required to coordinate proper S and G2 cell cycle progression with differentiation and cell cycle gene expression.

Introduction

A conserved eukaryotic transcriptional oscillator controls cell cycle gene expression in proliferating cells and underlies the well-studied Cyclin/Cdk cell cycle protein oscillator (ORLANDO *et al.* 2008; OIKONOMOU AND CROSS 2010). In metazoans, this oscillator depends upon transcriptional activation of several hundred cell cycle genes, initiated by E2F transcription factor complexes and followed by E2F inhibition (or degradation) (SHIBUTANI *et al.* 2008; ZIELKE *et al.* 2011; SADASIVAM AND DECAPRIO 2013). This generates an oscillation of chromatin opening and closing at cell cycle genes that is thought to properly coordinate G1/S and G2/M gene expression as well as the transition to a non-cycling state (LITOVCHICK *et al.* 2007; LITOVCHICK *et al.* 2011; FORRISTAL *et al.* 2014). Disruption of this coordination can affect cell cycle progression by causing inappropriate gene expression (REIS AND EDGAR 2004; WEN *et al.*

2008; FORRISTAL *et al.* 2014). While the oscillation of E2F activity is required for robust cell cycle gene expression (DIMOVA *et al.* 2003; KORENJAK *et al.* 2012), E2F complexes are not absolutely essential for cell cycle progression or timely cell cycle exit in *Drosophila* (FROLOV *et al.* 2001; FROLOV *et al.* 2003; FROLOV *et al.* 2005). In the absence of E2F activity there must be E2F-independent factors or mechanisms that allow sufficient cell cycle gene regulation for cell cycle progression and timely cell cycle exit.

Cells entering non-proliferative or quiescent states are thought to repress the transcriptional oscillator by association of the tumor suppressor Retinoblastoma (RB) or RB family members with E2F. This association recruits a repressive complex termed the DREAM/MMB complex (*Drosophila*, Rbf, E2F and Myb/Multi-vulva class B) that is thought to promote the closing of chromatin and stable repression of cell cycle genes (KORENJAK *et al.* 2004; LEWIS *et al.* 2004; LITOVCHICK *et al.* 2007; SADASIVAM AND DECAPRIO 2013). Though DREAM/MMB has no apparent histone exchange component itself, recent findings suggest that its role in transcriptional repression is linked with histone H2A variant (H2Av) localization to target gene bodies (LATORRE *et al.* 2015). Perturbations in the DREAM/MMB complex have been reported to shift cells from quiescence towards proliferation in mammalian tissue culture and chondrocytes, but additional *in vivo* DREAM/MMB functions during terminal differentiation remain largely unknown (LITOVCHICK *et al.* 2007; LITOVCHICK *et al.* 2011; FORRISTAL *et al.* 2014). Furthermore, *Drosophila* tissues can still proliferate and exit the cell cycle normally in the complete absence of DREAM/MMB binding to chromatin, underscoring the importance of additional chromatin modulating factors in cell cycle progression and exit (KORENJAK *et al.* 2012).

The transition from proliferation to a post-mitotic state in *Drosophila*

Pulses of the hormone ecdysone control the developmental stages of *Drosophila*, with terminal differentiation of most adult tissues occurring during metamorphosis at the pupal stage (ASHBURNER 1989). Since ecdysone pulses control the onset of metamorphosis, subsequent developmental events are relatively naturally synchronized *in vivo*. This includes the final cell cycles in the *Drosophila* eyes and wings. All cell types in the eye become post-mitotic by 24 hours after pupa formation (APF) (CAGAN AND READY 1989). In the wing, there is a temporary G2 arrest early in metamorphosis, such that most cells complete their final cell cycle between 12 and 24 hours APF (SCHUBIGER AND PALKA 1987; MILAN *et al.* 1996; O'KEEFE *et al.* 2012). The synchronized cell cycle exit in the pupal fly wings and eyes provides a convenient *in vivo* context to identify genes that influence the proper timing of cell cycle exit.

The NuA4 complex

We took advantage of the synchronized cell cycle exit in the pupal fly eyes and wings to perform an RNAi-based screen for genes involved in the proper timing of cell cycle exit. This screen identified multiple components of the Tip60/NuA4 complex as important regulators of proper cell cycle exit, which we subsequently also found to be important for proper cell cycle progression in proliferating tissues.

Tip60/NuA4 is a multi-subunit complex conserved from yeast to humans, best characterized to open chromatin to promote gene expression (DOYON *et al.* 2004; LU *et al.* 2009). Tip60/NuA4 has histone acetyltransferase (HAT), DNA helicase, histone reading and histone exchange activities and plays an essential, conserved role in histone exchange for the

H2Ax variant (H2Av in *Drosophila*) that becomes phosphorylated upon DNA damage (KUSCH *et al.* 2004). NuA4 has been reported to engage many transcription factors, including Myc, p53 and E2F (MCMAHON *et al.* 2000; FRANK *et al.* 2003; LEGUBE *et al.* 2004; TAUBERT *et al.* 2004) to turn on target gene expression in proliferating cells. However, the NuA4 complex also acts as an essential repressor of gene expression in certain contexts, such as embryonic stem cells (FAZZIO *et al.* 2008; CHEN *et al.* 2013), and can promote closed chromatin formation in flies (QI *et al.* 2006). Furthermore, NuA4 components paradoxically act as both tumor suppressors and oncogenes, leaving their positive vs. negative roles in cell cycle control unresolved (SAPOUNTZI *et al.* 2006; JUDES *et al.* 2015).

Several studies suggest roles for NuA4 and H2Av in regulation of E2F target genes and genetic interactions with DREAM/MMB components (CEOL AND HORVITZ 2004; LU *et al.* 2007; DEBRUHL *et al.* 2013; LATORRE *et al.* 2015). Mammalian studies implicate Tip60/NuA4 as a transcriptional activator of E2F target genes, whereas a subset of NuA4 components in *Drosophila* cell culture were shown to repress E2F transcriptional targets (LU *et al.* 2007). Here we reveal contradictory roles for NuA4 in cell cycle progression and cell cycle gene expression during development. We find the loss of NuA4 function: (1) compromises proliferation (2) leads to accumulation of the DNA damage hallmark phosphoH2Av (3) causes aberrant expression of a transcriptional program associated with a DNA damage response and (4) disrupts the proper timing of cell cycle exit in pupal eyes and wings by delaying the final mitosis. We further show that NuA4's role in delaying cell cycle exit is independent of E2F/DP function as well as the DNA damage response pathway component p53 and that NuA4 acts to promote genetic stability in proliferating tissues.

Results

Compromising NuA4 delays cell cycle exit

To identify genes involved in the proper timing of cell cycle exit in *Drosophila* eyes and wings, we screened approximately 2,000 RNAi lines from the TRiP collection (NI *et al.* 2011) for ectopic cell cycle activity in pupal eyes or wings at timepoints when these tissues are normally fully post-mitotic (BUTTITTA *et al.* 2007). Our initial screen was performed in the eye and assayed a *PCNA-white* reporter transgene previously described as a readout for cell cycle activity (BANDURA *et al.* 2013). This screen used the *Glass Multimer Repeats* (*GMR)* promoter to drive Gal4/UAS induced RNAi expression in the eye during the transition to a post-mitotic state. From 36 hits in the initial eye screen, we verified 12 RNAi lines that led to ectopic mitoses in both the eye and wing at timepoints later than 24h after puparium formation (APF), a developmental timepoint when these tissues should be fully post-mitotic. Four of these RNAi hits fell within the same complex, the NuA4 complex. We therefore systematically tested the core subunits of NuA4 with additional RNAi lines and mutant alleles. We found that multiple, independent RNAi lines to six NuA4 subunits expressed in the posterior wing from larval stages (using *engrailed*-Gal4/UAS, *en*-Gal4) resulted in ectopic mitoses (as detected by phospho-Ser10-histone H3, PH3) at timepoints after the normal transition to a post-mitotic state (Fig. 2.1, Fig. 2.1a., Table 2.1). The effect of $Tip60^{RNAi}$ could be phenocopied by over-expression of a histone acetyltransferase (HAT)-inactive form of the catalytic subunit Tip60, ($Tip60^{E481Q}$ also termed $Tip60^{DN}$) previously shown to act as a dominant negative and reduce H4 acetylation (Fig. 2.1a. A,B) (LORBECK *et al.* 2011). By contrast, overexpression of a wild-type *Tip60* transgene ($Tip60^{WT}$) had no effect on the cell cycle, or wing and eye development in any of our assays.

Through a timecourse analysis (Fig. 2.1 J-N), we confirmed that cells with inhibited NuA4 were not permanently arrested in an aberrant mitosis. Inhibition of NuA4 delayed cell cycle exit for 4-6h in both eyes and wings, after which all cells became post-mitotic at 32h APF with a normal 2C DNA content as measured by flow cytometry (Fig. 2.1 N). The effects of NuA4 inhibition on cell cycle exit were compartment autonomous, as the anterior wing became post-mitotic normally (Fig. 2.1). We further verified the effects were cell autonomous by generating GFP-labeled clones of cells expressing $Tip60^{DN}$ in the wing. Cells within the clone delayed cell cycle exit, while non-expressing cells neighboring the clones became post-mitotic normally (Fig. 2.2a.1D). All 6 subunits with similar phenotypes are core NuA4 subunits, required for full function of the complex (DOYON AND COTE 2004) (Fig. 2.1 O). Thus, NuA4 HAT activity is required for the proper timing of developmentally controlled cell cycle exit.

We next examined whether the delay of cell cycle exit associated with NuA4 inhibition was an indirect effect due to earlier developmental defects. Using temporal restriction of Gal4/UAS transgene activation via *engrailed*-Gal4 combined with a temperature sensitive Gal80 (hereafter termed en^{TS}), we limited expression of $Tip60^{DN}$ to the final cell cycle in the pupal wing. Inhibition of Tip60 HAT function during only the final cell cycle also recapitulated the cell cycle exit delay observed with RNAi to NuA4 subunits (Fig. 2.1a. C,E). Similar to the wing, inhibition of NuA4 HAT activity during the final cell cycle in the eye (using *GMR-Gal4*) also delayed the timing of cell cycle exit for several hours (Fig. 2.1a. F-H). To test whether the effects of $Tip60^{DN}$ on cell cycle exit reflect a general requirement for H4 acetylation, we inhibited another major H4 HAT, *Drosophila* CBP (PARKER *et al.* 2008). Inhibition of CBP in the wing reduced overall levels of histone H4 acetylation, but did not delay cell cycle exit (Fig. 2.1a. I),

suggesting that NuA4 performs a specific function required for the proper timing of cell cycle exit.

Compromising NuA4 does not alter the timing of terminal differentiation

Since NuA4 has histone H4 acetyltransferase activity, it could be responsible for promoting gene expression globally. To determine if NuA4 inhibition simply slows developmental progression, we examined whether the 4-6h delay of cell cycle exit was also associated with a delay in the acquisition of characteristics associated with terminal differentiation. In the pupal wing, the formation of actin-rich hairs is a physical marker for terminal differentiation (MITCHELL *et al.* 1983). At 25°C wing cells initiate hair formation at 32h APF (MITCHELL *et al.* 1983; FANG AND ADLER 2010). Inhibition of Tip60 or other NuA4 components using en^{TS} did not alter wing hair initiation or growth (33h APF shown, Fig. 2.2a. A-C), when compared to the anterior non-expressing compartment despite a 4-6hr delay of cell cycle exit. We also examined whether Tip60/NuA4 inhibition altered the timing of differentiation in the eye (Fig. 2.2a. D-F). Terminal differentiation of many cell types in the late 3rd larval instar (L3) eye disc is spatially synchronized, following the morphogenetic furrow (MF) that sweeps from posterior to anterior across the tissue. Posterior to the MF, a new row of differentiated cells is established every 2h which can be marked by the expression of post-mitotic neural and cone cell markers (TREISMAN 2013). A 4-6h delay in development would be expected to cause a 2-3 row posterior shift in the onset of differentiation marker expression. We used heat-shock induced recombination to create non-overlapping GFP-labeled clones expressing $Tip60^{DN}$ that span the MF and the first few rows of differentiated cells. We did not observe any delay in photoreceptor or cone cell marker expression upon NuA4 inhibition, compared to the surrounding non-clonal cells (Fig. 2.2a. D-F).

This suggests that compromising NuA4 does not delay cell cycle exit simply by slowing overall developmental progression.

Inhibition of NuA4 leads to ectopic cell cycle gene expression

NuA4 is a chromatin remodeler and components of NuA4 have been shown to repress E2F-dependent gene expression in cultured *Drosophila* S2 cells (LU *et al.* 2007). We therefore examined whether NuA4 inhibition altered cell cycle gene repression in pupal wings and eyes during cell cycle exit. We examined three reporters previously shown to be accurate readouts of endogenous cell cycle gene regulation including transcriptional repression at cell cycle exit; a PCNA-GFP transgene which reports E2F-dependent G1-S gene expression, and the Mad2-GFP and Stg-GFP protein traps that report endogenous levels of G2-M phase cell cycle regulators (THACKER *et al.* 2003; WEN *et al.* 2008; INABA *et al.* 2011). Inhibition of Tip60/NuA4 in the posterior pupal wing by RNAi or $Tip60^{DN}$ expression led to ectopic PCNA-GFP and Mad2-GFP expression at stages that are normally post-mitotic (Fig. 2.2 A-G). NuA4 inhibition during the final cell cycle in the eye also caused a subset of interommatidial cells to exhibit ectopic PCNA-GFP expression at post-mitotic pupal stages (Fig. 2.2 H). In clones with Tip60/NuA4 inhibited in the late L3 eye, we observed higher and prolonged Stg-GFP expression in the G1 arrested cells of the morphogenetic furrow as well as the post-mitotic region posterior to the MF (Fig. 2.1 I-K). To confirm that the reporters reflect the endogenous transcripts we performed quantitative RT-PCR for cell cycle genes in pupal wings at 26h APF expressing $Tip60^{WT}$ and $Tip60^{DN}$. Transcripts for *pcna* and *mad2* were increased in wings expressing $Tip60^{DN}$, consistent with our reporter assays (Fig. 2.1 L). However, we did not observe an increase in *stg* expression in pupal wings. Unlike the eye, endogenous *stg* levels normally peak at the time of cell cycle exit in the

pupal wing (BUTTITTA *et al.* 2007), and NuA4 inhibition may not increase *stg* beyond the already high levels of expression at this stage. The ectopic expression of the known E2F1 targets *pcna* and *mad2* (NEUFELD *et al.* 1998; THACKER *et al.* 2003; WEN *et al.* 2008) raised the possibility that NuA4 impacts E2F1 expression or activity. Surprisingly, expression of Tip60^{DN} reduced both *e2f1* transcript and E2F1 protein levels in the pupa wing (Fig. 2.1 L,M). Altogether our data suggests that NuA4 function is needed for the proper shut-off of specific cell cycle genes at cell cycle exit, but seemingly paradoxically is also required for the proper maintenance of E2F1 levels.

Compromising NuA4 disrupts cell cycle progression

Our finding that NuA4 is required both for the proper shutoff of cell cycle gene expression as well as the proper maintenance of E2F1 levels, raised the question of whether the delayed cell cycle exit observed upon NuA4 inhibition is due to extra cell cycles or the result of a slowed final cell cycle. To address this we performed a clonal lineage tracing experiment in the wing blade to quantify the number of cell divisions occurring before the delayed cell cycle exit. Non-overlapping, GFP-labeled clones expressing *Tip60*^{DN} were induced at 0h APF during the final cell cycle in the wing. Pupa wings were examined at 36h APF, (12h after normal exit and 4-6h after the delayed cell cycle exit) and the number of cells per clone was counted blind for at least 100 clones per genotype (Fig. 2.3 A). We also co-expressed the apoptosis inhibitor P35, to avoid the effects of apoptosis on counting cell divisions. Control clones expressing GFP+P35 averaged 2.22±0.08 cells/clone, while clones expressing *Tip60*^{DN} +P35 averaged 2.11±0.05 cells/clone (Fig. 2.3 A). We confirmed that this method is sensitive enough to detect even one extra cell cycle in the wing, as clones overexpressing CycD/Cdk4 +P35 caused one extra cell cycle in

approximately 50% of clones resulting in 2.59±0.11 cells/clone. Thus, inhibition of Tip60 HAT activity delays cell cycle exit by slowing the final cell cycle, rather than by causing additional cycles.

We next examined whether loss of Tip60/NuA4 function prolongs the cell cycle during asynchronous proliferation in the larval wing. We again created non-overlapping GFP-marked clones and compared cells/clone 30 and 46h after induction for $Tip60^{DN}$+P35 vs. $Tip60^{WT}$+P35 (Fig. 2.3 B). Clonal cell counts for $Tip60^{WT}$ averaged 4.26 ± 0.12 cells/clone at 30h corresponding to a normal cell doubling time (DT) of approximately 15h in the wandering L3 larval wing, consistent with other reports (REIS AND EDGAR 2004). By contrast, clones expressing $Tip60^{DN}$ averaged 3.39 ± 0.11 cells/clone (Fig. 2.3 B), corresponding to an average DT almost 4h longer than the control (18.93h). This indicates that Tip60 HAT activity is required for proper cell cycle progression.

Slowed cell cycle progression was also observed upon inhibition of other NuA4 subunits. RNAi to E(Pc) or Nipped-A in the presence of P35 to block apoptosis resulted in smaller clones in the larval wing (Fig. 2.3 C) despite little change to cell size (Fig. 2.3a. A). *domino* (*dom*) null clones generated by mitotic recombination in a $dom^{+/-}$ background were also significantly smaller than their $dom^{+/+}$ sibling twinspot clones, even when one copy of the H99 locus was removed to minimize cell death (Fig. 2.3 D, Fig. 2.3a. B-D). Using flow cytometry to measure DNA content, we determined that *dom-/-* cells accumulated in the late S, G2 phase of the cell cycle (with >2C DNA content) in proliferating L3 wings (Fig. 2.3.D'). We observed similar results with RNAis to the other NuA4 subunits and $Tip60^{DN}$, when expressed in the GFP-positive posterior compartment of the late L3 wing (Fig. 2.3 E). To ensure the changes in cell cycle phasing were not due to non-autonomous effects on the non-Gal4 expressing anterior

compartment of the wing, we also performed posterior-to-posterior wing comparisons of flow cytometry profiles to control genotypes including w^{1118}, $white^{RNAi}$ and $Tip60^{WT}$ (Fig. 2.3 F). We consistently observed an increase in cells with >2C DNA content when NuA4 is inhibited, although we also found a mild compensatory non-autonomous effect on the cell cycle distribution in the anterior wing as well (Fig. 2.3 G). This, together with the slowed cell cycle progression suggests that full Tip60/NuA4 function is required for proper S/G2/M progression *in vivo*; which is consistent with data from other organisms (CLARKE *et al.* 1999; CHOY *et al.* 2001; LI *et al.* 2004; HU *et al.* 2009; TAPIAS *et al.* 2014).

A previous study of the NuA4 subunits *Brd8, YL-1* and *dom* in cultured *Drosophila* S2 cells described an effect of NuA4 on E2F activity, but did not describe a cell cycle phenotype (LU *et al.* 2007). To examine whether NuA4 impacts cell cycle progression in S2 cells, we used an S2 cell line containing the FUCCI (fluorescent ubiquitination-based cell cycle indicator) reporters and performed RNAi to NuA4 subunits for 5 days, followed by E2F reporter assays, flow cytometry and cell counts (ZIELKE *et al.* 2014). NuA4 inhibition in S2 cells had the previously described effects on an E2F-Luciferase reporter (not shown), but also reduced EdU incorporation during S-phase and lengthened the S-G2 transition (Fig. 2.3a. E-G). This resulted in altered cell cycle phasing, mainly by increasing the proportion of cells in late S and early G2 (Fig. 2.3 H). Altogether our data suggests inhibition of NuA4 leads to cell cycle alterations that slow S/G2 cell cycle progression.

NuA4 inhibition deregulates cell cycle gene expression during active proliferation

A well-known readout of E2F transcriptional activity, PCNA-GFP is increased upon NuA4 inhibition in pupal wings (Fig. 2.1). We observed similar increases in PCNA-GFP and Stg-GFP

reporters when NuA4 was inhibited in the proliferating late L3 wing, despite the slowed proliferation and prolonged S and G2 phases under these conditions (Fig. 2.4 A-H). Similar to the pupa wing, expression of $Tip60^{DN}$ in the posterior L3 wing caused a reduction in E2F1 protein levels (Fig. 2.4 I, J). Since E2F1 is degraded in S-phase but accumulates during G1 and late G2 phases (SHIBUTANI *et al.* 2008; ZIELKE *et al.* 2014) cells in a prolonged late S/early G2 would be expected to have lower E2F1 protein levels. However we were puzzled by the apparently contradictory results of a delay in S/G2 progression when NuA4 is inhibited, accompanied by higher levels of Stg. This suggested that compromising NuA4 may activate a checkpoint to offset the increased levels of Stg. Stg acts on the CycB/Cdk1 complex to promote its activity by removing the inhibitory Cdk1 phosphorylation catalyzed by the Wee and Myt kinases. However we observed no obvious changes in total Cdk1 or Wee levels by immunofluorescence. Instead, we found that expression of $Tip60^{DN}$ reduced CycB protein within 24h of expression in the larval wing, while $Tip60^{WT}$ expression had no effect on CycB (Fig. 2.4 K-M). RNAi to other NuA4 subunits also recapitulated this effect, leading to a ~15-20% reduction in CycB protein levels which we also confirmed by qRT-PCR (Fig. 2.4a. A,B). By contrast we did not observe consistent changes in another G2-M regulator CycA (Fig. 2.4a. C-E). We suggest that the reduced levels of CycB may contribute to the slowed S/G2 progression when NuA4 is compromised. Importantly, a previous study of Tip60 localization on the genome by DamID resolved one of the top 5 strongest peaks of Tip60 binding on the entire chromosome to the 5' region of the *cycB* gene, suggesting the regulation of *cycB* by Tip60 could be direct (Fig. 2.4 N) (FILION *et al.* 2010).

The transcriptional response to Tip60 inhibition

To get a more global view of the gene expression changes caused by inhibition of Tip60, we performed RNAseq on dissected late L3 wings containing large, overlapping clones expressing *Tip60*^{WT} or *Tip60*^{DN}. We used *flipout*^{TS} to restrict expression of *Tip60*^{WT} or *Tip60*^{DN} to 48 or 78h prior to RNA extraction. *Tip60*^{WT} expression caused minimal changes in the transcriptome compared to control wings expressing Gal4/GFP alone (112-133 transcripts out of the entire genome), while *Tip60*^{DN} expression for 48 and 78h led to a largely overlapping program of 860 genes that significantly change expression >1.4-fold compared to *Tip60*^{WT}.

Tip60 has been primarily reported to play roles as a transcriptional co-activator with several factors including nuclear hormone receptors, Myc and E2F (BRADY *et al.* 1999; FRANK *et al.* 2003; TAUBERT *et al.* 2004; HATTORI *et al.* 2008). We were therefore surprised to find that the majority of genes with changed expression (72.5%) are upregulated when Tip60 HAT function is inhibited (Fig. 2.4 O). We observed few significant changes to core G2 cell cycle regulators, with the exception of a mild (1.4-fold) upregulation of *tribbles*, a mitotic inhibitor involved in String degradation (MATA *et al.* 2000; SEHER AND LEPTIN 2000). Also consistent with our qRT-PCR results, *cycB* (and *cycB3)* were mildly reduced (32-41%) at both timepoints. We examined the genes altered by *Tip60*^{DN} for overlap with Tip60 binding based upon published Tip60 ChIP-Seq and Tip60-DamID data (FILION *et al.* 2010; XU *et al.* 2014). We found that 35% of upregulated and 33% of downregulated genes are also bound by Tip60 in *Drosophila* cells, suggesting our dataset includes targets of both direct and indirect Tip60 regulation.

We next compared the genes upregulated by *Tip60*^{DN} to transcriptional targets identified for the DREAM/MMB complex (GEORLETTE *et al.* 2007). At the same time, due to the known

roles for Tip60/NuA4 in DNA damage signaling (reviewed by SQUATRITO *et al.* 2006; SUN *et al.* 2010; GURSOY-YUZUGULLU *et al.* 2015) we also included a comparison to a transcriptional response (both p53-dependent and p53-independent) to DNA damage by ionizing radiation (IR) in wings (VAN BERGEIJK *et al.* 2012) (Fig. 2.4 P). We found a significant overlap with the genes upregulated by $Tip60^{DN}$ expression and the DNA damage response (DDR) profile (104 out of 634 genes, Table 2.1a), and a lesser overlap with the DREAM/MMB regulated genes (68 out of 634 genes). The DNA damage response also partially overlaps with DREAM/MMB regulated genes, as several DNA repair and synthesis enzymes are regulated by DREAM, but only 24% (14 out of 48) of the shared DREAM/DNA damage response genes are also significantly upregulated by $Tip60^{DN}$ (Table 2.2a). Thus, the inhibition of Tip60/NuA4 results in the upregulation of over 100 genes associated with a DNA damage response. These include the known direct targets of p53 such as *reaper*, *eiger* and *Xrp1 (BRODSKY et al. 2000; AKDEMIR et al. 2007; LINK et al. 2013)*, as well as several p53-independent targets such as *Gadd45*, *Snap25* and *Traf4 (VAN BERGEIJK et al. 2012).* A subset of targets, their regulation by p53 and DREAM, as well as whether they overlap with known locations of Tip60 binding is shown in Fig. 2.4 Q. Importantly orthologs of several of these targets (e.g. *Snap25, Gadd45, Traf4, trbl, eiger*) are also upregulated in mammalian cells in response to replication stress induced by aphidicolin treatment (MAZOUZI *et al.*).

Tip60/NuA4 may act to quench DNA damage signaling in *Drosophila* via its modification and replacement of phosphorylated H2A variant (pH2Av), with an unmodified variant (KUSCH *et al.* 2004). Consistent with this role, Tip60/NuA4 inhibition in the proliferating wing (using en^{TS}) led to a significant increase in formation of pH2Av foci in wings, even in the absence of any exogenous DNA damaging agents (Fig. 2.4 R-T, Fig. 2.4a. F). This suggests that

Tip60/NuA4 is required to limit or prevent a DNA damage response due to some form of endogenous stress. Tip60/NuA4 has been shown to catalyze the acetylation and exchange of pH2Av for H2Av, which is required for resolution of the DNA damage response (KUSCH *et al.* 2004). Consistent with this, we found that S2 cells treated with RNAi to Tip60 or E(Pc) failed to resolve pH2Av foci 16h after a pulse of the DNA damaging agent Camptothecin (CPT, Fig. 4a. G-I). Altogether our data suggests unresolved pH2Av and/or possibly unrepaired DNA damage, contributes to the transcriptional response and cell cycle defects we observe when NuA4 is inhibited.

NuA4 inhibition does not delay cell cycle exit through the p53-dependent DNA damage response

To test whether DNA damage signaling could cause a delay in cell cycle exit, we overexpressed p53 in the posterior wing with en^{TS} starting at L3 and examined pupal wings for mitoses at 26-30h APF. We found that overexpression of p53 is sufficient to induce a compartment autonomous delay of cell cycle exit, with similar timing to NuA4 inhibition (Fig. 2.5 A). We next tested whether p53 is necessary for the cell cycle exit delay caused by loss of NuA4. We co-expressed a DNA-binding defective p53 ($p53^{DN}$) with $Tip60^{DN}$ in the posterior wing (BRODSKY *et al.* 2000), or expressed $Tip60^{DN}$ or $Brd8^{RNAi}$ in a p53 null background ($p53^{5A\text{-}1\text{-}4/11\text{-}1B\text{-}1}$) (RONG *et al.* 2002; XIE AND GOLIC 2004). We verified that these p53 alleles were functional and blocked p53-induced apoptosis in the wing (Fig 2.5a. A-C) and loss of p53 does not affect the normal timing of cell cycle exit (Fig. 2.5a. D,E). However, despite the inhibition or loss of p53, the cell cycle exit delay caused by NuA4 inhibition persisted (Fig. 2.5 B-D). Instead we observed a severe enhancement of wing defects, a reduction in wing size and animal survival, suggesting

Tip60/NuA4 and p53 may be required in parallel for proliferation and survival in the absence of exogenous DNA damage (Fig. 2.5 E, Fig. 2.5a. F). Loss of p53 did not prevent the reduction in CycB levels in the wing caused by NuA4 inhibition (Fig. 2.5a. G-I), and inhibition of p53 by $p53^{DN}$ could not rescue the poor growth or survival of *dom-/-* cells in the proliferating larval wing (Fig. 2.5a. J). Knockdown of the DDR kinases upstream of p53, *ATM (mei-41), chk1 (grp)*, and *ATR (tefu),* also did not suppress the delayed cell cycle exit caused by $Tip60^{DN}$ expression. However similar to our results with p53, the posterior wing size was significantly reduced by coexpression of *ATM* and ATR^{RNAi} with $Tip60^{DN}$, creating notches in the wing blade (arrows, Fig. 2.5a. K-M). Because *ATM* and *ATR* can act redundantly in *Drosophila (Bi et al. 2005; Joyce et al. 2011; Kondo and Perrimon 2011)*, we also attempted to simultaneously knockdown *ATM* with expression of $Tip60^{DN}$ in an *ATR* mutant background. However we were unable to recover any animals of the correct genotype, suggesting possible synthetic lethality. Finally blocking apoptosis, the most downstream component of DDR signaling, also could not suppress the delayed cell cycle exit caused by NuA4 inhibition (Fig. 2.5a. N,O). This suggests that the effects of NuA4 on cell cycle progression act independent of, but in parallel to components of the canonical DDR pathway.

NuA4 inhibition does not delay cell cycle exit through altered E2F/DP function

Tip60 and NuA4 subunits genetically interact with components of a repressive RB/E2F/DP DREAM-like complex in *C. elegans*, while in *Drosophila* cell culture specific NuA4 components have been shown to repress E2F target gene expression (Ceol and Horvitz 2004; Lu *et al.* 2007). Our results *in vivo* suggest the effects of the NuA4 complex on cell cycle genes are complicated, as we see context-dependent evidence of both activating (e.g. *cycB, e2f1*) and

repressive (e.g. *pcna, stg, mad2, tribbles*) effects on cell cycle gene expression. Tip60 physically interacts with the E2F dimerization partner DP as assayed by co-immunoprecipitation (Fig. 2.6a. A), consistent with the reported interactions between Dom and E2F in both *Drosophila* and mammalian cells (LU *et al.* 2007). We therefore examined whether E2F/DP function could be required for the delayed cell cycle exit caused by Tip60/NuA4 inhibition.

We used a severe *Dp* hypomorphic mutation over a null allele ($Dp^{a1/a4}$) to obtain pupal wings with normal developmental timing (ROYZMAN *et al.* 1997). The strong loss of *Dp* function neither suppressed nor enhanced the delay of cell cycle exit caused by $Tip60^{DN}$ in the pupa wing (Fig. 2.6 A-C). The loss of *Dp* also did not suppress the S/G2 cell cycle phase elongation in the larval wing, or alter the reduction in CycB caused by Tip60 inhibition (Fig. 2.6a. B-D). By contrast, the loss of *Dp* enhanced a phenotype of ectopic Elav-positive neurons at the posterior wing margin (PWM) caused by $Tip60^{DN}$ or inhibition of another NuA4 subunit Brd8 (Fig. 2.6D-H, Fig.. 2.6a. E). This is a phenotype previously associated with the loss of repressive components of the DREAM/MMB complex, that is thought to be independent of the cell cycle functions of DREAM/MMB (ROVANI *et al.* 2012). The loss of *Dp* also enhanced the severity of defects caused by $Tip60^{DN}$ in adult wings (Fig. 2.6a. F), and the loss of another DREAM/MMB component, *Rbf* is synthetically cell-lethal with $Brd8^{RNAi}$ in pupal eyes and wings (Fig. 2.6a. G). Altogether our data suggests that while NuA4 and DREAM/MMB genetically interact in some contexts, the impacts of NuA4 loss on cell cycle progression and cell cycle exit appear to be independent of E2F/DP function.

Delaying the final G2-M transition impacts the proper repression of cell cycle genes at cell cycle exit

NuA4 inhibition elongates late S/early G2 phases (Fig. 2.3) and reduces the expression of a major G2-M regulator CycB in proliferating tissues (Fig. 2.4). We therefore directly examined whether slowing the final cell cycle in the pupal wing could recapitulate the cell cycle exit defects we observe when NuA4 is inhibited. We used the en^{TS} system to over-express transgenes that prolonged the final G2-M transition, through the expression of the Cdk1 inhibitory Wee kinase, or an RNAi to Cdk1. Prolonging the final G2-M transition effectively delayed cell cycle exit with timing similar to that observed when we compromise NuA4 function (up to 30h APF, Fig. 2.7 A,B), while prolonging the final cell cycle with an RNAi to *e2f1* or the expression of a dominantly active Rbf, Rbf^{280} did not perturb the overall timing of cell cycle exit (Fig. 2.7a. A-D). Other genetic conditions known to prolong the cell cycle such as generating $Minute^{+/-}$ clones or slowly dividing *Dp* null mutant clones also did not detectibly delay cell cycle exit in the pupal wing (MARTIN AND MORATA 2006; SUN AND BUTTITTA 2015). This demonstrates that simply slowing cell cycles during the proliferative phases or slowing the final G1-S does not delay cell cycle exit in the wing.

What is the biological consequence then, of slowing the final G2-M? We find that delaying the final mitosis results in a failure to properly shut down the expression of cell cycle genes in the pupal wing. Elongation of the final G2 phase via expression of Wee kinase or Cdk1 inhibition led to ectopic PCNA-GFP and Mad2-GFP expression for several hours after they are normally repressed (PCNA-GFP shown, Fig. 2.7 C-D). This was particularly striking in the case of $cdk1^{RNAi}$, where expression starting from the proliferating larval stages led to an early arrest of cell proliferation in the posterior wing, but with ubiquitously high PCNA-GFP expression that

persisted for several hours beyond the transition to a post-mitotic state (Fig. 2.7 D). Why does an elongation of the final G2-M transition lead to aberrant expression of cell cycle genes? The lengthening of either gap phase in the proliferating larval wing has previously been shown to result in an accumulation of E2F1 activity that drives a compensatory shortening of the next gap phase to maintain the overall cell doubling time. This is termed "cell cycle compensation" and is dependent upon the negative regulation of E2F1 activity by Cyclin/Cdks (REIS AND EDGAR 2004). This creates a situation where G2 elongation, for example by Wee expression, results in increased E2F transcriptional activity that can be detected by the PCNA-GFP reporter (Fig. 2.7a. E). Our results suggest that cell cycle compensation also occurs during the final cell cycle in the pupal wing, but due to the absence of a subsequent cell cycle this results in aberrant E2F activity and cell cycle gene expression in tissues entering into a post-mitotic state. Based on these results, we suggest that the aberrant cell cycle gene expression and de-repression of E2F targets observed when NuA4 is inhibited may be due in part to the S/G2 delay and subsequent activation of the cell cycle compensation mechanism.

We also observed additional consequences of altering the final G2 phase on cell fate at the posterior wing margin. A developmentally regulated G2 arrest is essential for proper cell fate decisions in sensory organ precursors (SOPs), as disruption of proper Cdk1 activity in SOPs can alter cell division timing and asymmetric cell fate decisions (FICHELSON AND GHO 2004; AYENI *et al.* 2016). Consistent with this, we observed that inhibition of Cdk1 activity was sufficient to fully recapitulate the ectopic neuron phenotype in the posterior wing margin, similar to that observed when components of the DREAM or the Myb component of MMB are inhibited (ROVANI *et al.* 2012) (Fig. 2.6 F, Fig. 2.7 E,F). We suggest this phenotype is similar to that shown previously in SOPs of the notum where a delay in G2 caused a cell fate change in the pI

SOP to the pIIb fate, which produces a neuron and sheath cell (FICHELSON AND GHO 2004). Importantly, activation of the DDR pathway via p53 expression in the posterior wing is also sufficient to recapitulate this phenotype (Fig. 2.7 G), suggesting that multiple pathways impacting timely S/G2 progression converge on this phenotype. Altogether our results suggest that the Tip60/NuA4 complex is required for proper S/G2 progression, likely through its roles in modulating CycB levels and pH2Av removal. This impacts proper cell cycle exit, cell identity in the posterior wing and as described further below, is essential for genetic stability (Fig. 2.7 H).

Promoting G2 progression when NuA4 is inhibited leads to aberrant mitoses and genetic instability

A reduction in CycB occurs within 24h of $Tip60^{DN}$ expression in proliferating wings, even in *p53* null and in strong *Dp* hypomorphic backgrounds. To determine whether increasing CycB/Cdk1 activity could suppress the G2 elongation and proliferation defects caused by Tip60/NuA4 inhibition, we co-overexpressed String to increase the activity of the remaining CycB/Cdk1. In larval wings, co-expression of Stg with $Tip60^{DN}$ effectively suppressed the effect of $Tip60^{DN}$ on increased S and G2 populations (Fig. 2.8 A). However when we examined the pupal wing, we found that the delay in cell cycle exit persisted even in the presence of high levels of Stg and CycB (Fig. 2.8 B-D, H-J). Closer examination of the PH3 staining in wings co-expressing $Tip60^{DN}$ and Stg or CycB (not shown) revealed many mitotic defects, including defects in chromosome alignment, condensation, anaphase bridges and mis-segregated chromosomes, defects we do not observe in wings expressing $Tip60^{DN}$ alone (Fig. 2.8 E-F). Inhibition of Tip60/NuA4 function leads to defects in cell cycle progression that elongate the late S/early G2 phases of the cycle. This elongation may occur in part through a reduction in CycB expression

and activation of a DNA damage response, which effectively increases the chances for repair prior to mitosis. When cells with compromised NuA4 are forced into mitosis without delay by high CycB/Cdk1 activity, severe mitotic defects occur ultimately resulting in defects in the adult wing (Fig. 2.8 G, J). Thus NuA4 plays an essential role in S/G2 progression to promote genetic stability.

Discussion

Here we show that compromising the Tip60/NuA4 complex *in vivo* leads to a delay of cell cycle exit and ectopic cell cycle gene expression in terminally differentiating cells. NuA4 components physically and genetically interact with DREAM components and can impact specific targets of RB/E2F repression (Lu *et al.* 2007). But we find that other essential roles for NuA4 in promoting S and G2-phase progression leads to slower cycling and confounding indirect effects on E2F cell cycle targets *in vivo* when NuA4 is compromised. When NuA4 is inhibited, cells accumulate pH2Av and exhibit transcriptional changes associated with a DNA damage response. In addition, E2F1 and CycB levels are reduced when NuA4 is inhibited. This leads to an elongation of the cell cycle, coupled with de-repression of specific RB/E2F targets, resulting in a paradoxical cell cycle gene expression program where certain cell cycle genes become highly expressed in cells that are exiting the cell cycle. We suggest that NuA4 acts as an essential component to coordinate proper pH2Av removal with S/G2 phase completion prior to mitotic entry, in addition to its other roles in modulating chromatin for gene expression.

The Tip60/NuA4 complex and cell cycle gene expression

NuA4 components directly localize to the promoters of many cell cycle genes in several organisms, and most often Tip60/NuA4 is thought to promote cell cycle gene expression via HAT activity (LI *et al.* 2004; TAUBERT *et al.* 2004; TAPIAS *et al.* 2014). We show that the Tip60/NuA4 complex in *Drosophila* impacts cell cycle gene expression in complex ways. Tip60/NuA4 is required to prevent the expression of a cluster of DNA damage response and specific cell cycle genes, but is also required for the normal expression of *cycB* (Fig. 2.4, Fig. 2.4a.). Tip60/NuA4 binds to the *cycB* promoter and 5' intron, suggesting that *cycB* could be directly regulated by NuA4 (FILION *et al.* 2010). Interestingly, *cycB* is located in the genome as a divergently paired gene (DPG) (YANG AND YU 2009) with *stall*, which is upregulated 6.5-fold upon Tip60 inhibition. Tip60/NuA4 may therefore act to direct the proper transcription of certain DPGs with differential expression patterns. Consistent with this idea we noted that 18 of the 20 strongest Tip60 binding peaks in the genome (FILION *et al.* 2010), are associated with DPGs.

While specific components of NuA4 have been shown to repress certain E2F targets in cell culture, a repressive function for the Tip60 subunit on expression of many other genes was unexpected, as HAT activity is usually associated with increased gene expression. Some of the effects we observe on gene expression are indirect, likely due to an inability to remove pH2Av from chromatin and resolve DNA damage signaling (Fig. 2.4, Fig. 2.4a.). However, Tip60 HAT activity may also act on chromatin to directly repress target genes, as 35% of genes upregulated by $Tip60^{DN}$ in the *Drosophila* wing have Tip60 binding sites (FILION *et al.* 2010; XU *et al.* 2014). Tip60/NuA4 has been shown to catalyze histone exchange to incorporate the H2A variant H2AZ in yeast (AUGER *et al.* 2008; ALTAF *et al.* 2010), and the H2A variant in *Drosophila* H2Av, has been associated with gene repression (SWAMINATHAN *et al.* 2005; QI *et al.* 2006; HANAI *et al.*

2008). Recent work in *C. elegans* has revealed that target genes of RB/E2F repression, including cell cycle genes bound by the DREAM complex, exhibit deposition of the H2Av homolog H2A.Z, along the gene body (LATORRE *et al.* 2015). H2A.Z localization on the gene body is associated with repression as opposed to H2A variant localization at promoters, which is associated with transcriptional activation (BARSKI *et al.* 2007; HARDY *et al.* 2009), and loss of H2A.Z at the majority of DREAM bound genes in *C. elegans* de-represses their expression. Thus the function of NuA4 in H2Av incorporation could act to directly repress gene expression. While we did not observe large changes in expression of most *Drosophila* DREAM targets in our RNAseq data (Table 2.3a), compromising Tip60/NuA4 function may prevent proper H2Av deposition at the 17% of genes affected by $Tip60^{DN}$ that overlap with *Drosophila* DREAM regulated genes. Consistent with this idea, we found that 60% of the genes upregulated by Tip60 inhibition that are shared with DREAM targets exhibit significant H2Av localization on the gene body, including *pcna* and *mad2* (modencode.org, dataset #4953).

Elongation of G2 phase can lead to an upregulation of E2F activity and activation of the E2F transcriptional reporter PCNA-GFP (Fig. 2.7, Fig. 2.7a). This is due to cell cycle compensation, where E2F1 protein accumulates during the G2 delay resulting in an increased E2F transcriptional output (REIS AND EDGAR 2004). When NuA4 is inhibited we observe hallmarks of increased E2F1 activity and cell cycle delay, but without an accumulation of E2F1. Instead we observe a reduction in E2F1 protein and transcript levels (Fig. 2.2, Fig. 2.4). This suggests that either NuA4 inhibition acts on the cell cycle reporters in an E2F-independent manner, possibly by the H2Av mechanism described above, or that the reduced levels of E2F1 may somehow have increased activity when NuA4 is inhibited. E2F1 activity can be increased through reduced levels of the repressor Rbf or increased phosphorylation of Rbf by Cyclin/Cdks.

We examined whether there were higher levels of G1 and S Cyclins CycE and CycA when NuA4 was inhibited (Fig. 2.4a. , CycE data not shown) but did not observe any significant differences from controls. We also did not see significant changes in expression of other direct or indirect negative E2F1 regulators including *ago*, *dacapo e2f2*, *Rbf*, *Rbf2*, *cycD* or *cdk4* in our RNAseq data. Because we could not ultimately rule out the possibility of a change in Rbf phosphorylation or protein levels, we genetically eliminated *Rbf* in cells expressing $Brd8^{RNAi}$. We found that this combination was strongly synthetically cell-lethal, suggesting the two pathways may act independently but in parallel (Fig. 2.6a. G).

The Tip60/NuA4 complex and DNA damage signaling

Tip60/NuA4 plays multiple roles, both positive and negative, at several levels within the DNA damage response and repair pathway. Tip60 can acetylate the ATM kinase to promote its activation and phosphorylation of targets in response to DNA damage (SUN *et al.* 2005; SUN *et al.* 2007). Tip60 also acetylates p53 protein to modulate its activity (TANG *et al.* 2006), as well as acts with p53 at the chromatin to promote expression of target genes (LEGUBE *et al.* 2004). We find that inhibition of Tip60/NuA4 leads to high levels of pH2Av, a hallmark of high ATM/ATR kinase activity, as well as activation of several direct transcriptional targets of p53 (Fig. 2.4). This demonstrates that activating ATM and p53 target expression are not the key roles for Tip60/NuA4 *in vivo* in *Drosophila*. Instead, our results are consistent with an essential role for the Tip60/NuA4 complex in acetylating and exchanging phospho-H2Av for H2Av to resolve DNA damage signaling (KUSCH *et al.* 2004) (Fig. 2.4, Fig. 2.4a.). We show that Tip60/NuA4 inhibition or loss leads to an accumulation of pH2Av, possibly in response to endogenous DNA damage. We believe this is why loss of Tip60/NuA4 leads to ectopic activation of DNA damage

response genes encompassing both a p53-dependent and p53-independent response (Fig. 2.4), as well as enhances the loss of function phenotypes for multiple components of the DNA damage response pathway (Fig. 2.5). We suggest a delayed progression through S/G2 becomes essential when NuA4 is inhibited, to allow for pH2Av removal or DNA/chromatin repair. This is demonstrated by the severe mitotic defects and genetic instability that occur when NuA4 is compromised but the cell cycle delay is bypassed (Fig. 2.8).

NuA4 and cancer

Previous studies have paradoxically characterized NuA4 as both a tumor suppressor and an oncogene (GORRINI *et al.* 2007; JUDES *et al.* 2015). Maintenance of proper cell cycle gene expression may in part underlie some roles for NuA4 in cancer, while others may be due to its roles in DNA damage signaling (SQUATRITO *et al.* 2006). Our data suggests Tip60/NuA4 may behave as a tumor suppressor by ensuring genetic stability (Fig. 2.4, Fig. 2.8). However, we also observe cell cycle gene upregulation when NuA4 is compromised (Fig. 2.3). While the increased cell cycle gene expression we observe upon NuA4 inhibition was insufficient to cause extra or accelerated cell cycling in our experiments, additional hits (which may be caused by increased genetic instability) could cooperate with compromised NuA4 to further de-regulate E2F targets or bypass the slowing of the cell cycle due to the late S/G2 phase elongation. This is of concern for the development and use of Tip60 HAT and bromodomain inhibitors in cancer therapy (GAO *et al.* 2014; SANCHEZ *et al.* 2014) which could cause further genetic instability and impair NuA4-dependent cell cycle gene repression and cell cycle exit.

NuA4 inhibitors may be highly effective in some contexts however. Inhibition of Brd8 by RNAi in *Rbf* null cells strongly enhances their elimination in pupal eyes and wings, even more

strongly than a combination previously shown to completely bypass cell cycle exit (Fig. 2.6a. G) (BUTTITTA *et al.* 2010). This is reminiscent of other Rbf synthetic lethal genes such as TSC1 and 2 that lead to a lethal accumulation of DNA damage when *Rbf* is lost, which can effectively eliminate RB mutant cancer cells (LI *et al.* 2010; GORDON *et al.* 2013). This suggests NuA4 inhibitors could be highly effective for elimination of cancer cells that have lost or inactivated RB.

Materials and Methods

Fly stocks and genetics:
Inhibition of NuA4 in the posterior wing:
w/y, w, hs-FLP; en-GAL4, UAS-GFP; UAS-Tip60$^{WT\ or\ DN}$ or UAS-NuA4^{RNAi}/ tub-gal80^{TS}
w/y, w, hs-FLP; en-GAL4, UAS-GFP/+; UAS-P35/ UAS-Tip60^{DN} UAS-NuA4^{RNAi}
Inhibition of NuA4 during the final cell cycle in the eye:
w/y, w, hs-FLP; GMR-GAL4/+; UAS-Tip60$^{WT\ or\ DN}$ or UAS-NuA4^{RNAi}/ PCNA-GFP
Clonal lineage analysis:
w/ y, w, hs-FLP; UAS-P35/+; UAS-Tip60$^{WT\ or\ DN}$ or UAS-NuA4^{RNAi} /act>CD2>GAL4, UAS-GFP$_{NLS}$
Clones to assess terminal differentiation in the eye and qRT-PCR
w/ y, w, hs-FLP; tub>CD2>GAL4, UAS-GFP/+; tub-gal80^{TS}, UAS-dIAP/ UAS-Tip60^{DN} or UAS-NuA4^{RNAi}
Fluorescent reporters and inhibition of NuA4
w/ y, w, hs-FLP; en-GAL4, UAS-His2Av::RFP/+; mad2-GFP, mRFP-Nup107/ UAS-NuA4^{transgene}
y,w/ y,w, hs-FLP;+; PCNA-GFP, act>CD2>GAL4/ UAS-NuA4^{transgene}
y,w, hs-FLP;+;stg-GFP^{YD0246}, act>CD2>GAL4, UAS-His2Av::RFP/UAS-NuA4^{transgene}
RNAi and over-expression lines (also refer to Table 2.1)
y, w, hs-FLP;+; UAS-Tip60^{E431Q}B/Tm6B
y, w, hs-FLP; UAS-Tip60^{WT}/CyO-GFP; +
y, w, hs-FLP; UAS-CycD, UAS-cdk4/CyO-GFP;+
UAS-Wee (NEUFELD et al. 1998)
BDSC 28368 *UAS-Cdk1^{RNAi}*
UAS-Stg (on II) (NEUFELD *et al.* 1998)
BDSC 6583: *w^{1118};+; PGUS-p53.Ct3.1/TM6B, Tb^{1}*
BDSC 6584: *w^{1118}; PGUS-p53.2.1*
BDSC 27277: *y,v;+; UAS-grp^{RNAi}*
BDSC 31635: *y,v;+; UAS-atm^{RNAi}*
Mutant alleles:
dom^{LL05537} (TEA AND LUO 2011)
Dp^{a1} (ROYZMAN *et al.* 1997), *Dp^{a4}* (FROLOV *et al.* 2005)

p53$^{5A\text{-}1\text{-}4/11\text{-}1B\text{-}1}$ (RONG *et al.* 2002; XIE AND GOLIC 2004)
Brd8^{G19099} (BDSC#31838)

To reduce lethality, some crosses used temperature sensitive Gal80 (tub-Gal80^{TS}) (MCGUIRE *et al.* 2004) to suppress transgene expression until later in development. In these cases animals were raised at 18^{o}C, then shifted to 28^{o}C for Gal4 induction at the indicated times. For cell cycle gene reporter assays (PCNA-GFP, Mad-GFP, Stg-GFP), animals were raised at room temperature due to the lack of Gal80^{TS} in these stocks (23^{o}C). For inhibition of NuA4 in the pupal eye, GMR-GAL4 was used to over-express the transgenes starting in the posterior terminally differentiating, third larval instar eye and continuing until late development stages. For maximum GAL4 production with weak UAS-RNAi lines (e.g. *domino*^{RNAi}), animals were raised at 28^{o}C and staged at 0h APF.

Clone size and lineage counting:

Clone counts in pupal wings were performed as described (BUTTITTA *et al.* 2007). In brief, a 35mm dish containing pupae on a wetted tissue, was sealed with parafilm and submerged in a 37^{o}C water bath for two minutes. Pupae were then incubated at 25^{o}C until dissection. For *Tip60*^{DN} and *Tip60*^{WT} clone counts at L3, animals were reared in un-crowded conditions and heat-shocked in a 37^{o}C water bath for 7.5mins. Mitotic Flp/FRT clones for the *dom-/-* analysis were counted 48hrs after a 13min (37^{o}C) heatshock. Clone areas and cell numbers were counted blind.

Histology:

Pupae were staged from white pre-pupae (0h after pupa formation). Development at 28^{o}C occurs 1.15 times faster than at 25^{o}C, 1.25 times faster at 31^{o}C, and 2.2 times more slowly at 18^{o}C

(ASHBURNER 1989; BUTTITTA *et al.* 2007). All incubation times were adjusted accordingly and the hours APF presented as the 25^{o}C equivalent. Wings and eyes from animals equivalent to 26-32h APF or from wandering larvae at the third larval instar, were fixed with 4% paraformaldehyde/1X PBS for 30min. Tissues were washed twice in 1x PBS, 0.1% Triton X, 10min each and then used for immunostaining (BUTTITTA *et al.* 2007).

Immunohistochemistry:

Fixed tissues were blocked with 1x PBS, 0.1% Triton X-100, 1% BSA for 20min prior to primary antibody incubation either at room temperature (RT) for 4hrs or overnight at 4^{o}C with rotation. After removal of the primary antibody, tissues were washed with 1x PBS, 0.3% Triton X-100, 0.1% BSA, 2% NGS three times for 20min each. Tissues were incubated with secondary antibody conjugated to Alexa-Fluor 488, 568 or 633 1:4000 (Molecular Probes) for 4h at RT or overnight at 4^{o}C with nutation. Höechst 33258 was used to label nuclei, tissues were mounted in vectashield (Vector Labs). F-actin staining was performed in 1XPBS using 1:100 rhodamine-labelled phalloidin (Invitrogen R415) for 2-4 hours.

Antibodies and reagents:

Anti-phospho-Ser10 histone H3: 1:4000 rabbit (Millipore #06-570) or 1:1000 mouse (Cell Signaling #9706), Anti-GFP: 1:1000 chicken (Life Technologies A10262) or 1:1000 rabbit (Life Technologies A11122), Anti-Elav: 1:100 rat (DSHB 7E8A10), Anti-Cut: 1:100 mouse (DSHB 2B10). Anti- CycB 1:100 (DSHB, F2F5) Anti-CycA 1:100 (DSHB, A12), Anti-pH2Av 1:100 (DSHB, UNC93-5.2.1) Anti-DP rabbit (1:1,000, kindly provided by Dr. M. Frolov) mouse anti-FLAG (1:1,000, Sigma). Secondary antibodies to the appropriate animals were labeled with

Alexa fluor 488, 568 or 633 (Invitrogen) and used at 1:2,000. Co-immunoprecipitation was performed as described (SUN AND BUTTITTA 2015) using $3X10^6$ S2R+ cells transiently transfected with pMT-$Tip60^{FLAG}$. Mouse anti-FLAG-agarose (Sigma) was used to immunoprecipitate endogenous DP which was detected by western blot with Rabbit anti-DP.

Microscopy:

Images were obtained using a Leica DM1600 epi-fluorescence system with de-convolution (ImageQuant) or a Leica SP5 confocal. All images were cropped, rotated, and processed using Adobe Photoshop. All brightness/contrast adjustments were applied equally on the entire image.

Flow cytometry:

Flow cytometry on larval and pupal wings was performed on an Attune cytometer with dissociation and gating/detection parameters as described (FLEGEL *et al.* 2013).

Mounting and scoring of Adult wings:

Mounting and microscopy of adult wings was performed as described (O'KEEFE *et al.* 2012). For scoring phenotype severity, 7 classes of defects (notched margin, ectopic vein, ectopic bristles, L4 truncation, loss of crossveins, L5 truncation and smaller posterior compartment) were generated and wings were scored according to the same rubric for the total number of defects.

qRT-PCR and RNAseq:

Animals were reared in un-crowded conditions and heat-shocked in a 37°C water bath for 30min. to induce overlapping clones. Transgene expression was silenced by keeping animals at 18°C

until they reached the developmental stage appropriate for either RT-qPCR or RNA-seq analysis. For RT-qPCR, animals were shifted to 28°C at 0wpp and wings were dissected in 1x PBS from animals equivalent to 26h APF. RNA was isolated per the TRIzol manual, resuspended in water, and then treated with DNase I to remove contaminating DNA. Using 300ng of RNA per sample, cDNA was synthesized using oligo$(dT)_{20}$ and the Superscript III First-Strand Synthesis System (Invitrogen 18080051). qPCR using 0.5µL of cDNA per reaction was then performed using the 7500 Fast Real-Time PCR and StepOnePlus Real-Time PCR Systems (Applied Biosystems).

For RNA-seq, heat-shocked animals were shifted to 28°C either 48h or 78h prior to their dissection as wandering L3 larvae. Twenty wing discs were dounce homogenized in TRIzol with ten strokes of a tight pestle. Samples were vortexed at speed 10 for 1min, incubated for 5mins at room temperature then frozen in liquid nitrogen. Samples were kept at -80°C until they were pooled to make a total of 40 wing discs per replicate of each condition and genotype. The pooled RNA was phase separated with chloroform and RNA was precipitated in isopropanol at -30°C overnight prior to 20min 4°C centrifugation at 12,000x g. The RNA pellet was resuspended in 30µL of RNase-Free water.

Using PolyA selection, the University of Michigan's Sequencing Core generated directional barcoded libraries for each sample and confirmed the quality via the Bioanalyzer and qPCR. Sequencing was performed with the Illumina HiSeq 2000 platform and high read quality was confirmed using FastQC. Reads were aligned to the BDGP6.82 *D. melanogaster* genome using Rsubread (v1.21.5), with featureCounts resulting in >83% of the reads being successfully assigned to genes (LIAO *et al.* 2014). Counts per million (cpm) were determined with edgeR (v3.13.4) and transcripts with low expression were identified and removed using the data-based Jaccard similarity index determined with HTSFilter (v1.11.0). The cpm were TMM normalized

(calcNormFactors), voom transformed (LAW *et al.* 2014), fit to a linear model (lmFit), then differential gene expression calls were made with eBayes.

For significance of overlap with other datasets (Fig. 2.4), hypergeometric probabilities were calculated using the hypergeometric distribution. In our case: (1) the population size equals the total number of genes that align to the genome and pass our filters for the RNAseq (2) the number of successes in the population is the total number of genes that are represented in both our dataset and the published dataset under comparison, (3) the sample size is the total number of genes upregulated by $Tip60^{DN}$ and for which there is data in the published dataset under comparison, and (4) the number of successes in the sample equals the total number of genes that overlap in our $Tip60^{DN}$ upregulated dataset and are significantly upregulated in the published dataset under comparison.

S2R+ RNAi, EdU labeling and Camptothecin treatment and recovery:

S2R+ Fucci cells were cultured as previously described (ZIELKE *et al.* 2014). (Note that in Fig. 2.3 the graphs are color-coded according to the indicated cell cycle phase, not according to the FUCCI red/green readout.) RNAi was performed as described (ROGERS AND ROGERS 2008) with the following modifications; cells were incubated in 1mL of serum free medium with 10 µg/mL of dsRNA for 4-24h, followed by addition of 1mL of 10% serum medium for 4 days. dsRNA was synthesized using the T7 Megascript Kit (Ambion) and primer sequences are provided in Table 2.4a. For flow cytometry cells were stained with DyeCycleViolet (for samples run live in Fig.3) or FX Cycle Violet for fixed cells (Fig. 2.3a) and were run on the Attune flow cytometer (Life Technologies). EdU incorporation was performed on S2R+ cells (without FUCCI reporters) and detected using reagents from the Click-IT EdU 488 flow cytometry kit (Life Technologies).

For Camptothecin (CPT) treatment, S2R+ cells were treated with the indicated dsRNA for 3 days. On the 4th day 10 μM CPT was added for 6 hours, followed by washing and recovery in fresh media without CPT for 16h. Cells were subsequently fixed with 4% paraformaldehyde/PBS and stained for pH2Av.

Acknowledgements

We thank Dr. F. Elefant for sharing the Tip60^{DN} line and Dr. M. Frolov for sharing *Dp* alleles and antibodies. Additional stocks for this study were obtained from the Yale Flytrap collection the TRiP collection and the Bloomington Drosophila Stock Center (NIH P40OD018537). Additional antibodies were obtained from the Developmental Studies Hybridoma Bank (DSHB), created by the NICHD of the NIH and maintained at The University of Iowa. We thank Dr. B. Edgar in whose lab the initial pilot RNAi screen was performed. We also thank C. Sifuentes for help with RNAseq data analysis and an anonymous reviewer for encouraging us to examine the role of G2 phase in the PWM phenotype. This work was supported by the National Institutes of Health, grants R00GM086517 and R21AG047931, the Biological Sciences Scholars Program (BSSP) and startup funding from the University of Michigan to L. Buttitta. K. Flegel was supported by a Rackham Merit Fellowship from the University of Michigan and an NIH Genetics Training Grant

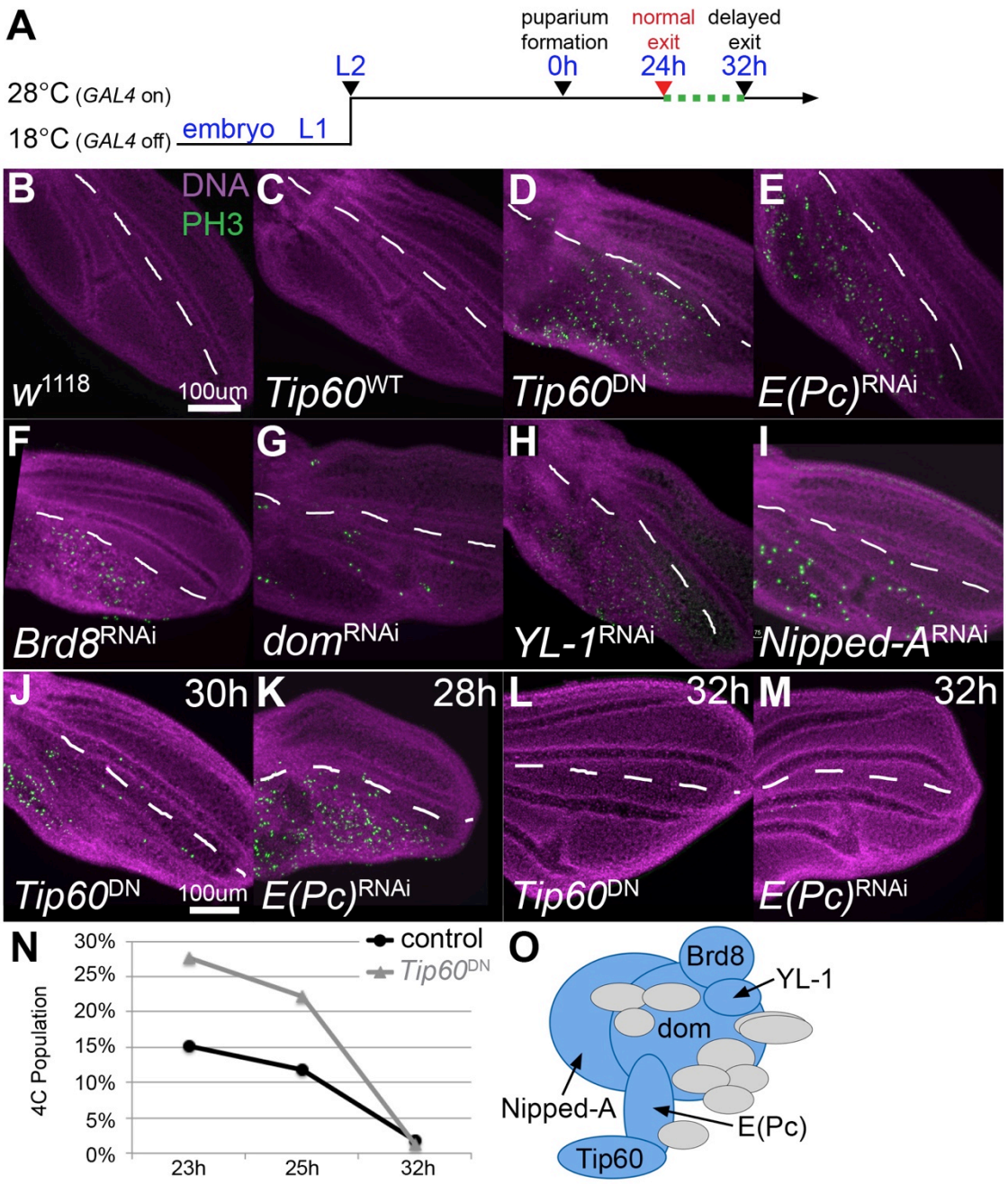

Fig. 2.1. NuA4 inhibition delays cell cycle exit

(A-I) Using *engrailed*-Gal4 modified with a temperature sensitive Gal80 (en^{TS}), a UAS-driven HAT-inactive form of Tip60 ($Tip60^{E431Q}$, "dominant negative" Tip60, $Tip60^{DN}$) or the indicated UAS-RNAis were expressed in the posterior wing from the second larval instar (L2). Pupa were collected at 0hr after puparium formation (APF) and aged to 27h APF or the indicated stages while being kept at the permissive temperature for Gal4-induced transgene expression. The dotted line indicates the wing anterior/posterior boundary. NuA4 inhibition increased the number of mitoses (indicated by phospho-Ser10 histone H3, PH3) in the posterior wing, at timepoints when the wing is normally post-mitotic. (J-N) Ectopic mitoses persist for <8h past the time of normal cell cycle exit. (N) Flow cytometry at the indicated timepoints (h APF) showed an

increased proportion of cells with a 4C DNA content (G2/M) in wings expressing *Tip60*^{DN}. (O) Schematic of the NuA4 complex. Multiple RNAi lines for the core subunits were tested (Table 2.1). Subunits required for proper cell cycle exit are shown in blue.

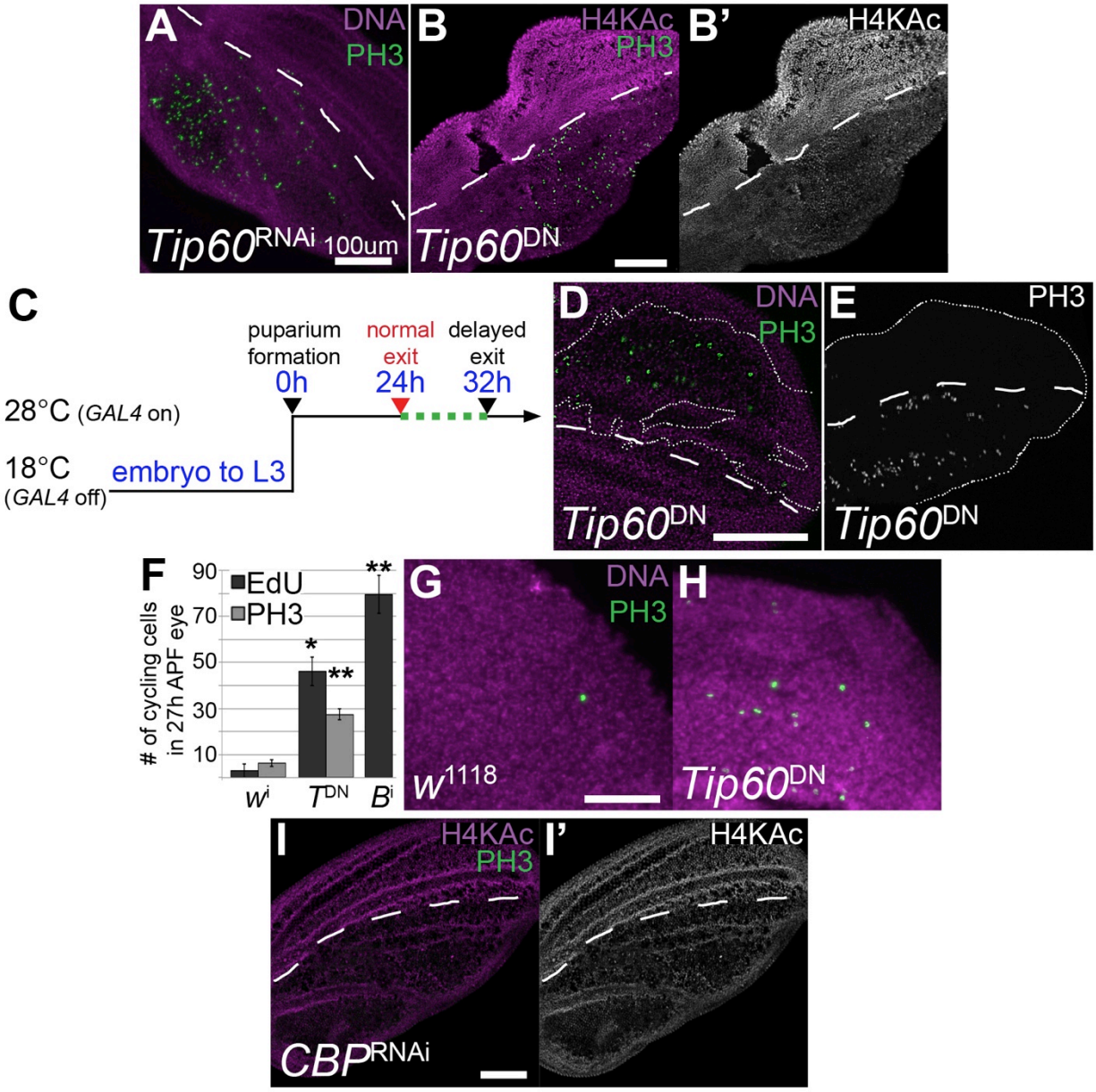

Fig. 2.1a. Compromising NuA4 delays the timing of the final cell cycle
(A-C, E, I) Using *en*^{TS}, *Tip60*^{DN} or the indicated RNAis were expressed in the posterior wing from the second larval instar. Pupa were collected at 0hr after puparium formation (APF) and aged to 27h APF at the permissive temperature for Gal4-induced transgene expression. The dashed line indicates the anterior/posterior boundary. (A) *Tip60*^{RNAi} in the posterior wing recapitulates the delayed cell cycle exit phenotype of *Tip60*^{DN} (compare to Fig. 2.1D, mitoses indicated by PH3). (B) *Tip60*^{DN} expression compromises endogenous H4 HAT activity as indicated by an antibody for H4K5/8/12/16 acetylation. (C,D) Using heat-shock induced flipase (*hs-flp*) with a *tub>stop>Gal4* transgene combined with Gal80^{TS}, (*flipout*^{TS}) we generated clones of cells expressing Gal4 beginning at 24 h after embryo hatching, but restricted the UAS-induced expression of *Tip60*^{DN} to stages after 0h APF using temperature shifts to limit cell death (the clonal border and wing anterior-posterior boundary are respectively indicated by the dotted and

dashed lines). In pupa staged to 26h APF, clonal *Tip60*^{DN} expression delays cell cycle exit (as indicated by PH3) in a manner similar to that observed with *en*^{TS}. (C,E) Using *en*^{TS} we restricted *Tip60*^{DN} expression in the posterior wing to the final cell cycle in the wing (from 0h APF). Inhibition of Tip60 during the final cell cycle delayed cell cycle exit. (F-H) Inhibition of Tip60/NuA4 during the final cell cycle in the eye was performed using GMR-GAL4/*UAS*. Inhibition of Tip60/NuA4 delayed cell cycle exit in the pupal eye, as indicated by persistent mitoses and S phases (indicated by EdU labeling) in interommatidial cells 3h after normal cell cycle exit. (I) RNAi of CBP does not delay cell cycle exit, despite reducing H4 acetylation. p-values were determined with an unpaired t-test, * p-value<0.05, ** p-value<0.01.

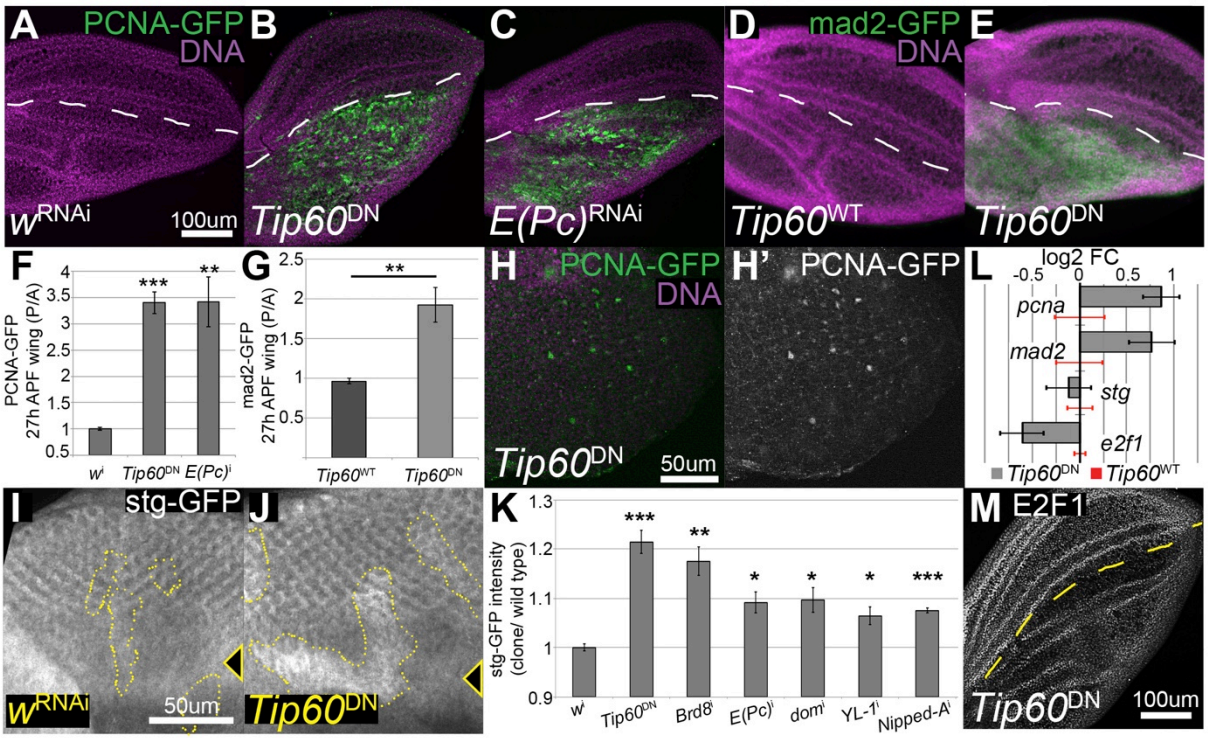

Fig. 2.2. NuA4 is essential for proper cell cycle gene repression at cell cycle exit
(A-G) Using *en*-Gal4, the indicated transgenes were expressed in the posterior wing. RNAi to *white* (w^{RNAi}) and Tip60^{WT} serve as negative controls that do not affect the cell cycle. Pupa were collected at 0h APF and aged to 27h APF. The dashed line indicates the wing anterior/posterior boundary. (B,C,F) NuA4 inhibition resulted in high levels of PCNA-GFP expression. (D,E,G) A G2-M reporter Mad2-GFP, also accumulated when Tip60 HAT activity was inhibited. (H) Tip60^{DN} was expressed during the final cell cycle in the eye using *GMR-GAL4/UAS*, resulting in PCNA-GFP expression in the interommatidial bristle precursors at 27h APF. (I-K) Using heat-shock induced *flipout-Gal4* we generated clones expressing $Tip60^{DN}$ in the larval eye in a background carrying a String-GFP protein trap insertion (Stg-GFP). Cells expressing $Tip60^{DN}$ posterior to the morphogenetic furrow (MF) increased Stg-GFP expression (MF indicated by arrowhead, posterior is at top.) (L) Using *flipout-Gal4* in combination with Gal80^{TS} (*flipout* ^{TS}) we generated large, overlapping clones of cells expressing Gal4 24h after embryo hatching, but restricted the UAS-induced expression of *Tip60*^{DN} or $Tip60^{WT}$ to pupal stages only (from 0h APF) using temperature shifts. In pupa expressing *Tip60*^{DN} staged to 26h APF, quantitative RT-PCR revealed aberrant *pcna* and *mad2* in the wing, compared to the $Tip60^{WT}$ expressing controls. By contrast, *e2f1* transcript is reduced by Tip60^{DN}. Levels of *stg* in the pupa wing are unchanged by Tip60^{DN}. (M) E2F1 protein levels are decreased in 27h APF pupal wings expressing $Tip60^{DN}$ in the posterior. p-values were determined by an unpaired t-test, * p-value<0.05, ** p-value<0.01, *** p-value<0.001

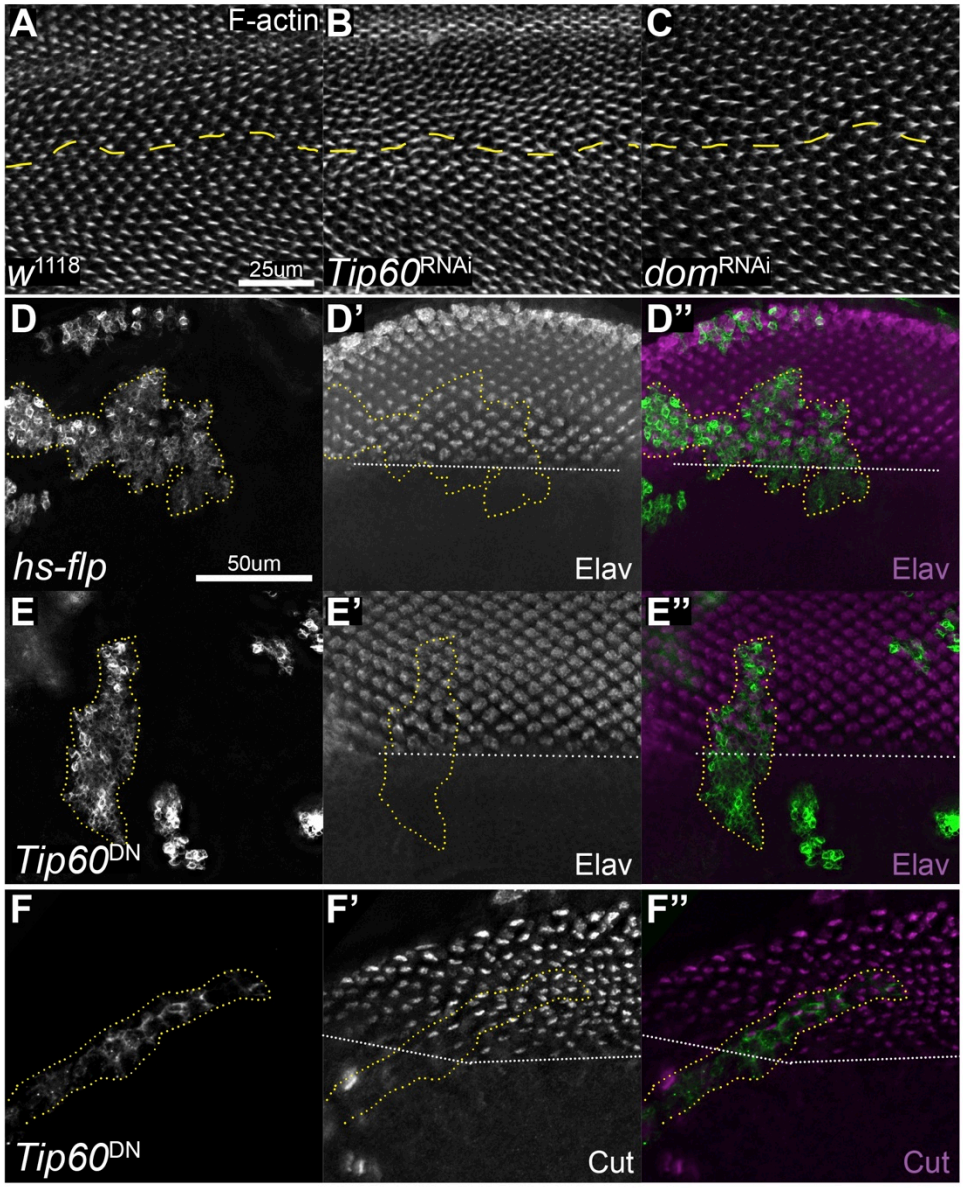

Fig. 2.2a. NuA4 inhibition does not delay terminal differentiation
(A-C) NuA4 was inhibited in the posterior wing using *en*^{TS} and the indicated UAS transgenes (the dashed line indicates the wing anterior-posterior boundary). Images are oriented with the posterior below the line. Developing pupal wing hairs were stained with rhodamine-phalloidin at 33h APF. NuA4 inhibition did not alter the timing or growth of wing hairs. (D-F) GFP-labeled clones were generated using *flipout*^{TS}. *Tip60*^{DN} expression in clones that crossed the boundary of photoreceptor differentiation in the late L3 larval eye, did not delay or prevent the differentiation of photoreceptors labeled with Elav (D,E) or cone cells labeled by Cut (F) compared to neighboring non-Gal4 expressing cells. For D-F images are oriented with posterior at top.

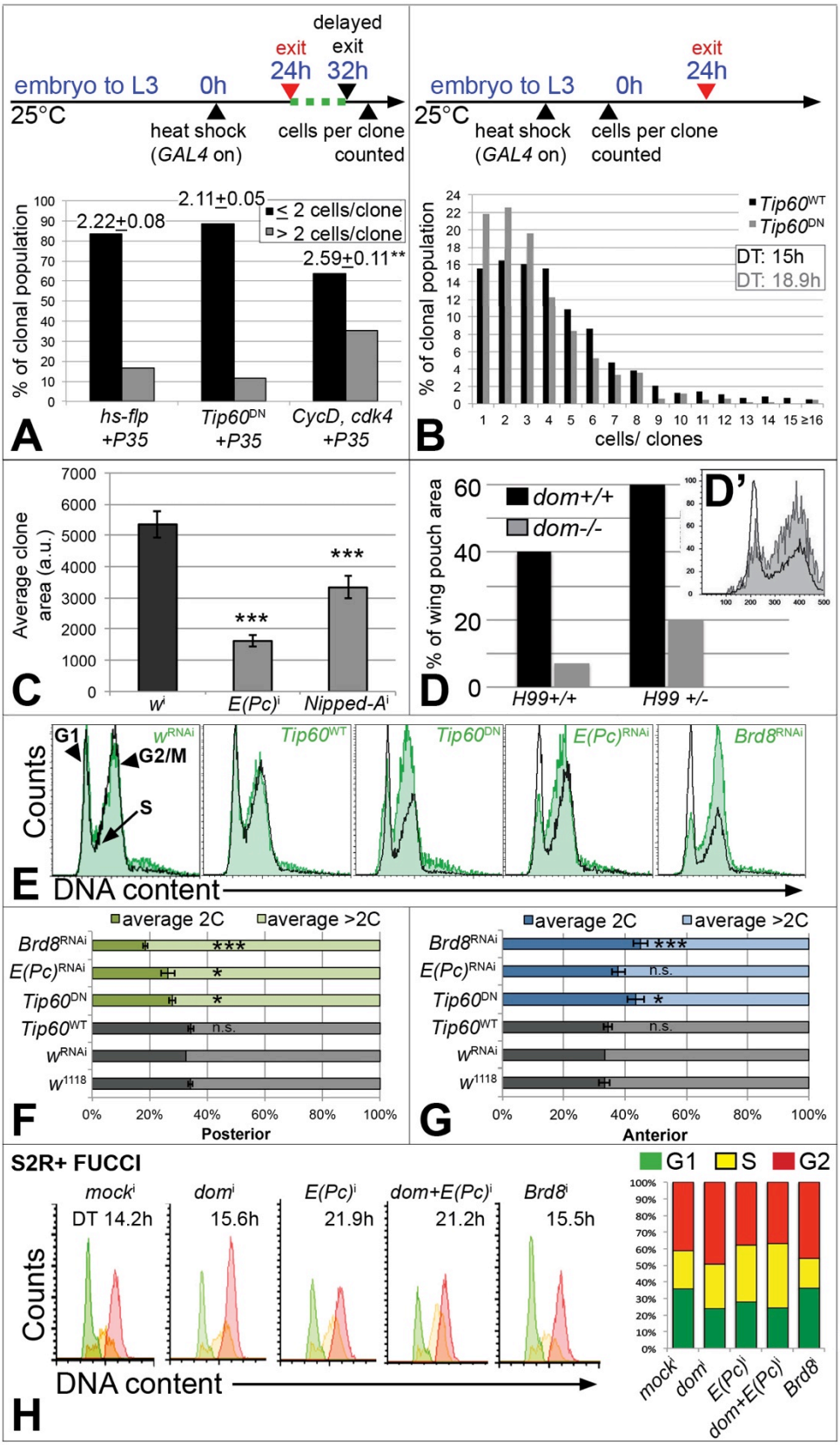

Fig. 2.3. Compromising NuA4 disrupts cell cycle progression

(A) Using heat-shock induced *flipout-Gal4* we generated non-overlapping clones of cells co-expressing *UAS-Tip60*^{DN}, an inhibitor of apoptosis P35, and GFP at 0h APF. Pupa were aged to 36h APF and the average number of cells per clone was counted blind from a minimum of 100 clones per genotype. *CycD/cdk4* serves as a positive control (Buttitta *et al.* 2007). (B) We generated clones expressing *Tip60*^{WT} or *Tip60*^{DN} and P35 in the proliferating L3 wing for 30h, to measure cell doubling times (DT). *Tip60*^{DN} expression lengthened cell doubling time by ~4h (*Tip60*^{WT}: 15h, *Tip60*^{DN}: 18.93h). (C) Clones expressing the indicated UAS-RNAis and *P35* were induced for 72h and measured in the late L3 wing. (D) FRT-mediated mitotic recombination was used to generate *domino* null (*dom*^{LL05537}) mosaic wings. Sibling clones generated from the same recombination event (+/+ and -/-) were measured after 48h in the late L3 wing. A heterozygous deficiency for the pro-apoptotic *H99* locus (*H99*$^{+/-}$) could not rescue the small size of *dom*$^{-/-}$ clones. (D') Flow cytometry was performed on late L3 wings to examine the DNA content of GFP-labeled *dom*$^{-/-}$ cells (grey). Cells lacking *dom* (grey trace) exhibit an increased proportion of >2C DNA content (cells in S/G2/M phases) compared to *dom*$^{+/-}$ and *dom*$^{+/+}$ cells (black trace). (E-G) Flow cytometry was performed on wandering L3 wings with *en*^{TS}, UAS-*Tip60*^{DN} or the indicated UAS-RNAis with GFP. (E) NuA4 inhibition increased the proportion of cells with >2C DNA content (green trace) compared to the non-Gal4 expressing cells (black trace). (F) Quantification of flow cytometry replicates are shown. NuA4 inhibition in the posterior wing (green bars, F) increases the >2C (S/G2/M) population compared to the posterior wing of control genotypes (grey bars, F). (G) NuA4 inhibition in the posterior wing also non-autonomously increased the proportion of anterior cells with 2C DNA content (G1, blue bars G) compared to the anterior wing of control genotypes (grey bars, G). (H) RNAi to NuA4 subunits was performed in S2R+ FUCCI cells (Zielke *et al.* 2014). Inhibition of NuA4 increased cell doubling time (DT) and the proportion of cells in S and G2, with the exception of Brd8. p-values were determined with an unpaired t-test,* p-value<0.05, *** p-value<0.001

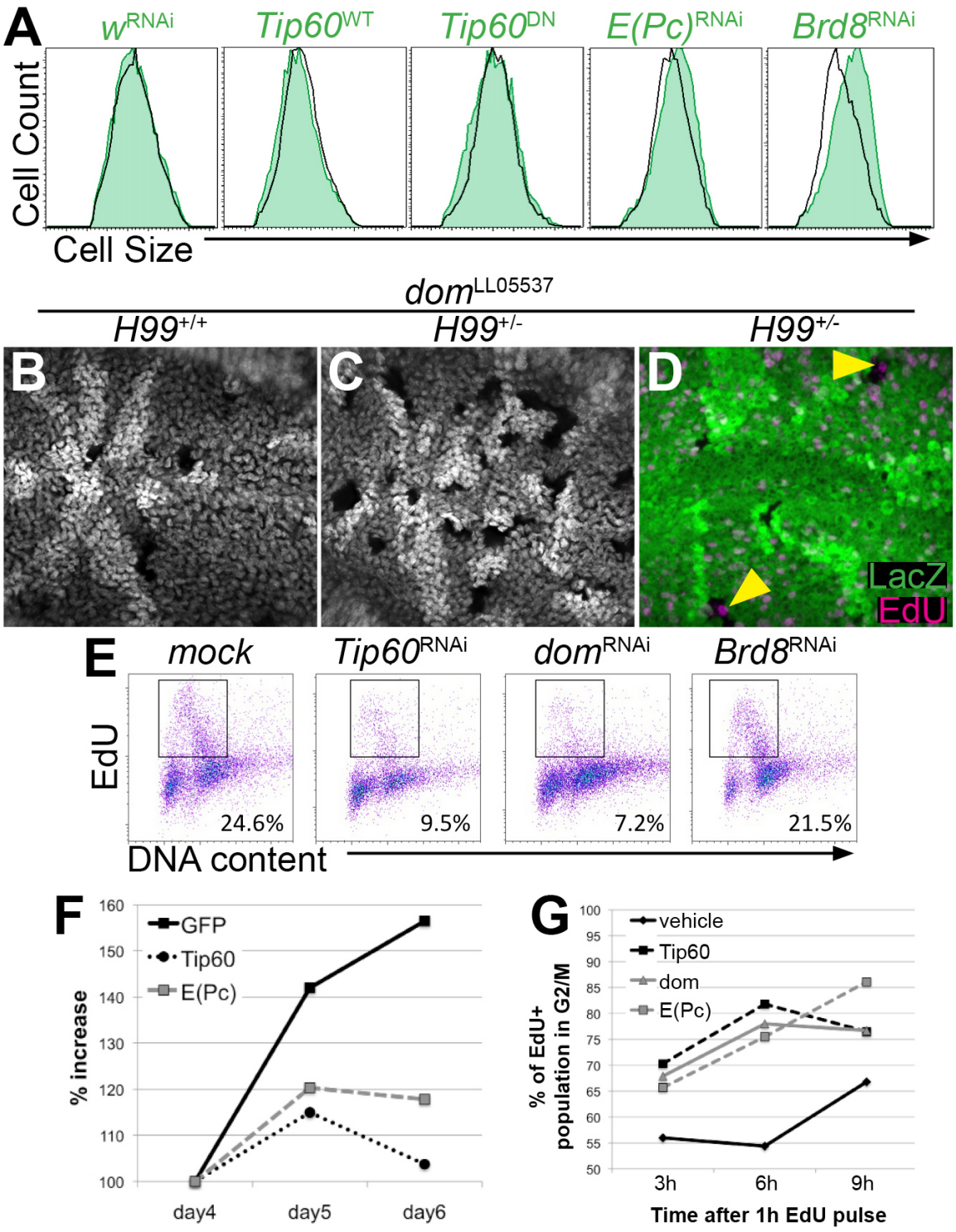

Fig. 2.3a. NuA4 is needed for proper proliferation

(A) Cell size (as measured by Forward Scatter in flow cytometry) is not significantly altered by RNAi to NuA4 components (compare to cell cycle alterations in Fig. 2.3E). Brd8^{RNAi} mildly increases cell size, likely due to the increased proportion of cells in G2 in the wing. (B-D) FRT-mediated mitotic recombination was used to generate *domino* null (*dom*^{LL05537}, *dom*$^{-/-}$) clones in

the proliferating L3 wing. (C) Heterozygosity for the pro-apoptotic *H99* locus ($H99^{+/-}$) increased the recovery of small lacZ-negative $dom^{-/-}$ clones, but did not rescue their poor growth. (D) LacZ-negative $dom^{-/-}$ cells do cycle, as indicated by EdU labeling (arrowheads). (E) RNAi to *Tip60* and *domino* in S2R+ cells decreased EdU incorporation (provided in a 30 min. pulse). However, consistent with the results shown in Fig. 2.3H, RNAi to *Brd8* did not compromise proliferation in S2R+ cells, as it does *in vivo*. (F) Cell proliferation is reduced for S2R+ cells exposed to RNAi for Tip60 and E(Pc) (presented as % increase from day 4). RNAi to GFP did not affect cell proliferation. (G) An EdU pulse-chase experiment was performed in dsRNA treated S2R+ cells to measure the duration of G2. Cells were labeled with EdU for 1hr and DNA content of EdU+ cells was quantified by flow cytometry for the indicated timepoints following EdU removal. Cells exposed to RNAi to *Tip60*, *E(Pc)* or *dom* and labeled with EdU during the pulse, accumulated in G2 for 6-9 hours after the pulse. Vehicle indicates a mock RNAi treatment without any dsRNA added.

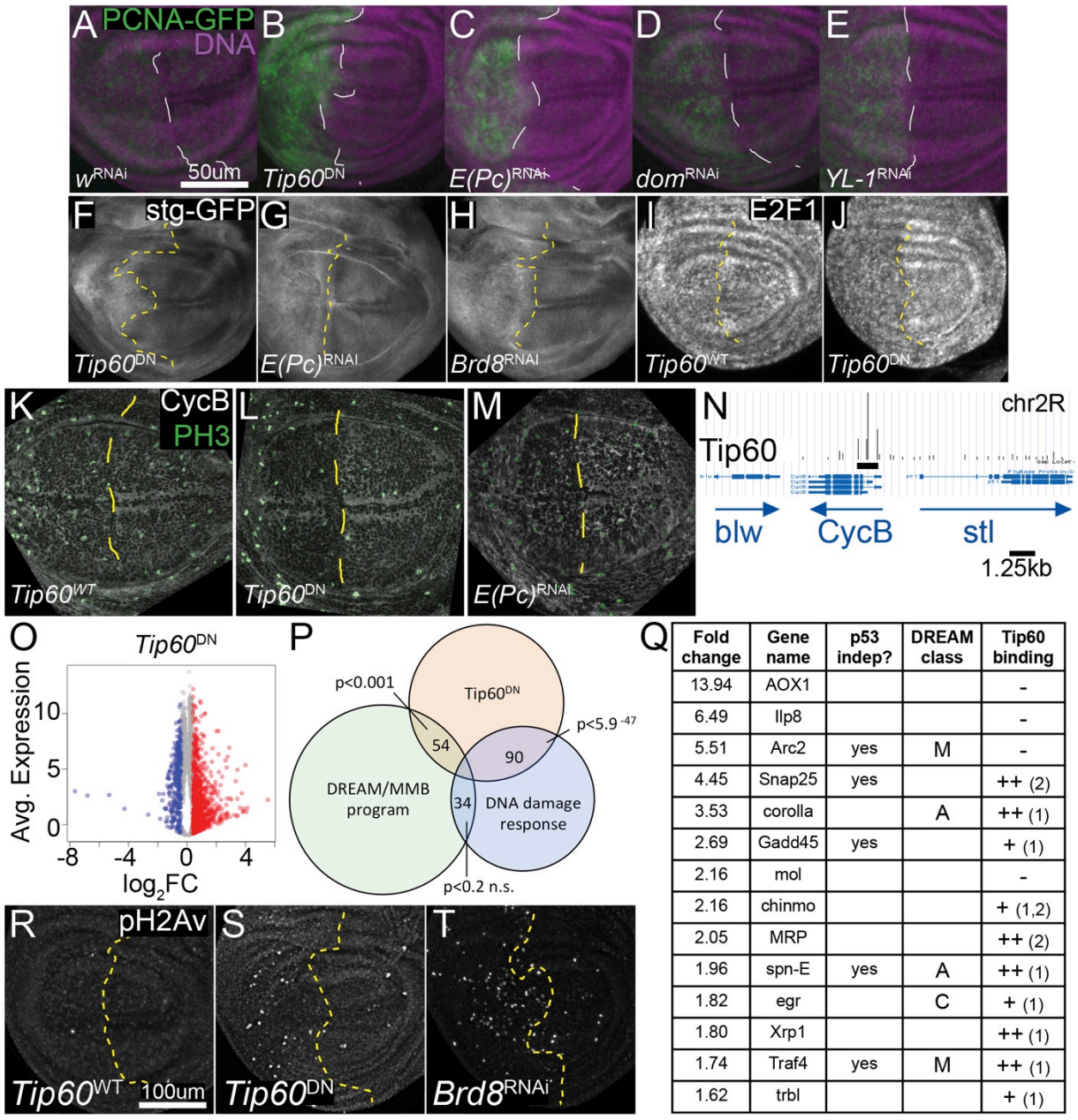

Q

Fold change	Gene name	p53 indep?	DREAM class	Tip60 binding
13.94	AOX1			-
6.49	Ilp8			-
5.51	Arc2	yes	M	-
4.45	Snap25	yes		++ (2)
3.53	corolla		A	++ (1)
2.69	Gadd45	yes		+ (1)
2.16	mol			-
2.16	chinmo			+ (1,2)
2.05	MRP			++ (2)
1.96	spn-E	yes	A	++ (1)
1.82	egr		C	+ (1)
1.80	Xrp1			++ (1)
1.74	Traf4	yes	M	++ (1)
1.62	trbl			+ (1)

Fig. 2.4. NuA4 inhibition deregulates cell cycle gene expression during active proliferation
(A-M, R-T) Using *en-Gal4/UAS* the indicated transgenes were expressed in the posterior larval wing. The dashed line indicates the wing anterior/posterior boundary. Wings are oriented with the posterior to the left. (A-H) NuA4 inhibition leads to high levels of PCNA-GFP and Stg-GFP. (I-J) NuA4 inhibition causes a decrease in E2F1 protein levels. (K-M) NuA4 inhibition reduced CycB protein levels after 24h of expression in the L3 wing. $Tip60^{WT}$ had no effect on CycB. (N) Tip60 binds to the 5' region of CycB (FILION *et al.* 2010). (O-Q) RNAseq was performed on dissected late L3 wings containing large, overlapping clones of cells expressing $Tip60^{WT}$ or $Tip60^{DN}$ using $flipout^{TS}$. (O) The majority (72.5%) of genes that change upon $Tip60^{DN}$ expression are upregulated. Genes with increased log Fold Change (logFC, $Tip60^{DN}/Tip60^{WT}$) are indicated in red, while genes that decrease expression are indicated in blue. (P) A comparison of genes significantly upregulated by $Tip60^{DN}$ to DREAM targets in proliferating Kc *Drosophila* cells,

and targets of the DNA damage response to IR in wings. Fourteen genes overlap in all three datasets. The *Tip60*^{DN} transcriptional response highly overlaps with the DNA damage response profile (90+14 out of 635 genes), with a lesser overlap with the DREAM/MMB program (54+14 out of 635 genes). p-values indicate overlap greater than that expected by chance for the comparisons. (Q) The table shows a subset of IR response genes that are also upregulated upon *Tip60*^{DN} expression, encompassing both p53-dependent and p53-independent targets with Tip60 binding. (R-T) NuA4 inhibition leads to an accumulation of pH2Av foci in the absence of exogenous DNA damage. [1] (FILION *et al.* 2010) [2] (XU *et al.* 2014)

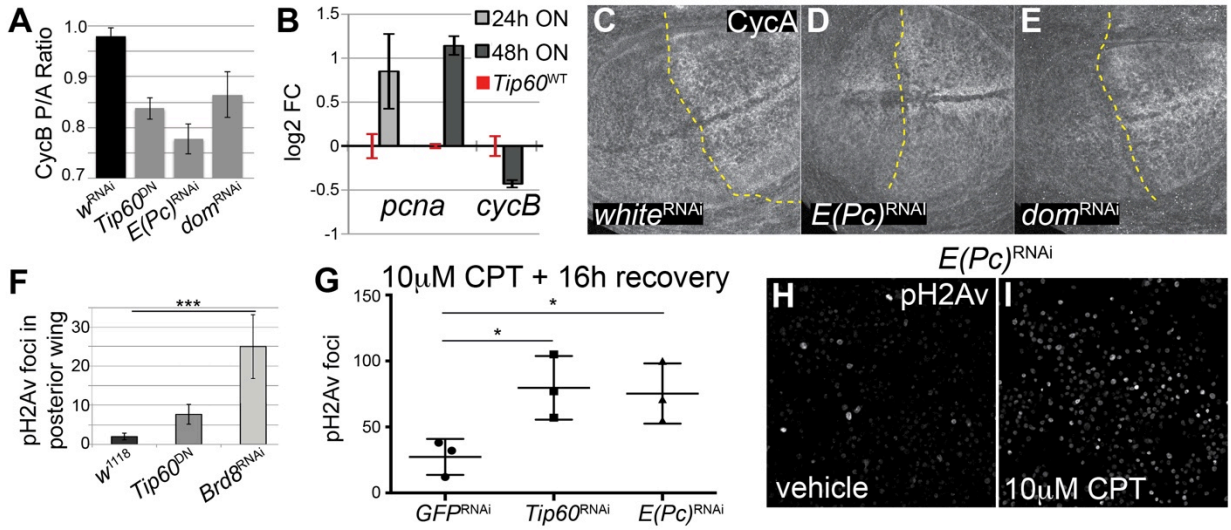

Fig. 2.4a. Loss of NuA4 function alters expression of specific cell cycle genes
(A, C-F) Using *en-Gal4/UAS* the indicated transgenes were expressed in the posterior larval wing. The dashed line indicates the anterior/posterior boundary (left side is posterior). (A) CycB is reduced 15-20% in the posterior wing when NuA4 is inhibited (n=5 discs). (B) Using *flipout-Gal4* in combination with Gal80^{TS} (*flipout ^{TS}*) we generated large, overlapping clones of cells expressing Gal4 24h after embryo hatching, but restricted the UAS-induced expression of *Tip60*^{DN} or *Tip60*^{WT} to 24h or 48h prior dissection at wandering L3 larval stages using temperature shifts. We confirmed by quantitative RT-PCR that *Tip60*^{DN} expression in L3 wings caused aberrant mRNA expression of *pcna* and reduction of *cycB*, compared to the *Tip60*^{WT} expressing controls. (C-E) CycA were not significantly affected by NuA4 inhibition compared to controls expressing *white*^{RNAi}, which exhibited no cell cycle phenotypes in any of our FACS assays. (F) Inhibition of Tip60 HAT activity or expression of *Brd8*^{RNAi} led to formation of phospho-H2Av foci in L3 wings in the absence of exogenous DNA damaging agents. (G-I) Inhibition of NuA4 in S2R+ cell culture by dsRNA to *Tip60* and *E(Pc)* decreased the cells' ability to recover from the DNA damage inducing agent Camptothecin (CPT). NuA4 inhibition resulted in more pH2Av+ cells compared to the GFP^{RNAi} control. p-values were determined by an unpaired t-test, *p-value<0.05 *** p-value<0.001.

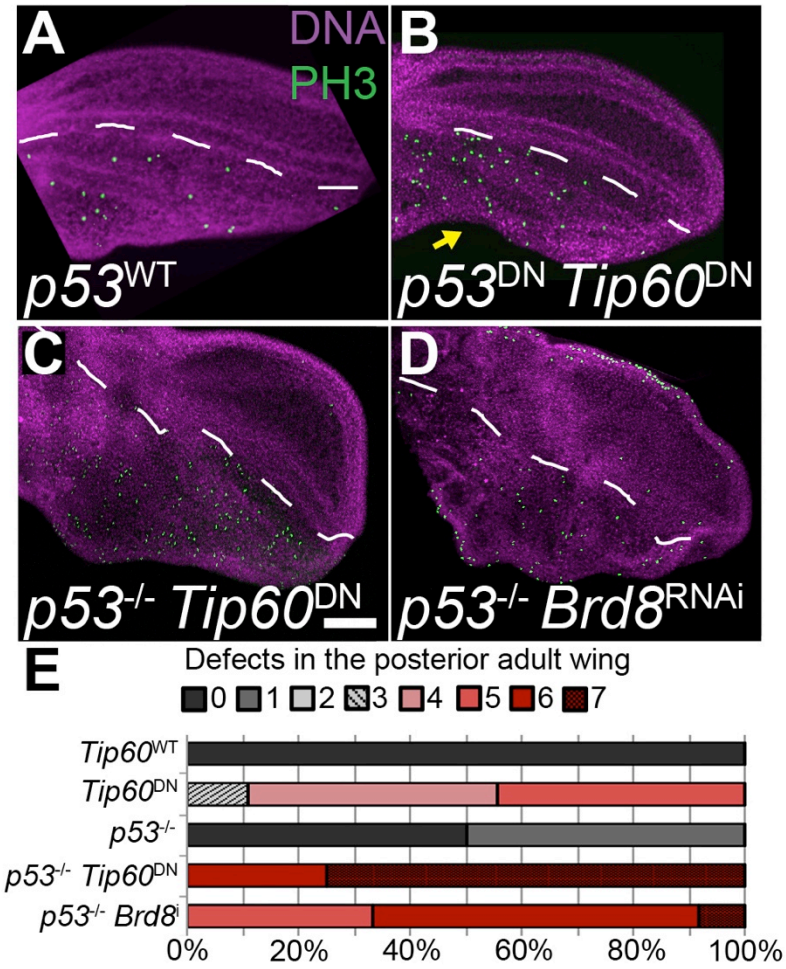

Fig. 2.5. NuA4 inhibition delays cell cycle exit independent of the p53-dependent DNA damage response (DDR)

Pupa expressing the indicated transgenes in the posterior wing (*en*-GAL4/UAS) were collected at 0hr APF, aged to 25-28h APF, and stained for mitoses using PH3. The dashed line indicates the anterior/posterior boundary. (A) Overexpression of wild-type p53 ($p53^{WT}$) was sufficient to delay cell cycle exit similar to NuA4 inhibition in the posterior wing (compare to Fig. 2.1). (B-E) Overexpression of a p53 allele that cannot bind DNA ($p53^{DN}$) or p53 null alleles ($p53^{5A\text{-}1\text{-}4/11\text{-}1B\text{-}1}$) did not prevent the delay of cell cycle exit caused by NuA4 inhibition in the posterior wing. (E) Loss of p53 strongly enhanced the severity of adult wing defects, suggesting loss of NuA4 function and p53 cooperate to increase genetic instability (The full details of the adult wing defect scoring are described in the Methods).

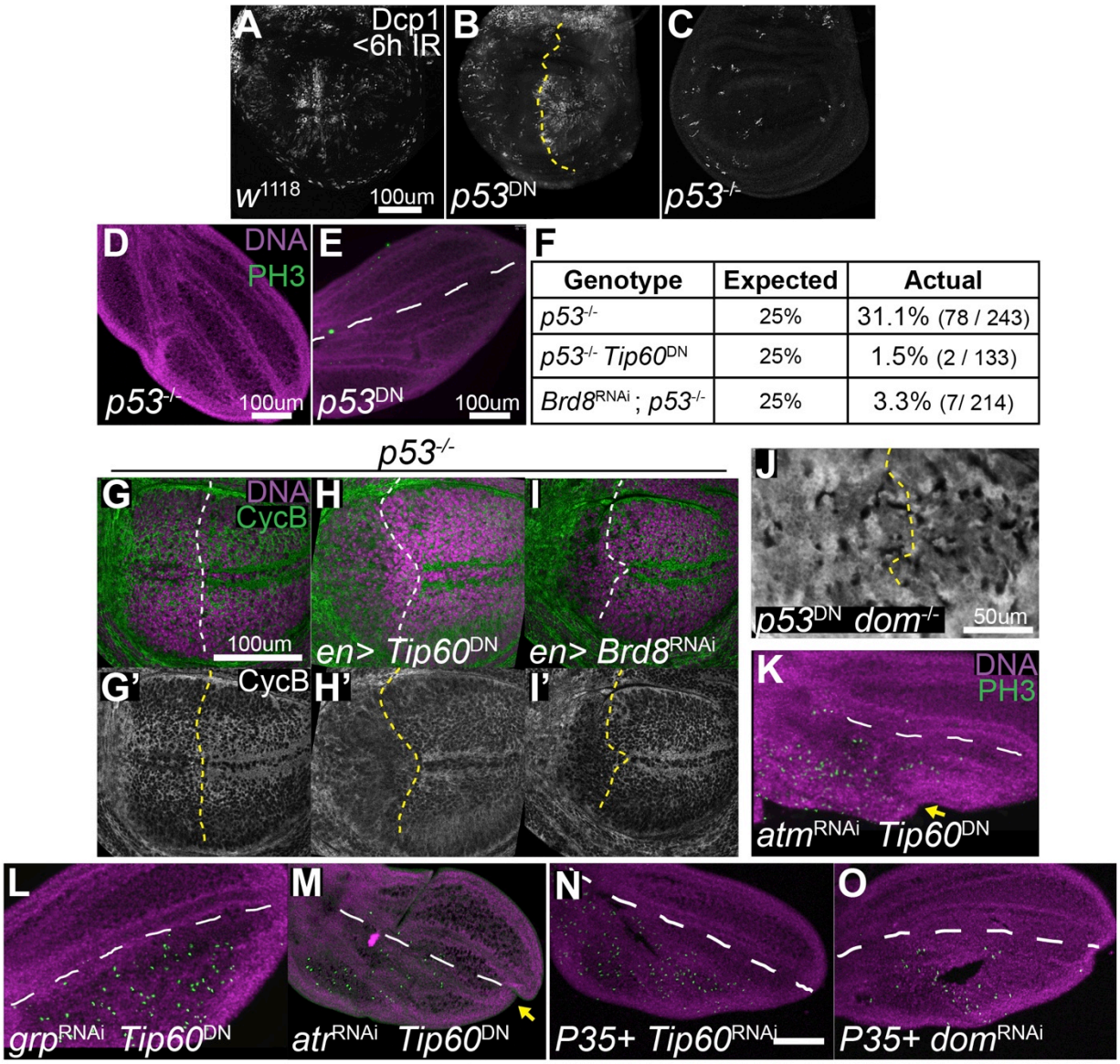

Fig. 2.5a. NuA4 inhibition delays cell cycle exit and slows the cell cycle independent of several DDR components

Using *en*-GAL4/UAS the indicated transgenes were expressed in the posterior wing. The dashed line indicates the anterior/posterior boundary (left is posterior). (A-C) p53-dependent apoptosis (as indicated by staining for the cleaved caspase, Dcp1) induced by 40 Grays of irradiation is substantially reduced by *en*-Gal4 expression of a p53 allele that cannot bind DNA ($p53^{DN}$) or in a p53 null background ($p53^{5A\text{-}1\text{-}4/11\text{-}1B\text{-}1}$) compared to the w^{1118} control. (D,E, K-O) Pupa expressing the indicated transgenes in the posterior wing were collected at 0hr APF, aged to 25-28h APF, and stained for mitoses using PH3. (D, E) Loss of *p53* or expression of $p53^{DN}$ in the posterior wing, does not alter cell cycle exit in the pupal stages nor does it reduce the size of the posterior wing (27h APF shown). (F) Loss of p53 severely enhances larval and pupal lethality when combined with NuA4 loss of function transgenes driven by *en*-Gal4. Numbers indicate eclosed adults for each genotype. (G-I) $p53^{-/-}$ mutant larvae expressing RFP only, or RFP with $Tip60^{DN}$ or $Brd8^{RNAi}$ in the posterior L3 larval wing were stained for CycB protein. Loss of p53 does not

rescue the reduction in CycB levels. (J) *en*-Gal4/UAS driven expression of $p53^{DN}$ in the posterior larval wing cannot rescue the small size of LacZ negative $dom^{-/-}$ clones. (KI-O) Pupa expressing the indicated transgenes in the posterior wing were collected at 0hr APF, aged to 25-28h APF, and stained for mitoses using PH3. (K-M) RNAi knockdown of the DDR kinases *tefu*/*ATM*, *grp/chk1,* and *mei-41/ATR* in combination with $Tip60^{DN}$ expression could not prevent the delayed cell cycle exit in the posterior wing caused by inhibition of NuA4. (N, O) Blocking apoptosis by co-expression of P35 did not prevent the cell cycle exit delay when NuA4 is inhibited in the posterior wing.

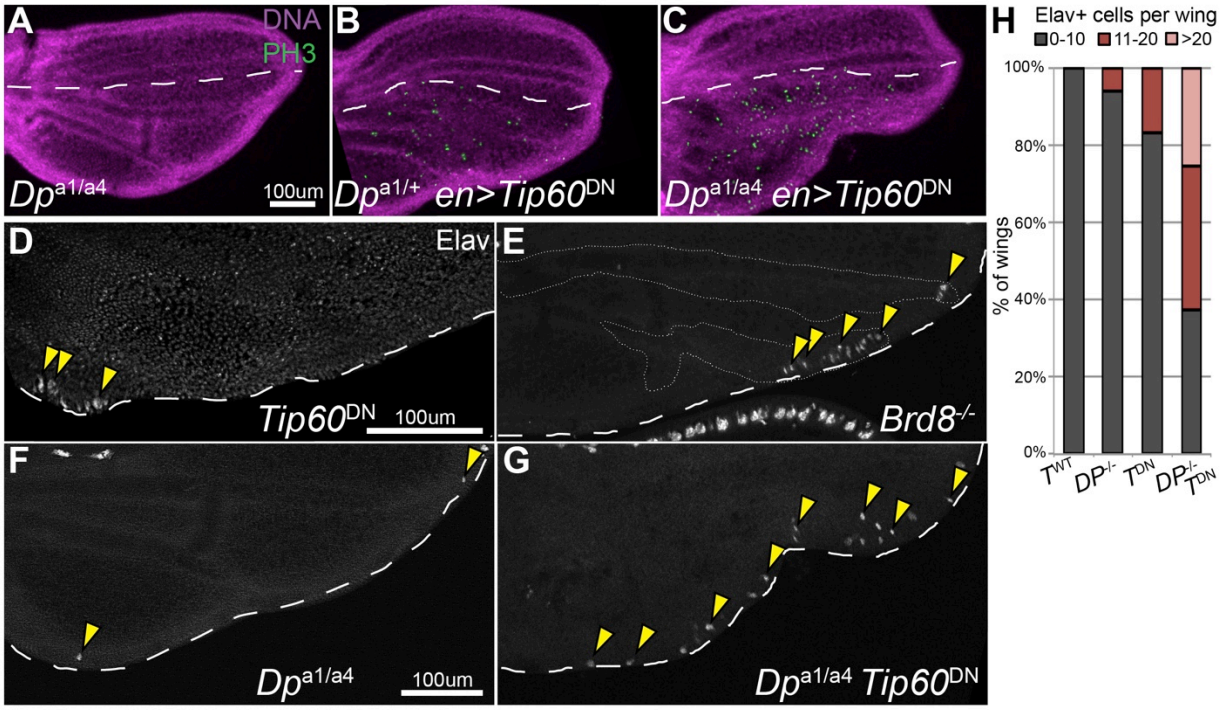

Fig. 2.6. NuA4 affects cell cycle exit independent of DP function
(A) $Dp^{a1}/^{a4}$ wings with *en-Gal4/UAS-GFP* exhibit normal cell cycle exit. (B,C) Expression of $Tip60^{DN}$ in the posterior wing delays cell cycle exit (as shown by PH3) in $Dp^{a1}/^{+}$ and $Dp^{a1}/^{a4}$ wings. All wings shown are at 27h APF. (D) $Tip60^{DN}$ expression in the posterior pupal wing leads to ectopic neurons (as indicated by Elav staining, arrowheads) at the posterior wing margin (indicated by the dashed line). (E) $Brd8^{-/-}$ (Brd^{G19099}) clones in the pupal wing often contain ectopic neurons at the posterior wing margin (clone boundaries are indicated by dotted lines). (F,G) *Dp* mutant wings ($Dp^{a1}/^{a4}$) occasionally exhibit ectopic neurons at the posterior wing margin, which becomes strongly enhanced when $Tip60^{DN}$ is expressed in the posterior wing using *en-Gal4/UAS*. (H) Quantification of the ectopic posterior wing margin neurons in the indicated genetic backgrounds.

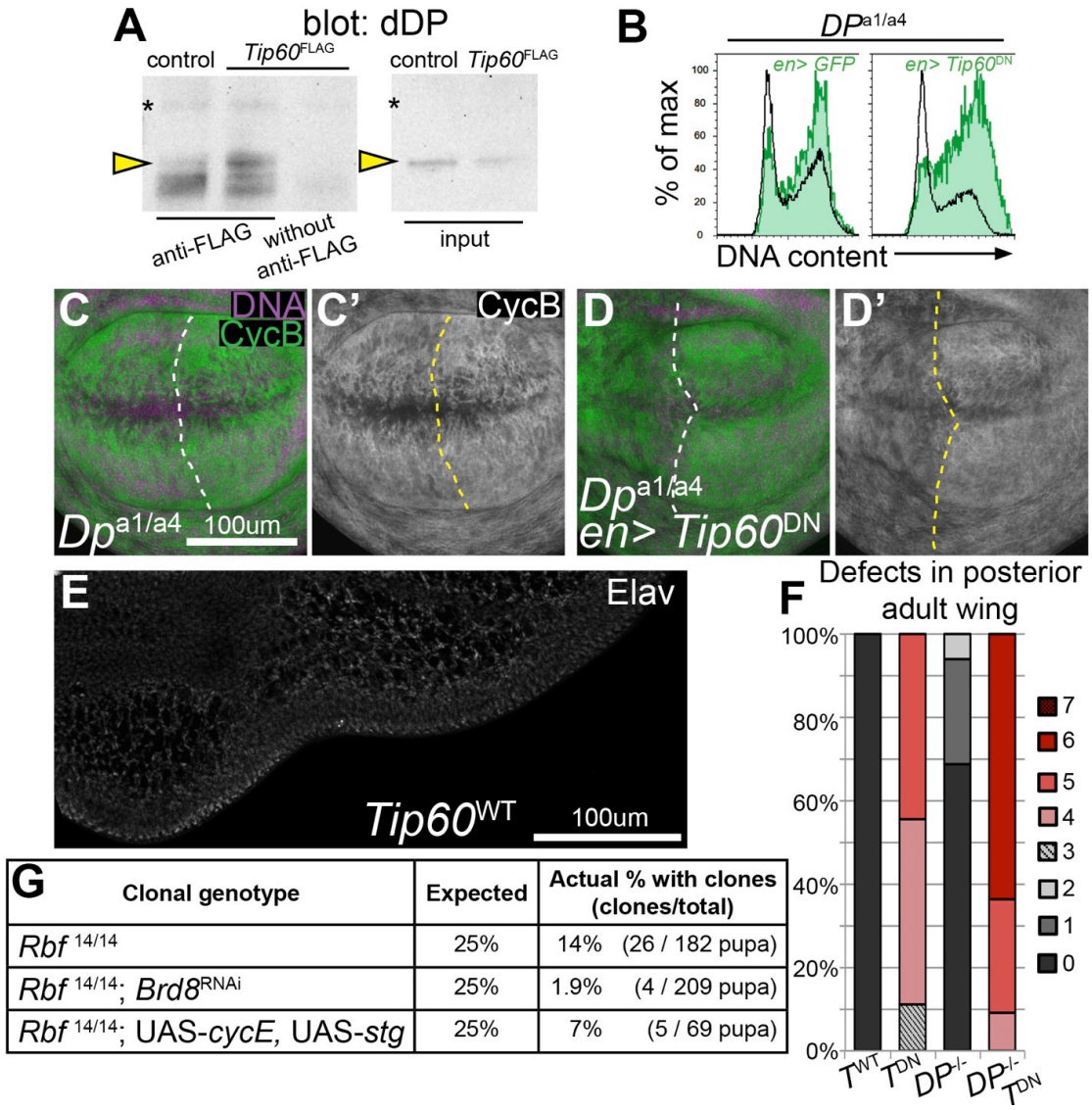

G

Clonal genotype	Expected	Actual % with clones (clones/total)
Rbf $^{14/14}$	25%	14% (26 / 182 pupa)
Rbf $^{14/14}$; *Brd8*^{RNAi}	25%	1.9% (4 / 209 pupa)
Rbf $^{14/14}$; UAS-*cycE,* UAS-*stg*	25%	7% (5 / 69 pupa)

Fig. 2.6a. NuA4 and DREAM genetically and physically interact

(A) FLAG-tagged Tip60 co-immunoprecipitates endogenous Dp (arrowhead) in S2 cells. Controls were transfected with empty vector. (B) Using *en*-Gal4/UAS, either GFP alone, or GFP+Tip60^{DN} was expressed in *Dp*$^{a1/a4}$ mutant larval wings and cell cycle phasing was examined by flow cytometry. *Dp*$^{a1/a4}$ mutant wings show an increase in the G2/M population with GFP expression alone, but Tip60^{DN} expression in *Dp*$^{a1/a4}$ mutants further increases the proportion of cells in late S/early G2. (C,D) *Dp*$^{a1/a4}$ mutant larvae expressing GFP only, or GFP with *Tip60*^{DN} in the posterior L3 larval wing were stained for CycB protein. The dashed line indicates the anterior/posterior boundary (left side is posterior). (E) Overexpression of Tip60 in the posterior wing (*en*-Gal4/UAS-*Tip60*^{WT}) does not cause ectopic posterior wing margin neurons in the pupal wing at 27hAPF as indicated by Elav staining (this is a control for Fig. 2.6D). (F) Loss of *Dp* enhances the adult wing defects caused by expression of *en*-Gal4/UAS-*Tip60*^{DN}. The adult wing defect scoring system is described in the Methods. (G) Loss of NuA4 function enhances the lethality of Rbf loss in pupal clones, to a degree even more severe than that caused by a genetic combination causing a complete bypass of cell cycle exit, *Rbf*$^{-/-}$,CycE/Stg (BUTTITTA *et al.* 2010).

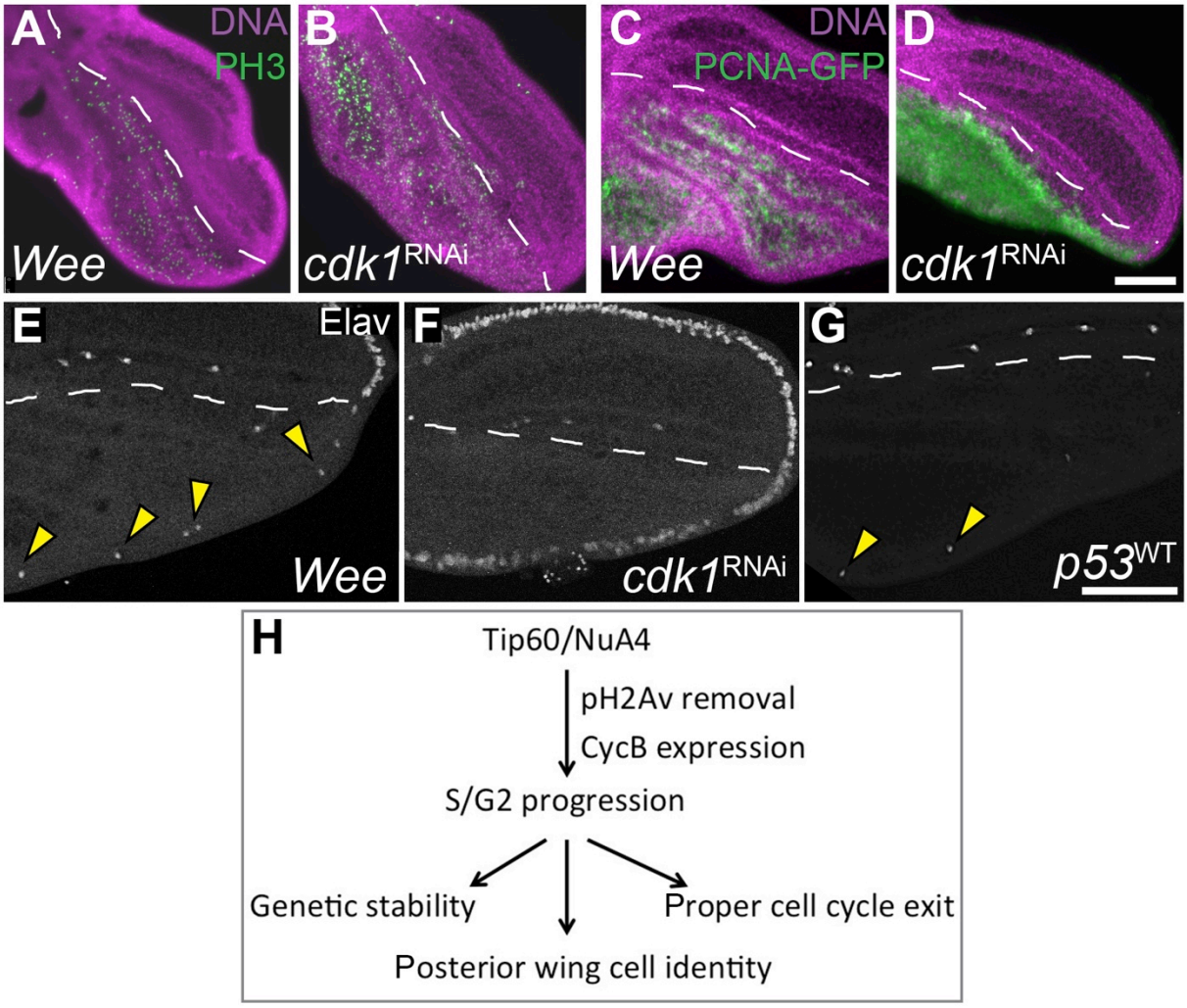

Fig. 2.7. Prolonging the final G2 delays cell cycle exit, de-represses cell cycle genes and causes ectopic neurons at the posterior wing margin

(A-G) Using *en*-GAL4/UAS the indicated transgenes were expressed in the posterior wing. Inhibition of Cdk1 activity by expression of *Wee* or *Cdk1* RNAi in the posterior wing delays the timing of cell cycle exit (A, B) and leads to ectopic E2F activity (C,D) similar to inhibition of NuA4. (Note that the posterior wing in D is smaller, because there is no $Gal80^{TS}$ in the PCNA-GFP background.) (E, F) Inhibition of Cdk1 activity leads to Elav positive ectopic neurons in the posterior wing margin. (G) Overexpression of p53 ($p53^{WT}$) also led to Elav positive ectopic neurons in the posterior wing margin. (H) Schematic of the Tip60/NuA4 functions described in our study.

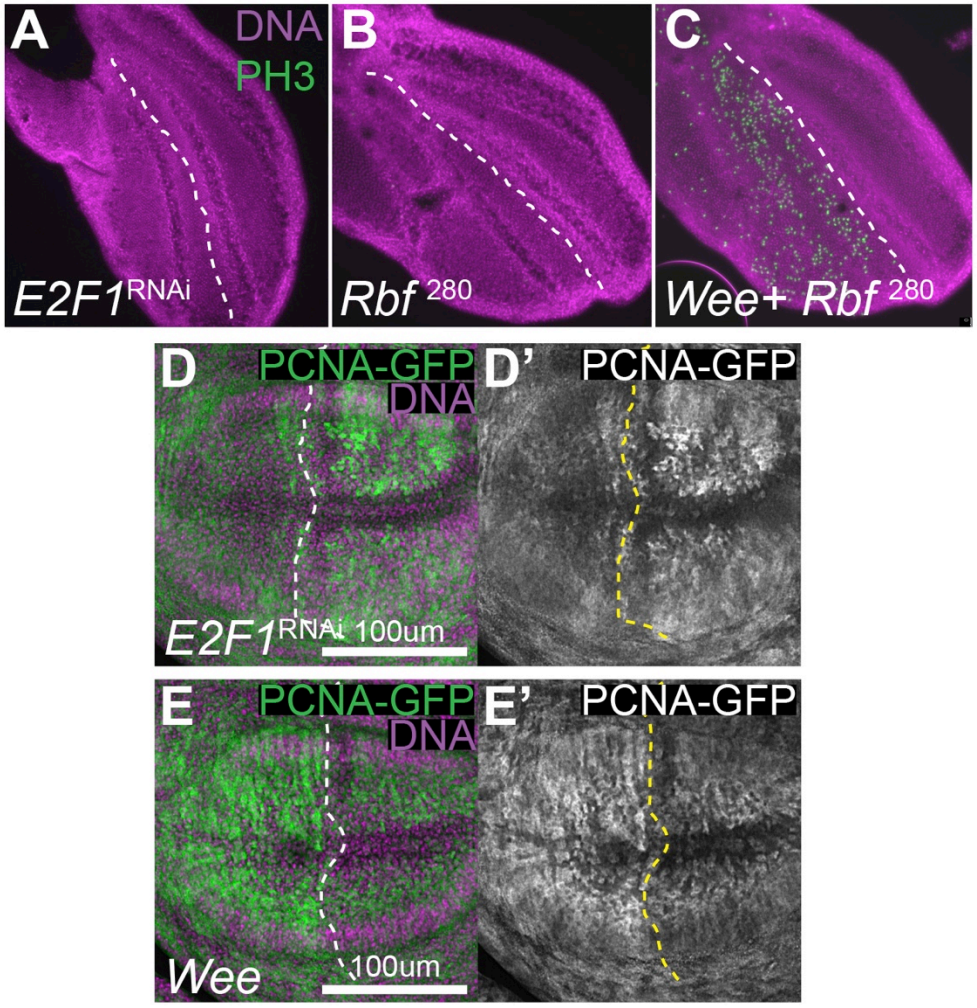

Fig. 2.7a. Slowing the final cell cycle does not delay cell cycle exit
Using *en*-GAL4/UAS the indicated transgenes were expressed in the posterior wing. The dashed line indicates the anterior/posterior boundary (left side is posterior). (A, B) Slowing the cell cycle with RNAi to E2F or expression of a constitutively repressive Rbf, Rbf^{280}, in the posterior wing did not alter the timing of cell cycle exit. (C) By contrast, co-expression of Rbf^{280} with Wee delayed the timing of cell cycle exit in a manner similar to Wee alone. (D) RNAi to E2F in the posterior wing effectively reduced E2F activity as shown by PCNA-GFP. (E) By contrast, expression of Wee in the posterior wing increased PCNA-GFP, similar to inhibition of NuA4 (compare to Fig. 2.4A-E).

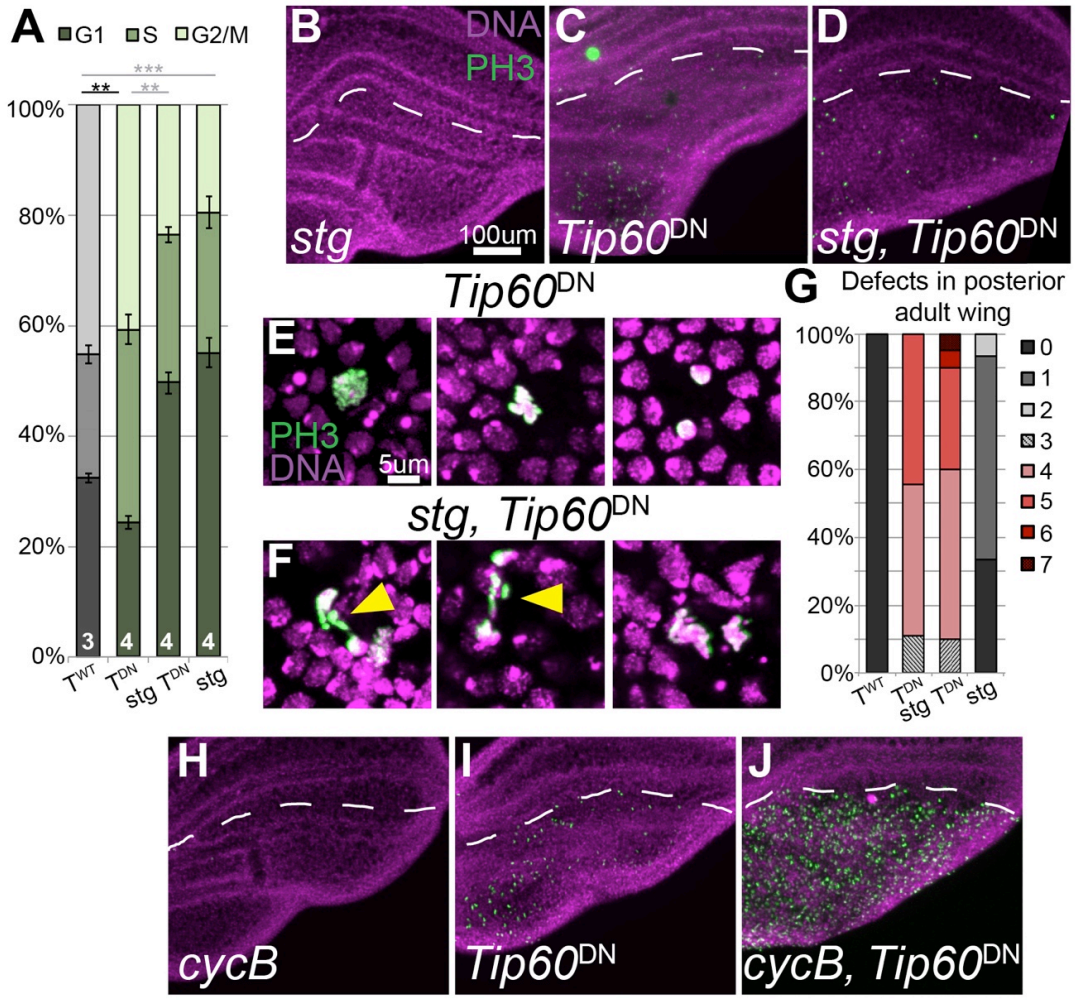

Fig. 2.8. Accelerating G2-M when NuA4 is inhibited leads to severe mitotic defects
(A) Using *en*^{TS} the indicated transgenes were expressed in wings from the L2 stage. Cell cycle phasing was subsequently examined by flow cytometry at the late L3 stage. *Tip60*^{DN} expression increases the proportion of cells in S/G2 compared to *Tip60*^{WT} but co-expression of *Stg* with *Tip60*^{DN} forces cells through G2/M, similar to *Stg* expression alone. (B-D) Using *en*^{TS} we drove expression of the indicated transgenes in the posterior wing, starting from L2. Pupa were collected at 0h APF and aged to 26-28h APF at the permissive temperature for transgene expression. (B) *Stg* expression does not alter normal cell cycle exit, (C) while *Tip60*^{DN} expression delayed cell cycle exit as observed by ectopic PH3 staining. (D) Co-expression of *Stg* with *Tip60*^{DN} did not rescue the delayed cell cycle exit, but defects in mitosis occurred when cells with inhibited NuA4 were forced through G2. (E) Delayed mitoses in *Tip60*^{DN} expressing wings appeared relatively normal in prometaphase, metaphase and telophase. (F) By contrast, many defective mitoses were observed in wings co-expressing *Stg* and *Tip60*^{DN} including anaphase bridges (arrowhead) and improperly segregated DNA. (G) Co-expression of *Stg* with *Tip60*^{DN} increased the number of defects observed in the adult wing. (H) *cycB* expression does not alter normal cell cycle exit (J) Co-expression of *cycB* with *Tip60*^{DN} delayed cell cycle exit of even more cells than (I) *Tip60*^{DN} alone. p-values were determined with an unpaired t-test, ** p-value<0.01, *** p-value<0.001

Table 2.1. RNAi lines for core NuA4 subunits
RNAi lines for the core NuA4 subunits tested for a delay in cell cycle exit.

en > GAL4	EdU at 22h APF	PH3 at 27h APF	stock number(s)
white^{RNAi}	N	N	BDSC#35573
Tip60^{RNAi}	Y	Y	BDSC#28563
E(Pc)^{RNAi}	Y	Y	BDSC#28686
Brd8^{RNAi}	Y	Y	v41530, v104879
dom^{RNAi}	Y	Y	BDSC#31054, v7789
Nipped-A^{RNAi}	Y	Y	BDSC#31255, #34849
YL-1^{RNAi}	Y	Y	v21903, v107951
Mrg15^{RNAi}	N	N	v43800, v43802
Reptin^{06945}	N	N	BDSC# 11706
Pontin$^{5.1}$	N	N	PMID: 16087886

Table 2.1a. Genes induced by *Tip60*^{DN} and the DNA damage response
Transcriptional program induced by *Tip60*^{DN} expression that also overlaps with the DNA damage response (DDR) from (VAN BERGEIJK *et al.* 2012).

Gene name	log FC 48h	log FC 78h	p53 indep?	Tip60 binding (DamID)	Tip60 binding (ChIP-Seq)
Act57B		1.342216064		-	
AOX1	3.801490374	3.301794879		-	
Arc2	1.215181446	1.034855483	yes	-	
babos		0.418713017		-	
CG10283		0.433444083		-	
CG10445	0.465519089			++	
CG11897	2.245622593	1.600368667	yes	++	
CG12868	0.939229825	0.865127822		++	
CG12880	0.976410376	1.158980571		-	
CG1299	0.495174603			-	
CG13082		0.68835997		-	
CG13272	0.803148204	0.516431244		-	
CG14304	1.093800673	0.753920145		-	
CG14906	0.785916726			++	
CG15212		0.924881684	yes	-	
CG15611	0.903978898	0.653038717		-	
CG16947	0.72647539	0.928485339		-	
CG17124	0.86546946	0.734796299		-	
CG2064	0.466489153			-	
CG2909	0.549313473			++	
CG3008	0.524269958			++	
CG3036	1.058351625	1.428808634		-	
CG31705	0.520564086			-	
CG31728	0.675036303	0.923457292	yes	-	
CG32099	0.635967699	0.609609741		-	
CG32549		0.540903248	yes	-	
CG3376	0.403461924	0.40848306		+	
CG33978	0.42565307			-	
CG4096	0.696812108	0.580545009		++	

CG43366	0.781221336	0.712964268		-	
CG44085	1.312354838			+	
CG4858	0.405236616			+	
CG5953	1.608032473	1.368840213		+	
CG6071	1.949376604	1.626851016		-	
CG6272	0.556560007	0.553892692		+	
CG6353	0.447686561			-	
CG6739	1.090821225	1.147412068		-	
CG7054	0.495430562			+	
CG7587		2.628726912		-	
CG9192	0.911997434	1.378796065		-	
CG9411	0.64687876	0.948425397	yes	-	
CG9689	0.570699579	0.719950785		-	
CG9850	0.841627595	0.690785423	yes	-	
chinmo	1.107781665			+	++
clt	0.429276272			-	
CR32207	0.578413568	0.514878676		-	
Cyp9f2	1.197893534	0.804763201		+	
Cyp9f3Psi	0.707765408			-	
DAAM		0.414447167		-	
dlp	0.567400273	0.566626183		-	
Ef1alpha100E	1.800520907	2.460928756	yes	-	
egr	0.862643263	0.999696729		+	
Gadd45	1.429339908	1.357381446	yes	+	
Gclc		0.445761634		++	
Glt	1.354925071	1.548219214		-	
Ilp8	2.697269829			-	
ImpL3	4.051401102	2.311946537		-	
insc		0.434949876		++	
IP3K2		0.469238654		+	
Men	1.046098012	0.524298472		++	
mfas	0.521014147	0.583992439		-	
Mmp1	0.413081884	0.588866613		+	

Mmp2		0.553214543		++	
Mocs1	0.618731138			++	
mtg	0.850179279	0.764570301		-	
Osi14	0.660001447			-	
PEK	0.440366963			+	
Pka-C3		0.724937275		++	
Pvf2	0.709124596	0.764676259		-	
Rab32		0.58043333		-	
rho-4	0.407496054	0.418121348		-	
RpL12	0.404517067			-	
Rpt3R	0.811634277	0.708548239		-	
sage	0.879251662			-	
sda	0.688492015	0.605342175		-	
slow	0.566129725	0.451540876		-	
Snap25	2.153476912	2.59429639	yes	-	++
Socs36E	0.426088603			+	
sog	0.429506453			-	
spir		0.400539333		-	
Spn47C	3.495951559	3.491517574		-	
ssp3		0.433282689		-	
Sulf1		0.427977501		-	
Tep4	0.726897945	0.694545929		-	
Traf4	0.802301311	0.584587098	yes	++	
trbl	0.697977603	0.465379635		+	
twz		0.554252434		-	
unc-13	1.03890413	1.12947619		+	
upd1	0.884009089	0.885374101		-	
Xrp1	0.849617743	0.732286277		++	

Table 2.2a. Genes induced by *Tip60*^{DN}, DREAM, and the DNA damage response
Transcriptional program induced by *Tip60*^{DN} expression that overlaps with both the DNA damage response and targets of DREAM (GEORLETTE *et al.* 2007; VAN BERGEIJK *et al.* 2012).

Gene name	log FC 48h	log FC 78h	p53 independent?
CG15784	2.830843772	2.006137895	yes
Arc1	2.462872484	2.452627785	yes
corolla (mei-39)		1.820713845	
mol	1.113604616	0.678560687	
MRP	1.032300087	0.813099375	
spn-E	0.972779342	0.883056532	yes
agt	0.918326335	0.623356841	
rpr	0.658195641	0.464573596	
CG3448	0.624751423		yes
glob1	0.624270474	0.437249977	yes
vir-1		0.714230166	
kay	0.454967406	0.60817313	
CG18213	0.419637685		
CG5399		1.64980284	

Table 2.3a. Genes regulated by *Tip60*^{DN} that are also targets of DREAM
Transcriptional program induced by *Tip60*^{DN} expression that overlaps with targets of DREAM (GEORLETTE *et al.* 2007). Genes upregulated logFC >0.5 by *Tip60*^{DN} are shaded in red and genes downregulated logFC >0.5 by *Tip60*^{DN} are green. A total of 511 genes significantly regulated by *Tip60*^{DN} that were also on the array used by GEORLETTE *et al.* (2007) were entered for comparison and had an overlap of 88/511. H2Av localization is from H2Av ChIP-Seq on L3 larvae from modencode data file 4953. Significant H2Av signal on gene body coding region as well as enrichment on 5' end is indicated by "enriched at 5' ". H2Av was on the gene body of 36/60 (60%) of shared Tip60/DREAM upregulated genes and 14/27 (51%) of downregulated genes.

FBgn	gene symbol	DREAM/MMB class	H2Av on gene body?
FBgn0003483	spn-E	A	+ (enriched at 5')
FBgn0029147	NtR	A	+ (enriched at 5')
FBgn0030852	corolla	A	+
FBgn0035542	CG11347	A	-
FBgn0037742	Rpt3R	A	+
FBgn0000246	c(3)G	B	-
FBgn0034075	Asph	B	+ (enriched at 5')
FBgn0000533	ea	C	+
FBgn0014469	Cyp4e2	C	-
FBgn0024366	CG11409	C	N/D
FBgn0031011	CG8034	C	-
FBgn0033483	egr	C	+ (enriched at 5')
FBgn0038037	CG17227	C	+ (enriched at 5')
FBgn0052412	CG32413	C	+
FBgn0003087	pim	D	+
FBgn0011828	Pxn	D	-
FBgn0014135	bnl	D	-
FBgn0027657	glob1	D	-
FBgn0030362	regucalcin	D	+
FBgn0033712	CG13163	D	+ (enriched at 5')
FBgn0053969	CG5571	D	+ (enriched at 5')
FBgn0001122	G-oalpha47A	E	-
FBgn0001297	kay	E	-
FBgn0005683	pie	E	+
FBgn0012037	Ance	E	-
FBgn0031816	CG16947	E	+
FBgn0039006	Cyp6d4	E	+
FBgn0033051	dream	F	+
FBgn0043364	cbt	F	-
FBgn0016694	Pdp1	H	-

FBgn0023129	aay	H	-
FBgn0023537	CG17896	H	+ (enriched at 5')
FBgn0025885	Inos	H	+
FBgn0027570	Nep2	H	-
FBgn0033313	Cirl	H	-
FBgn0034997	CG3376	H	+ (enriched at 3')
FBgn0016715	Reg-2	I	-
FBgn0033205	CG2064	I	+ (enriched at 5')
FBgn0024920	Ts	K	+
FBgn0000071	Ama	L	-
FBgn0030309	CG1572	L	+
FBgn0037617	CG8145	L	+ (enriched at 5')
FBgn0001168	h	M	-
FBgn0022069	Nnp-1	M	+ (enriched at 5')
FBgn0026319	Traf4	M	-
FBgn0031286	CG3862	M	+ (enriched at 5')
FBgn0031888	Pvf2	M	-
FBgn0032620	CG12288	M	+ (enriched at 5')
FBgn0033088	CG3271	M	+ (enriched at 5')
FBgn0033928	Arc2	M	+
FBgn0036549	CG10516	M	+ (enriched at 5')
FBgn0038455	CG14907	M	+
FBgn0038601	CG18600	M	+
FBgn0038893	CG6353	M	+
FBgn0039644	CG11897	M	+
FBgn0040308	Jafrac2	M	+
FBgn0050382	CG30382	M	+ (enriched at 5')
FBgn0000299	Cg25C	N	-
FBgn0004133	blow	N	-
FBgn0014380	RhoL	N	-
FBgn0016075	vkg	N	+
FBgn0022710	Ac13E	N	-
FBgn0031307	CG4726	N	-
FBgn0033538	CG11883	N	-
FBgn0040398	CG14629	N	-
FBgn0019952	Orct	O	-
FBgn0025683	CG3164	O	-
FBgn0026562	BM-40-SPARC	O	+
FBgn0029791	CG4096	O	-
FBgn0035356	CG16986	O	+
FBgn0035767	CG8596	O	-

FBgn0038972	CG7054	O	+
FBgn0041629	Hexo2	O	+
FBgn0051673	CG31673	O	+
FBgn0029167	Hml	P	-
FBgn0011722	Tig	Q	-
FBgn0052702	CG32699	Q	-
FBgn0001114	Glt	R	-
FBgn0023540	CG3630	R	+
FBgn0030057	Ppt1	R	+
FBgn0030628	CG9114	R	+
FBgn0031053	CG14223	R	+
FBgn0032213	CG5390	R	+
FBgn0032889	CG9331	R	+
FBgn0037028	CG3618	R	+ (enriched at 5')
FBgn0039128	CG13599	R	+
FBgn0039774	Cdase	R	-

Table 2.4a. Primer sequences for NuA4 dsRNA synthesis
List of primer sequences used for *in vitro* T7 transcription of dsRNA made for inhibition of NuA4 in S2R+ cell culture.

NuA4 dsRNA	5' to 3' primer sequence
T7-Brd8-fwd1	TAATACGACTCACTATAGG GAT AAA CCA AAA TCT GTG GAG
T7-Brd8-rev1	TAATACGACTCACTATAGG GTC TTT TCT TGC ATT GTT ACT G
T7-E(Pc)-fwd1	TAATACGACTCACTATAGG CAA CAA CAA CAA CAA TAC CG
T7-E(Pc)-rev1	TAATACGACTCACTATAGG CAG CTC ATT GCA GAT GTC TA
T7-Dom-fwd1	TAATACGACTCACTATAGG CTT TGT GGA AGA AAC TGG AG
T7-Dom-rev1	TAATACGACTCACTATAGG CGG ACT CTT CAG GTA CTC AG
T7-Tip60-fwd1	TAATACGACTCACTATAGG TTA AGC CCT GGT ATT TCT CA
T7-Tip60-rev1	TAATACGACTCACTATAGG TGA GAT CAC GTC CTC TTT TT

References

Akdemir, F., A. Christich, N. Sogame, J. Chapo and J. M. Abrams, 2007 p53 directs focused genomic responses in Drosophila. Oncogene 26**:** 5184-5193.

Altaf, M., A. Auger, J. Monnet-Saksouk, J. Brodeur, S. Piquet *et al.*, 2010 NuA4-dependent acetylation of nucleosomal histones H4 and H2A directly stimulates incorporation of H2A.Z by the SWR1 complex. J Biol Chem 285**:** 15966-15977.

Ashburner, M., 1989 *Drosophila; A laboratory handbook*. Cold Spring Harbor Press.

Auger, A., L. Galarneau, M. Altaf, A. Nourani, Y. Doyon *et al.*, 2008 Eaf1 is the platform for NuA4 molecular assembly that evolutionarily links chromatin acetylation to ATP-dependent exchange of histone H2A variants. Mol Cell Biol 28**:** 2257-2270.

Ayeni, J. O., A. Audibert, P. Fichelson, M. Srayko, M. Gho *et al.*, 2016 G2-phase arrest prevents bristle progenitor self-renewal and synchronizes cell divisions with cell fate differentiation. Development.

Bandura, J. L., H. Jiang, D. W. Nickerson and B. A. Edgar, 2013 The molecular chaperone Hsp90 is required for cell cycle exit in Drosophila melanogaster. PLoS Genet 9**:** e1003835.

Barski, A., S. Cuddapah, K. Cui, T. Y. Roh, D. E. Schones *et al.*, 2007 High-resolution profiling of histone methylations in the human genome. Cell 129**:** 823-837.

Bi, X., D. Srikanta, L. Fanti, S. Pimpinelli, R. Badugu *et al.*, 2005 Drosophila ATM and ATR checkpoint kinases control partially redundant pathways for telomere maintenance. Proc Natl Acad Sci U S A 102**:** 15167-15172.

Brady, M. E., D. M. Ozanne, L. Gaughan, I. Waite, S. Cook *et al.*, 1999 Tip60 is a nuclear hormone receptor coactivator. J Biol Chem 274**:** 17599-17604.

Brodsky, M. H., W. Nordstrom, G. Tsang, E. Kwan, G. M. Rubin *et al.*, 2000 Drosophila p53 binds a damage response element at the reaper locus. Cell 101**:** 103-113.

Buttitta, L. A., A. J. Katzaroff and B. A. Edgar, 2010 A robust cell cycle control mechanism limits E2F-induced proliferation of terminally differentiated cells in vivo. J Cell Biol 189**:** 981-996.

Buttitta, L. A., A. J. Katzaroff, C. L. Perez, A. de la Cruz and B. A. Edgar, 2007 A double-assurance mechanism controls cell cycle exit upon terminal differentiation in Drosophila. Dev Cell 12**:** 631-643.

Cagan, R. L., and D. F. Ready, 1989 The emergence of order in the Drosophila pupal retina. Dev Biol 136**:** 346-362.

Ceol, C. J., and H. R. Horvitz, 2004 A new class of C. elegans synMuv genes implicates a Tip60/NuA4-like HAT complex as a negative regulator of Ras signaling. Dev Cell 6**:** 563-576.

Chen, P. B., J. H. Hung, T. L. Hickman, A. H. Coles, J. F. Carey *et al.*, 2013 Hdac6 regulates Tip60-p400 function in stem cells. Elife 2**:** e01557.

Choy, J. S., B. T. Tobe, J. H. Huh and S. J. Kron, 2001 Yng2p-dependent NuA4 histone H4 acetylation activity is required for mitotic and meiotic progression. J Biol Chem 276**:** 43653-43662.

Clarke, A. S., J. E. Lowell, S. J. Jacobson and L. Pillus, 1999 Esa1p is an essential histone acetyltransferase required for cell cycle progression. Mol Cell Biol 19**:** 2515-2526.

DeBruhl, H., H. Wen and J. S. Lipsick, 2013 The complex containing Drosophila Myb and RB/E2F2 regulates cytokinesis in a histone H2Av-dependent manner. Mol Cell Biol 33**:** 1809-1818.

Dimova, D. K., O. Stevaux, M. V. Frolov and N. J. Dyson, 2003 Cell cycle-dependent and cell cycle-independent control of transcription by the Drosophila E2F/RB pathway. Genes Dev 17**:** 2308-2320.

Doyon, Y., and J. Cote, 2004 The highly conserved and multifunctional NuA4 HAT complex. Curr Opin Genet Dev 14**:** 147-154.

Doyon, Y., W. Selleck, W. S. Lane, S. Tan and J. Cote, 2004 Structural and functional conservation of the NuA4 histone acetyltransferase complex from yeast to humans. Mol Cell Biol 24**:** 1884-1896.

Fang, X., and P. N. Adler, 2010 Regulation of cell shape, wing hair initiation and the actin cytoskeleton by Trc/Fry and Wts/Mats complexes. Dev Biol 341**:** 360-374.

Fazzio, T. G., J. T. Huff and B. Panning, 2008 An RNAi screen of chromatin proteins identifies Tip60-p400 as a regulator of embryonic stem cell identity. Cell 134**:** 162-174.

Fichelson, P., and M. Gho, 2004 Mother-daughter precursor cell fate transformation after Cdc2 down-regulation in the Drosophila bristle lineage. Dev Biol 276**:** 367-377.

Filion, G. J., J. G. van Bemmel, U. Braunschweig, W. Talhout, J. Kind *et al.*, 2010 Systematic protein location mapping reveals five principal chromatin types in Drosophila cells. Cell 143**:** 212-224.

Flegel, K., D. Sun, O. Grushko, Y. Ma and L. Buttitta, 2013 Live Cell Cycle Analysis of Drosophila Tissues using the Attune Acoustic Focusing Cytometer and Vybrant DyeCycle Violet DNA Stain. J Vis Exp.

Forristal, C., S. A. Henley, J. I. MacDonald, J. R. Bush, C. Ort *et al.*, 2014 Loss of the mammalian DREAM complex deregulates chondrocyte proliferation. Mol Cell Biol 34**:** 2221-2234.

Frank, S. R., T. Parisi, S. Taubert, P. Fernandez, M. Fuchs *et al.*, 2003 MYC recruits the TIP60 histone acetyltransferase complex to chromatin. EMBO Rep 4**:** 575-580.

Frolov, M. V., D. S. Huen, O. Stevaux, D. Dimova, K. Balczarek-Strang *et al.*, 2001 Functional antagonism between E2F family members. Genes Dev 15**:** 2146-2160.

Frolov, M. V., N. S. Moon and N. J. Dyson, 2005 dDP is needed for normal cell proliferation. Mol Cell Biol 25**:** 3027-3039.
Frolov, M. V., O. Stevaux, N. S. Moon, D. Dimova, E. J. Kwon *et al.*, 2003 G1 cyclin-dependent kinases are insufficient to reverse dE2F2-mediated repression. Genes Dev 17**:** 723-728.
Gao, C., E. Bourke, M. Scobie, M. A. Famme, T. Koolmeister *et al.*, 2014 Rational design and validation of a Tip60 histone acetyltransferase inhibitor. Sci Rep 4**:** 5372.
Georlette, D., S. Ahn, D. M. MacAlpine, E. Cheung, P. W. Lewis *et al.*, 2007 Genomic profiling and expression studies reveal both positive and negative activities for the Drosophila Myb MuvB/dREAM complex in proliferating cells. Genes Dev 21**:** 2880-2896.
Gordon, G. M., T. Zhang, J. Zhao and W. Du, 2013 Deregulated G1-S control and energy stress contribute to the synthetic-lethal interactions between inactivation of RB and TSC1 or TSC2. J Cell Sci 126**:** 2004-2013.
Gorrini, C., M. Squatrito, C. Luise, N. Syed, D. Perna *et al.*, 2007 Tip60 is a haplo-insufficient tumour suppressor required for an oncogene-induced DNA damage response. Nature 448**:** 1063-1067.
Gursoy-Yuzugullu, O., N. House and B. D. Price, 2015 Patching Broken DNA: Nucleosome Dynamics and the Repair of DNA Breaks. J Mol Biol.
Hanai, K., H. Furuhashi, T. Yamamoto, K. Akasaka and S. Hirose, 2008 RSF governs silent chromatin formation via histone H2Av replacement. PLoS Genet 4**:** e1000011.
Hardy, S., P. E. Jacques, N. Gevry, A. Forest, M. E. Fortin *et al.*, 2009 The euchromatic and heterochromatic landscapes are shaped by antagonizing effects of transcription on H2A.Z deposition. PLoS Genet 5**:** e1000687.
Hattori, T., F. Coustry, S. Stephens, H. Eberspaecher, M. Takigawa *et al.*, 2008 Transcriptional regulation of chondrogenesis by coactivator Tip60 via chromatin association with Sox9 and Sox5. Nucleic Acids Res 36**:** 3011-3024.
Hu, Y., J. B. Fisher, S. Koprowski, D. McAllister, M. S. Kim *et al.*, 2009 Homozygous disruption of the Tip60 gene causes early embryonic lethality. Dev Dyn 238**:** 2912-2921.
Inaba, M., H. Yuan and Y. M. Yamashita, 2011 String (Cdc25) regulates stem cell maintenance, proliferation and aging in Drosophila testis. Development 138**:** 5079-5086.
Joyce, E. F., M. Pedersen, S. Tiong, S. K. White-Brown, A. Paul *et al.*, 2011 Drosophila ATM and ATR have distinct activities in the regulation of meiotic DNA damage and repair. J Cell Biol 195**:** 359-367.
Judes, G., K. Rifai, M. Ngollo, M. Daures, Y. J. Bignon *et al.*, 2015 A bivalent role of TIP60 histone acetyl transferase in human cancer. Epigenomics 7**:** 1351-1363.
Kondo, S., and N. Perrimon, 2011 A genome-wide RNAi screen identifies core components of the G-M DNA damage checkpoint. Sci Signal 4**:** rs1.
Korenjak, M., E. Anderssen, S. Ramaswamy, J. R. Whetstine and N. J. Dyson, 2012 RBF binding to both canonical E2F targets and noncanonical targets depends on functional dE2F/dDP complexes. Mol Cell Biol 32**:** 4375-4387.
Korenjak, M., B. Taylor-Harding, U. K. Binne, J. S. Satterlee, O. Stevaux *et al.*, 2004 Native E2F/RBF complexes contain Myb-interacting proteins and repress transcription of developmentally controlled E2F target genes. Cell 119**:** 181-193.
Kusch, T., L. Florens, W. H. Macdonald, S. K. Swanson, R. L. Glaser *et al.*, 2004 Acetylation by Tip60 is required for selective histone variant exchange at DNA lesions. Science 306**:** 2084-2087.

Latorre, I., M. A. Chesney, J. M. Garrigues, P. Stempor, A. Appert *et al.*, 2015 The DREAM complex promotes gene body H2A.Z for target repression. Genes Dev 29**:** 495-500.
Law, C. W., Y. Chen, W. Shi and G. K. Smyth, 2014 voom: Precision weights unlock linear model analysis tools for RNA-seq read counts. Genome Biol 15**:** R29.
Legube, G., L. K. Linares, S. Tyteca, C. Caron, M. Scheffner *et al.*, 2004 Role of the histone acetyl transferase Tip60 in the p53 pathway. J Biol Chem 279**:** 44825-44833.
Lewis, P. W., E. L. Beall, T. C. Fleischer, D. Georlette, A. J. Link *et al.*, 2004 Identification of a Drosophila Myb-E2F2/RBF transcriptional repressor complex. Genes Dev 18**:** 2929-2940.
Li, B., G. M. Gordon, C. H. Du, J. Xu and W. Du, 2010 Specific killing of Rb mutant cancer cells by inactivating TSC2. Cancer Cell 17**:** 469-480.
Li, H., C. Cuenin, R. Murr, Z. Q. Wang and Z. Herceg, 2004 HAT cofactor Trrap regulates the mitotic checkpoint by modulation of Mad1 and Mad2 expression. EMBO J 23**:** 4824-4834.
Liao, Y., G. K. Smyth and W. Shi, 2014 featureCounts: an efficient general purpose program for assigning sequence reads to genomic features. Bioinformatics 30**:** 923-930.
Link, N., P. Kurtz, M. O'Neal, G. Garcia-Hughes and J. M. Abrams, 2013 A p53 enhancer region regulates target genes through chromatin conformations in cis and in trans. Genes Dev 27**:** 2433-2438.
Litovchick, L., L. A. Florens, S. K. Swanson, M. P. Washburn and J. A. DeCaprio, 2011 DYRK1A protein kinase promotes quiescence and senescence through DREAM complex assembly. Genes Dev 25**:** 801-813.
Litovchick, L., S. Sadasivam, L. Florens, X. Zhu, S. K. Swanson *et al.*, 2007 Evolutionarily conserved multisubunit RBL2/p130 and E2F4 protein complex represses human cell cycle-dependent genes in quiescence. Mol Cell 26**:** 539-551.
Lorbeck, M., K. Pirooznia, J. Sarthi, X. Zhu and F. Elefant, 2011 Microarray analysis uncovers a role for Tip60 in nervous system function and general metabolism. PLoS One 6**:** e18412.
Lu, J., M. L. Ruhf, N. Perrimon and P. Leder, 2007 A genome-wide RNA interference screen identifies putative chromatin regulators essential for E2F repression. Proc Natl Acad Sci U S A 104**:** 9381-9386.
Lu, P. Y., N. Levesque and M. S. Kobor, 2009 NuA4 and SWR1-C: two chromatin-modifying complexes with overlapping functions and components. Biochem Cell Biol 87**:** 799-815.
Martin, F. A., and G. Morata, 2006 Compartments and the control of growth in the Drosophila wing imaginal disc. Development 133**:** 4421-4426.
Mata, J., S. Curado, A. Ephrussi and P. Rorth, 2000 Tribbles coordinates mitosis and morphogenesis in Drosophila by regulating string/CDC25 proteolysis. Cell 101**:** 511-522.
Mazouzi, A., A. Stukalov, André C. Müller, D. Chen, M. Wiedner *et al.*, A Comprehensive Analysis of the Dynamic Response to Aphidicolin-Mediated Replication Stress Uncovers Targets for ATM and ATMIN. Cell Reports 15**:** 893-908.
McGuire, S. E., Z. Mao and R. L. Davis, 2004 Spatiotemporal gene expression targeting with the TARGET and gene-switch systems in Drosophila. Sci STKE 2004**:** pl6.
McMahon, S. B., M. A. Wood and M. D. Cole, 2000 The essential cofactor TRRAP recruits the histone acetyltransferase hGCN5 to c-Myc. Mol Cell Biol 20**:** 556-562.
Milan, M., S. Campuzano and A. Garcia-Bellido, 1996 Cell cycling and patterned cell proliferation in the Drosophila wing during metamorphosis. Proc Natl Acad Sci U S A 93**:** 11687-11692.

Mitchell, H. K., J. Roach and N. S. Petersen, 1983 The morphogenesis of cell hairs on Drosophila wings. Dev Biol 95**:** 387-398.
Neufeld, T. P., A. F. de la Cruz, L. A. Johnston and B. A. Edgar, 1998 Coordination of growth and cell division in the Drosophila wing. Cell 93**:** 1183-1193.
Ni, J. Q., R. Zhou, B. Czech, L. P. Liu, L. Holderbaum *et al.*, 2011 A genome-scale shRNA resource for transgenic RNAi in Drosophila. Nat Methods 8**:** 405-407.
O'Keefe, D. D., S. R. Thomas, K. Bolin, E. Griggs, B. A. Edgar *et al.*, 2012 Combinatorial control of temporal gene expression in the Drosophila wing by enhancers and core promoters. BMC Genomics 13**:** 498.
Oikonomou, C., and F. R. Cross, 2010 Frequency control of cell cycle oscillators. Curr Opin Genet Dev 20**:** 605-612.
Orlando, D. A., C. Y. Lin, A. Bernard, J. Y. Wang, J. E. Socolar *et al.*, 2008 Global control of cell-cycle transcription by coupled CDK and network oscillators. Nature 453**:** 944-947.
Parker, D. S., Y. Y. Ni, J. L. Chang, J. Li and K. M. Cadigan, 2008 Wingless signaling induces widespread chromatin remodeling of target loci. Mol Cell Biol 28**:** 1815-1828.
Qi, D., H. Jin, T. Lilja and M. Mannervik, 2006 Drosophila Reptin and other TIP60 complex components promote generation of silent chromatin. Genetics 174**:** 241-251.
Reis, T., and B. A. Edgar, 2004 Negative regulation of dE2F1 by cyclin-dependent kinases controls cell cycle timing. Cell 117**:** 253-264.
Rogers, S. L., and G. C. Rogers, 2008 Culture of Drosophila S2 cells and their use for RNAi-mediated loss-of-function studies and immunofluorescence microscopy. Nat Protoc 3**:** 606-611.
Rong, Y. S., S. W. Titen, H. B. Xie, M. M. Golic, M. Bastiani *et al.*, 2002 Targeted mutagenesis by homologous recombination in D. melanogaster. Genes Dev 16**:** 1568-1581.
Rovani, M. K., C. B. Brachmann, G. Ramsay and A. L. Katzen, 2012 The dREAM/Myb-MuvB complex and Grim are key regulators of the programmed death of neural precursor cells at the Drosophila posterior wing margin. Dev Biol.
Royzman, I., A. J. Whittaker and T. L. Orr-Weaver, 1997 Mutations in Drosophila DP and E2F distinguish G1-S progression from an associated transcriptional program. Genes Dev 11**:** 1999-2011.
Sadasivam, S., and J. A. Decaprio, 2013 The DREAM complex: master coordinator of cell cycle-dependent gene expression. Nat Rev Cancer 13**:** 585-595.
Sanchez, R., J. Meslamani and M. M. Zhou, 2014 The bromodomain: from epigenome reader to druggable target. Biochim Biophys Acta 1839**:** 676-685.
Sapountzi, V., I. R. Logan and C. N. Robson, 2006 Cellular functions of TIP60. Int J Biochem Cell Biol 38**:** 1496-1509.
Schubiger, M., and J. Palka, 1987 Changing spatial patterns of DNA replication in the developing wing of Drosophila. Dev Biol 123**:** 145-153.
Seher, T. C., and M. Leptin, 2000 Tribbles, a cell-cycle brake that coordinates proliferation and morphogenesis during Drosophila gastrulation. Curr Biol 10**:** 623-629.
Shibutani, S. T., A. F. de la Cruz, V. Tran, W. J. Turbyfill, 3rd, T. Reis *et al.*, 2008 Intrinsic negative cell cycle regulation provided by PIP box- and Cul4Cdt2-mediated destruction of E2f1 during S phase. Dev Cell 15**:** 890-900.
Squatrito, M., C. Gorrini and B. Amati, 2006 Tip60 in DNA damage response and growth control: many tricks in one HAT. Trends Cell Biol 16**:** 433-442.

Sun, D., and L. Buttitta, 2015 Protein phosphatase 2A promotes the transition to G0 during terminal differentiation in Drosophila. Development 142**:** 3033-3045.
Sun, Y., X. Jiang, S. Chen, N. Fernandes and B. D. Price, 2005 A role for the Tip60 histone acetyltransferase in the acetylation and activation of ATM. Proc Natl Acad Sci U S A 102**:** 13182-13187.
Sun, Y., X. Jiang and B. D. Price, 2010 Tip60: connecting chromatin to DNA damage signaling. Cell Cycle 9**:** 930-936.
Sun, Y., Y. Xu, K. Roy and B. D. Price, 2007 DNA damage-induced acetylation of lysine 3016 of ATM activates ATM kinase activity. Mol Cell Biol 27**:** 8502-8509.
Swaminathan, J., E. M. Baxter and V. G. Corces, 2005 The role of histone H2Av variant replacement and histone H4 acetylation in the establishment of Drosophila heterochromatin. Genes Dev 19**:** 65-76.
Tang, Y., J. Luo, W. Zhang and W. Gu, 2006 Tip60-dependent acetylation of p53 modulates the decision between cell-cycle arrest and apoptosis. Mol Cell 24**:** 827-839.
Tapias, A., Z. W. Zhou, Y. Shi, Z. Chong, P. Wang *et al.*, 2014 Trrap-dependent histone acetylation specifically regulates cell-cycle gene transcription to control neural progenitor fate decisions. Cell Stem Cell 14**:** 632-643.
Taubert, S., C. Gorrini, S. R. Frank, T. Parisi, M. Fuchs *et al.*, 2004 E2F-dependent histone acetylation and recruitment of the Tip60 acetyltransferase complex to chromatin in late G1. Mol Cell Biol 24**:** 4546-4556.
Tea, J. S., and L. Luo, 2011 The chromatin remodeling factor Bap55 functions through the TIP60 complex to regulate olfactory projection neuron dendrite targeting. Neural Dev 6**:** 5.
Thacker, S. A., P. C. Bonnette and R. J. Duronio, 2003 The contribution of E2F-regulated transcription to Drosophila PCNA gene function. Curr Biol 13**:** 53-58.
Treisman, J. E., 2013 Retinal differentiation in Drosophila. Wiley Interdiscip Rev Dev Biol 2**:** 545-557.
van Bergeijk, P., J. Heimiller, L. Uyetake and T. T. Su, 2012 Genome-wide expression analysis identifies a modulator of ionizing radiation-induced p53-independent apoptosis in Drosophila melanogaster. PLoS One 7**:** e36539.
Wen, H., L. Andrejka, J. Ashton, R. Karess and J. S. Lipsick, 2008 Epigenetic regulation of gene expression by Drosophila Myb and E2F2-RBF via the Myb-MuvB/dREAM complex. Genes Dev 22**:** 601-614.
Xie, H. B., and K. G. Golic, 2004 Gene deletions by ends-in targeting in Drosophila melanogaster. Genetics 168**:** 1477-1489.
Xu, S., R. Wilf, T. Menon, P. Panikker, J. Sarthi *et al.*, 2014 Epigenetic control of learning and memory in Drosophila by Tip60 HAT action. Genetics 198**:** 1571-1586.
Yang, L., and J. Yu, 2009 A comparative analysis of divergently-paired genes (DPGs) among Drosophila and vertebrate genomes. BMC Evol Biol 9**:** 55.
Zielke, N., K. J. Kim, V. Tran, S. T. Shibutani, M. J. Bravo *et al.*, 2011 Control of Drosophila endocycles by E2F and CRL4(CDT2). Nature 480**:** 123-127.
Zielke, N., J. Korzelius, M. van Straaten, K. Bender, G. F. Schuhknecht *et al.*, 2014 Fly-FUCCI: A Versatile Tool for Studying Cell Proliferation in Complex Tissues. Cell Rep 7**:** 588-598.

CHAPTER III

Ecdysone signaling induces two phases of cell cycle exit in *Drosophila* cells

Portions of this chapter have been reviewed and were in revision for resubmission to the journal "Biology Open".

Author Contributions: I specifically performed the experiments found in Fig. 3.4 B-H, Fig 3.5 A-C, Fig. 3.1a. D, Fig. 3.3a. B and created the model diagram in Fig. 3.7. I assisted in the preparation of samples for RNA-seq. Jayashree Kumar and Daniel J. McKay performed the RNA-seq analysis.

Abstract

During development cell proliferation and differentiation must be tightly coordinated to ensure proper tissue morphogenesis. Because steroid hormones are central regulators of developmental timing, the links between steroid hormone signaling and cell proliferation are crucial. Here we examined the mechanism by which the steroid hormone ecdysone regulates the cell cycle in *Drosophila*. We find that a cell cycle arrest induced by ecdysone in *Drosophila* cell culture is analogous to a G2 cell cycle arrest observed in the early pupa wing. We show that in the wing, ecdysone signaling at the larva to puparium transition induces Broad which in turn represses the cdc25c phosphatase String. The repression of String generates a temporary G2 arrest that synchronizes the cell cycle in the wing epithelium during early pupa wing elongation and flattening. As ecdysone levels decline during early metamorphosis, Broad expression plummets

allowing String to become re-activated, which promotes rapid G2/M progression and a subsequent synchronized final cell cycle in the wing. In this manner, pulses of ecdysone can both synchronize the final cell cycle and promote the coordinated acquisition of terminal differentiation characteristics in the wing.

Introduction

Steroid hormones play a central role in coordinating the timing of developmental events. The insect steroid hormone ecdysone is a critical regulator of developmental transitions in hemi- and holometabolous insects, and has long served as a model to study the mechanisms by which steroid hormones control developmental timing (Yamanaka et al., 2013). The ecdysone nuclear hormone receptor signaling pathway is most closely related to the retinoic acid signaling pathway in vertebrates, which also acts a key modulator of cell differentiation in many cell types (Breitman et al., 1980). A pulse of ecdysone signaling occurs during the initiation of metamorphosis at the larval to pupal transition (Ashburner, 1989), where extensive changes in proliferation, cell shape, apoptosis and cell adhesion take place. For example the strong ecdysone pulse at the larva to puparium transition leads to activation of apoptotic programs in many larval cell types such as the salivary gland, muscle and midgut (Jiang et al., 1997; Jiang et al., 2000; Lee et al., 2002; Yin and Thummel, 2004; Zirin et al., 2013) while in other tissues such as the abdominal histoblasts or Dorsal Adult Progenitor (DAP) cells of trachea, proliferation of adult progenitors is triggered (Djabrayan et al., 2014; Ninov et al., 2009). In the case of abdominal histoblasts, these cells remain quiescent in the G2 phase of the cell cycle during larval development, and are poised to enter mitosis and proliferate when the rate-limiting G2-M cdc25c phosphatase String (Stg) is induced by ecdysone. Normally as a regulator of mitotic entry, Stg

itself is not sufficient to drive the entire cell cycle and therefore proliferation (Neufeld et al., 1998). However the dramatic proliferative response in histoblasts to the induction of Stg occurs because these cells accumulate high levels of the G1-S rate-limiting cyclin, Cyclin E (CycE) during the G2 arrest. The accumulation of CycE drives the subsequent G1-S transition, making Stg induction in these cells uniquely sufficient to induce a rapid proliferative response to remodel the abdomen during pupal stages (Ninov et al., 2009). In this manner the pulse of ecdysone that triggers the larval-puparium transition also induces rapid and sustained cell-type specific changes in cell cycle dynamics.

In contrast to the abdominal histoblasts, other adult precursors such as the imaginal eye, wing and leg discs exhibit reduced proliferation during the early pupal stages and ultimately become postmitotic one day after the larval to puparium transition (Buttitta et al., 2007; Graves and Schubiger, 1982; Milan et al., 1996; Schubiger and Palka, 1987). How can we explain the different cell cycle and survival responses of tissues to the same system-wide pulse of hormone? The differential effects of ecdysone on specific cell types has been postulated to be due in part to different ecdysone receptor (EcR) isoform expression (Cherbas et al., 2003; Davis et al., 2005; Gautam et al., 2015; Schubiger et al., 2003). The ecdysone receptor complex is a heterodimer of two nuclear receptors, EcR and Ultraspiracle (USP). The ecdysone ligand binds to the EcR subunit of the heterodimer and the *EcR* gene locus in *Drosophila* encodes 3 isoforms (EcR-A, EcR-B1 and EcR-B2) that have identical DNA and ligand binding domains but differ in their N-terminal domains. In the wing, the focus of our study here, EcR-A and EcR-B1 are both expressed in the pouch where the progenitors of the wing blade reside, but during early metamorphosis EcR-B1 levels drop and the predominant EcR in the wing becomes the EcR-A isoform (Schubiger et al., 2003; Talbot et al., 1993). This isoform of the receptor is thought to

contain a repressive domain that is absent from the other isoforms, such that in the absence of ecdysone it represses target gene expression, but in the presence of ecdysone, these targets become de-repressed (Mouillet 2001, Schubiger, Truman 2005). In contrast, the imaginal histoblasts predominantly express EcR-B1 (Talbot et al., 1993), but this changes upon the larval-puparium transition after which histoblasts express both EcR-A and EcR-B1 isoforms (Ninov et al., 2007). While different EcR receptor isoforms may shape some of the differential responses to ecdysone in the imaginal discs versus other tissues, it is becoming clear that many targets for each receptor isoform can also be cell type specific (Stoiber et al., 2016).

Several studies have investigated how ecdysone signaling impacts the cell cycle in larval imaginal discs. For example *ecdysoneless (ecd)* temperature sensitive mutants, which severely reduce ecdysone production at the restrictive temperature, exhibit disruption of cell cycle progression in a proliferative region of the developing eye disc termed the second mitotic wave (SMW). This wave of proliferation is preceded by the front of initial photoreceptor differentiation in the developing eye disc termed the morphogenetic furrow, which sweeps across the disc from the posterior to anterior during late larval and early prepupal stages. In the SMW of *ecd* mutants, proliferation and expression of the mitotic cyclin, Cyclin B (CycB) is dramatically reduced (Brennan et al., 1998). Consistent with ecdysone signaling promoting proliferation, disruption of the USP component of the ecdysone receptor complex also leads to fewer proliferating cells in the area of the SMW (Zelhof et al., 1997). Ecdysone signaling has also been linked to proliferation in the larval wing imaginal disc. For example, larval wings with suppressed ecdysone signaling contain fewer and smaller cells, in part due to upregulation of the growth suppressor Thor (Herboso et al., 2015). Ecdysone signaling is also required for expression of the zinc-finger transcription factor Crooked legs (Crol), which is required in the

larval wing for proper cell proliferation and survival (Mitchell et al., 2008). Furthermore ecdysone signaling also acts through Crol and Wingless to indirectly regulate CycB levels at the wing margin, an area at the dorso-ventral wing boundary where the cell proliferation pattern is distinct from the rest of the developing future wing blade (Mitchell et al., 2013). In addition, ecdysone signaling impinges on another growth and proliferation pathway in the wing, the Hippo signaling pathway (Saucedo and Edgar, 2007). An EcR co-activator Taiman (Tai) binds to the downstream Hippo pathway transcription factor Yorkie, and is also required for normal proliferation in the larval wing pouch (Zhang et al., 2015). Thus, in the larval stages where wing cells are largely asynchronously proliferating, ecdysone signaling is critical for proper proliferation and growth.

By contrast, the response of the imaginal wing disc to ecdysone during the larval-puparium transition and metamorphosis is quite different. Cell cycle regulation in the wing during metamorphosis is interesting because the wing undergoes precise temporally regulated cell cycle alterations prior to a permanent cell cycle exit. In the prepupal wing, a temporary G2 arrest precedes the final cell cycle, leading to a roughly synchronized final cell cycle followed by permanent cell cycle arrest (Fain and Stevens, 1982; O'Keefe et al., 2012). Leg discs also perform a temporary G2 arrest, that precedes the final cell cycle and ultimate arrest of proliferation with similar timing to the wing during metamorphosis (Graves and Schubiger, 1982). The final cell cycle arrest in these tissues occurs at 24h APF at 25°C, which corresponds to the beginning of the largest pulse of the active form of ecdysone 20-hydroxyecdysone (20-HE) during fly development. However, the temporary G2 arrest occurs just a few hours after the second-largest ecdysone pulse, which triggers the larva-puparium transition (Ashburner, 1989).

The model that the synchronized cell cycle alterations in the imaginal disc during metamorphosis are induced by ecdysone signaling is pervasive, and supported by the finding over 30 years ago that 20-HE exposure in *Drosophila* tissue culture cells can induce a cell cycle arrest in G2 phase (reviewed in Echalier, 1997; Stevens et al., 1980). Even more provocatively, removal of 20-HE after 3 days simulating a long pulse, was reported to trigger transient mitotic re-entry, potentially analogous to the final cell cycle observed in imaginal discs after the G2 arrest (Besson et al., 1987). Despite thorough descriptions of these ecdysone induced cell cycle alterations in cell culture, the mechanisms underlying the response of the cell cycle machinery to ecdysone and how they might relate to the cell cycle changes observed *in vivo* during wing metamorphosis have remained largely unknown. Here we reveal a pathway by which ecdysone signaling in the wing can modulate the cell cycle to coordinate cell cycle arrest with the events of cellular differentiation during metamorphosis.

Results

20-HE induces G2 phase cell cycle arrest

The levels of ecdysone signaling in specific tissues are difficult to manipulate *in vivo* without disrupting other aspects of metamorphosis. We therefore wondered whether *Drosophila* cell culture could be used as a model to examine the effects of ecdysone signaling on the cell cycle during wing metamorphosis. First, we examined the cell cycle arrest induced by 20-HE in a wing disc derived cell line, Clone 8 (cl-8) (Peel and Milner, 1990). Cl-8 cells arrest proliferation with a G2 DNA content in response to 0.1-1μg mL^{-1} HE treatment for 24h (Fig. 3.1a.) (Cottam and Milner, 1997b). Unfortunately this cell line had a propensity to clump due to the secretion of cuticle proteins in response to 20-HE (Cottam and Milner, 1997a; Cottam and

Milner, 1997b), which inhibited acquisition of clean, quantitative cell cycle profiles for cl-8 cells by flow cytometry. We therefore examined the cell cycle response to 20-HE in other cell lines. Treating the *Drosophila* embryonic plasmatocyte derived cell lines Kc167 (Kc) and S2R+ with 20-HE, also induced a G2 cell cycle arrest, similar to what we observe with cl-8 cells (Besson et al., 1987; Cherbas et al., 2011; Stevens et al., 1980). Kc cells undergo an easily visible cell shape change from a spherical shape to a spindle morphology in response to 20-HE within 18h (Courgeon, 1972; Echalier, 1997), providing a convenient readout to confirm ecdysone responsiveness (Fig. 3.1 A,B, Fig. 3.1a.) . Therefore, subsequent experiments examining cell cycle responses to 20-HE in culture were performed on Kc cells. At concentrations ranging from 0.01 - 1μg mL^{-1} (0.02-2.1μM) 20-HE, a cell cycle arrest occurs in G2 phase within 18h of exposure, reproducibly in 85-95% of cells (Fig. 3.1 C-F, I, Fig. 3.1a.). At time points after 24h of exposure, the cell cycle arrest is sustained and accompanied by cell death (Fig. 1E, Fig. 3.1a.) (Besson et al., 1987). Prolonged exposure to 20-HE beyond 3 days selected for a small population of cells that remain rounded and resistant to the cell cycle arrest and cell death. These results are consistent with previous observations that long-term exposure selects for cells that failed to respond or become non-responsive to 20-HE (Besson et al., 1987; Stevens et al., 1980).

When we performed RNAi mediated knockdown to all isoforms of the 20-HE receptor EcR, the cell cycle and cell death responses to 20-HE were completely abrogated (Fig. 3.1 F,I, Fig. 3.1a.). RNAi to EcR was highly effective (Fig. 3.2a.) and increased Kc cell proliferation and survival, even in the absence of exogenously provided 20-HE, suggesting that under normal culture conditions Kc cells respond to low levels of endogenous 20-HE (Fig. 3.1a.). This may be responsible for the increased G2 population we and others have observed in Kc versus S2R+ cells (Wu et al., 2007).

The Wee/Myt1 kinases are partially responsible for 20-HE induced G2 arrest

To determine how 20-HE blocks the cell cycle in G2, we performed RNAi treatments to knock down key cell cycle regulators of G2 phase and exposed cells to 1μg mL^{-1} 20-HE for 24-48h. We then examined cell cycle phasing by FACS (Fig. 3.1 F) and quantified cell cycle arrest by EdU incorporation (Fig. 3.1 G). A non-specific dsRNA fragment from the Bluescript SK vector, previously shown not to affect cell viability or cycling, served as our control RNAi (Rogers and Rogers, 2008). Knocking down the Cdc2 inhibitory kinases Wee and Myt1 together effectively bypassed the 20-HE induced G2 arrest in about half of the population (Fig. 3.1 F,G), but did not fully suppress the 20-HE induced increase in G2 cells (Fig. I, $p<0.001$). Knockdown of Wee and Myt1 was effective and also affected the cell cycle in cells exposed to vehicle only, leading to a substantially increased proportion of G1 cells compared to control RNAi (Fig. 3.1 F,I, Fig. 3.2a.) and increased cell proliferation (not shown).

We examined the phosphorylation state of Cdc2 using an antibody recognizing the inhibitory phosphorylation catalyzed by Wee and Myt1 (anti-pCdc2). The knockdown of Wee and Myt1 was effective, as it substantially reduced Cdc2 phosphorylation in unexposed Kc cells, which already exhibit a significant fraction of cells in G2-phase (Fig. 3.1 H, Fig. 3.2a.). 20-HE exposure together with Wee/Myt RNAi led to an increase in p-Cdc2 compared to treatment with the RNAi alone, consistent with our FACS showing that the G2 arrest induced by 20-HE partially persists even when Wee/Myt1 are strongly reduced (Fig. 3.1 F,I).

The 20-HE induced G2 arrest is reversible

Previous work mapping origins of replication in Kc cells used a protocol of 20-HE induced G2 arrest followed by release into media without 20-HE, containing hydroxyurea to synchronize cells in S-phase (MacAlpine et al., 2004). This suggested the 20-HE induced G2 arrest was reversible upon 20-HE removal for at least a proportion of cells. To examine how the exposure to a pulse of 20-HE affected subsequent cell cycles following 20-HE removal, we performed a 20-HE G2 arrest and release protocol with EdU labeling, to measure the fraction of cells that re-enter the cell cycle following G2 arrest. We exposed cells to 1μg mL^{-1} 20-HE for 24h and removed the 20-HE by performing washes and providing fresh media. After allowing cells to recover for the indicated times, we counted cells to measure their proliferation rate or exposed them to EdU for a duration sufficient to label about 50% of the total population to measure S-phase re-entry (Fig. 3.2 A,B). Since the addition of fresh media alone can alter cell cycle dynamics in culture, we treated mock controls the same way, in parallel using vehicle only.

We found that 18-32h after recovery from 20-HE induced cell cycle arrest, about 26% of the cells have completed mitosis and re-entered the cell cycle progressing into a subsequent S-phase (Fig. 3.2 A,B). This is in comparison to over 50% of the mock control, which suggests that roughly one half of cells can re-enter a subsequent cell cycle following a 20-HE induced G2 arrest and 20-HE removal. Cells exposed to 20-HE continually for 46h also exhibit a low level of EdU incorporation (about 16%), which may be due to a combination of prolonged cell death and arrest over 2 days selecting for a population of cells that failed to arrest initially or cells that lose responsiveness to 20-HE (Fig. 3.2 A,B).

20-HE removal leads to prolonged alterations in cell cycle dynamics

The proliferation rate of cells after a 20-HE induced arrest also remains slower than that of mock treated controls, even up to 97h after 20-HE removal (Fig. 3.2 C). This could be due to persistent cell death that continues in response to the 20-HE even after removal (Besson et al., 1987) or an alteration of the subsequent cell cycle, such as a prolonged G1 or G1 arrest (Fig. 3.2 D). To examine the effects on the cell cycle in more detail, we performed a timecourse analysis of the cell cycle phase after 20-HE removal. We performed this timecourse under conditions that reduce the amount of apoptosis in response to 20-HE, by reducing the concentration of 20-HE to 0.5µg mL^{-1}. Under these conditions, as quickly as 8h after 20-HE removal, a substantial fraction of cells have re-entered the cell cycle and proceed through mitosis and into the subsequent G1 phase (Fig. 3.2 E). By 24h after 20-HE removal many cells are in G1 phase (42%). By 32-48h after 20-HE removal we begin to see an increase in cycling cells in S and G2 phases, but the majority of the population remains in G1 (55%), suggesting a substantially prolonged G1 or a subsequent G1 arrest in a significant portion of the population occurs following 20-HE removal (Fig. 3.2 E, quantification in Fig. 3.2a. A).

We were interested to find that few cells were in S and G2 phases 24h after 20-HE removal, considering that our EdU labeling experiment indicated that about ½ of cells can re-enter the cell cycle and proceed through an S-phase after 20-HE removal (Fig. 3.2 A,B). This suggests that a prolonged G1 or G1 arrest may follow cell cycle re-entry after 20-HE removal. To confirm this we performed an EdU pulse chase experiment to follow the cell cycle timing of cells that re-enter S-phase after a pulse of 20-HE. We again exposed cells to 20-HE to 0.5µg mL^{-1} for 36-40h followed by removal. Cells were allowed to recover for 6h, then pulsed with EdU for an hour followed by a chase without EdU or 20-HE for the indicated times. We then assayed

the EdU labeled cells by FACS, starting 4h after the EdU pulse, which is equivalent to 12h after 20-HE removal. At this time, 15.2-23.2% of EdU labeled cells have progressed from S-phase through mitosis to the subsequent G1 phase. This is in contrast to 3.8% of the mock treated control, indicating that after 20-HE release the subsequent progression from S-phase to the next G1 proceeds much more rapidly than in mock treated controls. By 20-23h after 20-HE removal (13-16h post EdU labeling) 60.1-74.0% of 20-HE pulsed cells have completed mitosis and now exhibit a G1 DNA content, while only 24% have done so in the mock treated control. Altogether this suggests that after the release from a 20-HE induced G2 arrest, cells that re-enter the cell cycle exhibit a rapid S/G2/M progression, followed by a subsequent prolonged G1 phase (Fig. 3.2 D). This is consistent with the large G1 population we observe 24 and 32h after 20-HE removal in Fig. 3.2 E.

Cell cycle changes during wing metamorphosis are similar to those induced by pulsed 20-HE in cell culture.

The pattern of cell cycle changes we observed in cell culture in response to a pulse of 20-HE is highly reminiscent of the cell cycle dynamics in the *Drosophila* wing blade during early pupal stages (Fig. 3.3A, O'Keefe et al., 2012). The wing blade transitions from a largely asynchronously proliferating tissue in the late third instar larval stage (L3), to a mostly G2 arrested tissue at 6h after the larval-puparium transition (hours after puparium formation or h APF). After the G2 arrest in the wing, a fraction of cells re-enter the cell cycle at 12-18h APF and progress through an additional cell cycle followed by a sustained G1 arrest as the wing becomes quiescent and begins terminal differentiation (Milan et al., 1996; O'Keefe et al., 2012; Schubiger and Palka, 1987). As the larval-puparium transition is triggered by a pulse of ecdysone

(Ashburner, 1989), we wondered whether the temporary G2 arrest at 6h in the wing may be caused by ecdysone signaling at 0h APF, similar to what we observed in cell culture. In the larval wing disc, the EcR/USP complex acts in a repressive manner in the absence of ecdysone, and the binding of ecdysone at the larval-pupa transition relieves this repression. Therefore, knockdown of EcR by RNAi or mutation of USP (the EcR dimerization partner in the wing), mimics early ecdysone exposure and de-represses ecdysone target genes that are normally induced in the wing in response to the ecdysone pulse triggering the larval to puparium transition (Ghbeish et al., 2001; Schubiger and Truman, 2000). To determine whether the G2 arrest in the early pupal wing is due to ecdysone signaling, we knocked down EcR by expressing an EcR RNAi in the dorsal wing using *apterous-Gal4*, *UAS-GFP*, $Gal80^{TS}$ (*ap-Gal4*) for 24-96h and collected wings at 0h APF. We examined the cell cycle distribution in wings by FACS to determine the relative percentages of cells in G1 and G2 compared to controls without the EcR RNAi. Consistent with the G2 arrest we observe in cell culture, we find that inhibition of EcR in the wing resulted in a significant fraction of cells at 0h APF exhibiting a precocious G2 arrest (Fig. 3.3 B). This suggests that ecdysone signaling is sufficient to induce a G2 arrest in the larval *Drosophila* wing.

We performed an RNA- timecourse on wings from L3 to 44h APF to examine the global changes in gene expression during metamorphosis. These timepoints include the L3 larval stage (-10h APF), the temporary G2 arrest (6h APF) the final cell cycle (18h APF), the permanent cell cycle arrest (24h APF), and stages of terminal differentiation including vein differentiation, wing hair formation and cuticle protein production (36 and 44h APF). We observed a striking number of gene expression changes during this timecourse, with over 2,000 genes (~12% of the genome) significantly changing expression in the wing within the first 6h of metamorphosis (Fig. 3.3a.).

Subsequent timepoints also showed dramatic changes in gene expression ranging from over 1,900 genes changing between 6h and 18h APF during cell cycle re-entry from the G2 arrest to nearly 650 changing between 18 and 24h APF when cells complete the final cell cycle and enter quiescence (Supp. Fig. 3.3).

We next examined a set of 183 core cell cycle genes that include the cell cycle Cyclins/Cdks and their key targets and regulators (Fig. 3.3 C, Table 3.1). Cell cycle genes showed generally similar behavior during wing metamorphosis with high expression in the proliferating L3 wing and during the final cell cycle at 18h APF, but lower expression during the 6h G2 arrest and very low expression after completion of the final cell cycle at 24 and 36h APF. We observed reduced mRNA expression for many G2/M cell cycle regulators during the G2 arrest at 6h APF including the mitotic *aurora-A* and *polo* kinases, the G2/M cyclin *cyclinB* and the mitotic checkpoint regulators *mad2*, *bub3* and *fizzy,* the Drosophila homolog of cdc20 (Table 3.1). However we noted that the gene showing the most dramatic reduction specifically at 6h APF, was the rate limiting G2/M phosphatase *string* (*stg*) which removes the phosphorylation on cdc2 catalyzed by the Wee/Myt kinases (Fig. 3.3 C).

We next examined the global gene expression changes during wing metamorphosis for enrichment of specific gene ontology (GO) terms. Consistent with the changes in cell cycle genes we observed, we found that cell cycle-associated terms such as “M-phase”, “nuclear division” and “mitotic cell cycle” were greatly enriched in the genes that decrease expression at 6h APF (Fig. 3.3 D, Fig. 3.4a.). Conversely, the genes that increase expression between 6 and 18h APF during the final cell cycle are strongly enriched for this same set of cell cycle terms, which decrease expression again during cell cycle exit at 24h APF.

We noted that there is also a strong enrichment for genes involved in "RNA processing" (including rRNA) and "ribosome biogenesis" in the genes that decrease expression at 6h APF (Fig. 3.3 D). This is consistent with the observation that the final two cell cycles in the *Drosophila* wing are reductive divisions that occur in the absence of cellular growth, resulting in smaller cells which ultimately stretch and flatten to increase apical area during wing elongation (Aigouy et al., 2010, our unpublished observations; O'Keefe et al., 2012). Altogether our GO term analysis suggests that a significant fraction of the dramatic gene expression changes we observe in the wing during metamorphosis are driven by changes in the cell cycle dynamics of the pupal wing.

A peak of Broad-Z1 expression is correlated with the G2 arrest in the wing.

From our RNA-seq data we next extracted a set of known ecdysone signaling targets (Beckstead et al., 2005; Gauhar et al., 2009; Shlyueva et al., 2014) and plotted their expression levels over time in a clustered heat map, superimposed with the ecdysone titer and key events during these pupal timepoints (Fig. 3.4 A, 20-HE titer graph reproduced from Ashburner, 1989). This revealed multiple waves of ecdysone responses in the pupal wing, including early and late responses induced by the larval-prepupal pulse as well as distinct early and late responses to the larger pulse at 24h APF. We noted a cluster of ecdysone-direct targets that are expressed prior to or during the G2 arrest at 6h APF but are not induced by the second ecdysone pulse at 24h (Fig. 3.4 A, cluster indicated by red line). This cluster included 5 transcription factors, *Kr-h1*, *broad*, *ftz-f1*, *hairy (h)* and *CG9932.* We decided to examine Broad further as a potential regulator for the G2 arrest in the early pupa wing, since the knockdown of EcR by RNAi that induced a precocious G2 arrest in the wing (Fig. 3.3 B) was previously shown to induce precocious

expression of a specific isoform of Broad, Broad-Z1 (Schubiger and Truman, 2000). Importantly, we also found Broad-Z1 to be specifically enriched in wings at 6h APF by western blot (Fig. 3.4 B) and immunofluorescence (Fig. 3.4 C-E), coincident with the G2 arrest. We also detected total Broad expression in wings using an antibody to the Broad-core region that recognizes all Broad isoforms. We found that other isoforms of Broad, most likely transcripts encoding the Z3 isoform (based on our RNA-seq data), are expressed in the larval wing prior to the larval-puparium transition. However we saw no Broad expression at 27h APF following the largest ecdysone pulse, suggesting ecdysone only induces Broad-Z1 in the early prepupal wing (Fig. 3.4 F-H).

Broad regulates the ecdysone-induced G2 cell cycle arrest in early pupal wings

We have shown that the 20-HE–induced G2 arrest in cell culture relies in part upon the Wee/Myt kinases, which phosphorylate and inhibit Cdc2 activity (Fig. 3.1). We also found that *stg* expression, which counteracts the activity of the Wee/Myt kinases on Cdc2 is very low at 6h APF during an ecdysone induced G2 arrest in the wing. We therefore tested whether the G2 arrest in the early prepupa wing was dependent upon inhibitory Cdc2 phosphorylation. To do this, we used the *engrailed-Gal4* driver with a temperature sensitive Gal80 (*en-Gal4/Gal80^{TS}*) to turn on ectopic expression of UAS-driven *stg* and GFP in the posterior wing at 0hr APF. We then dissected wings at 6h APF and stained for the mitotic marker phosphorylated Ser-10 histone H3 (PH3) to determine whether cells in the posterior wing bypassed the G2 arrest and entered into mitosis. Indeed ectopic expression of *stg* robustly bypassed the G2 arrest in 100% of wings at this stage, demonstrating that the arrest is dependent upon inhibitory phosphorylation of Cdc2 (Fig. 3.5 A,B). Previous work had shown that ecdysone signaling could regulate Cyclin B

(CycB) levels in the larval wing margin indirectly through another ecdysone regulated transcription factor *crooked legs* (*crol*) (Mitchell et al., 2013). Since CycB also regulates Cdc2 activity and *cyclin B* levels were also low at 6h APF in our RNA-seq data, we tested whether overexpression of CycB could bypass the G2 arrest. However in 100% of wings robust expression of CycB failed to promote entry into mitosis (Fig. 3.5 C).

We next asked whether inhibition of Broad altered the G2 arrest in the early pupa wing. To inhibit Broad we used a UAS-driven RNAi that targets a common region of *broad* transcripts effectively knocking down all isoforms with the *en-Gal4/Gal80^{TS}* driver. Expression of the *broad* RNAi from the early second larval instar disrupted pupariation and resulted in visible defects in pupa cuticle tanning similar to those reported for overexpression of the repressive EcR-A isoform (Fig. 2.2a., Schubiger et al., 2003). By contrast expression of the RNAi from 0h APF was too weak to show any visible effects on pupal development. We therefore turned on Broad RNAi for only 18-24h prior to 6h APF, which likely results in only a partial knockdown. Nevertheless, expression of *broad* RNAi at these moderate levels resulted in ectopic mitoses (ranging from 3-14) in the posterior wing of 75% of animals (Fig. 3.5 D), consistent with a role for Broad in promoting the G2 cell cycle arrest.

To determine whether Broad may regulate Stg levels, we used a Stg-GFP protein trap line to monitor endogenous Stg expression (Inaba et al., 2011). We combined this protein trap with an *actin-"flipout stop"-Gal4* transgene (*act>Gal4*) to generate heat-shock induced *flp/FRT, UAS-RFP* labeled clones expressing Broad RNAi or a control RNAi to the *white* gene that has no effect on the cell cycle. Clones expressing Broad RNAi exhibit increased expression of Stg-GFP from L3 to 6h APF in the wing (Fig. 3.5 E-G, arrows, Fig. 3.2a.). Conversely ectopic Broad-Z1 overexpression reduces Stg-GFP expression in the proliferating L3 wing (Fig. 3.5 H-I, Fig.

3.2a.). Altogether our data suggests ecdysone signaling acts via Broad to downregulate String to induce a temporary G2 arrest in the pupa wing. The G2 arrest in the early pupal wing can be bypassed by reducing Broad or by providing exogenous String.

Broad binds to the *stg* regulatory locus and overlaps with wing enhancers.

To investigate whether Broad may regulate Stg expression directly, we examined Broad binding to the *string* gene locus at 0h APF using modencode dataset #3806 (www.modencode.org). The *string* regulatory region is modular and extensive spanning >40kb (Lehman et al., 1999; Lopes and Casares, 2015) and several regulatory elements that drive expression in the wing have been previously described (Andrade-Zapata and Baonza, 2014). These regions overlap with accessible potential regulatory elements identified by Formaldehyde-Assisted Isolation of Regulatory Elements (FAIRE) that become inaccessible after cell cycle exit in the late pharate adult tissues (McKay and Lieb, 2013). By aligning Broad binding data with FAIRE data at the *stg* locus, we found that several strong peaks of Broad binding overlap with potential wing regulatory elements (Fig. 3.6 A).

Two Gal4 reporters generated from *stg* regulatory regions (from the Janelia Gal4 collection) that drive expression in the wing overlap with peaks of Broad binding, 32B06 and 32C11. We therefore examined whether the loss of Broad alters the expression of these reporters. In males hemizygous for wild-type *broad*, we observed normal Broad levels and the previously reported expression patterns for these reporters in the wing (Andrade-Zapata and Baonza, 2014). (Fig. 3.6 B,C) By contrast, in animals hemizygous for the *broad npr3* null allele, Broad expression is lost and ectopic reporter expression is observed in the central wing pouch for 32B06, and additional expression in the wing pouch and hinge is observed for 32C11 (Fig. 3.6

D-E). Loss of Broad also disrupts larval development and wing patterning (Jia et al., 2016), resulting in reduced wing size and altered wing pouch shape. Altogether this data suggests that Broad can bind to *stg* regulatory regions that are known to drive expression in the wing and Broad may directly repress *stg* expression.

Discussion

We present a model for how the pulse of ecdysone at the larval to pupal transition impacts the cell cycle dynamics in the wing during metamorphosis (Fig. 3.7). Ecdysone signaling at the larva to puparium transition induces Broad, which in turn represses Stg to generate a temporary G2 arrest, which synchronizes the cell cycle in the wing epithelium. As ecdysone levels decline, Broad expression plummets, allowing Stg to be re-activated resulting in a pulse of cdc2 activity that promotes a rapid G2/M progression during the final cell cycle in the wing. This ultimately culminates in the relatively synchronized cell cycle exit at 24h APF (Milan et al., 1996; Schubiger and Palka, 1987), coinciding with the second large pulse of ecdysone. This second pulse in the pupa activates a different set of transcription factors (not Broad), promoting the acquisition of terminal differentiation characteristics in the wing. In this way, two pulses of ecdysone signaling can both synchronize the final cell cycle by a temporary G2 arrest and coordinate permanent cell cycle exit with the acquisition of terminal differentiation characteristics in the wing.

Over 30 years ago it was shown that 20-HE exposure in *Drosophila* tissue culture cells induces a cell cycle arrest in G2-phase (reviewed in Echalier, 1997; Stevens et al., 1980). This response appears to be shared among 3 different cell lines, Cl-8, Kc and S2 (Fig. 3.1a.). Here we show that in Kc cells, pulsed 20-HE exposure also leads to a G2 arrest followed by rapid cell

cycle re-entry after 20-HE removal and a subsequent prolonged G1 (Fig. 3.2). This cell cycle response to a pulse of 20-HE is reminiscent of the cell cycle changes that occur during early metamorphosis in the pupal wings and legs (Graves and Schubiger, 1982; O'Keefe et al., 2012). It is worth considering why Kc (and S2) cells, which are thought to be derived from embryonic hemocytes would exhibit a similar cell cycle response to 20-HE to the imaginal discs.

Relatively little is known about how ecdysone signaling impacts embryonic hemocytes, although recent work suggests that ecdysone signaling induces embryonic hemocyte cell death under sensitized conditions (Sopko et al., 2015). More is known about larval hemocytes, which differentiate into phagocytic macrophages and disperse into the hemolymph during the first 8h of metamorphosis (Grigorian et al., 2011). Ecdysone is involved in this maturation process, as lymph glands of *ecdysoneless* (*ecd*) mutants fail to disperse mature hemocytes and become hypertrophic in the developmentally arrested mutants (Sorrentino et al., 2002). This suggests that the high levels of systemic ecdysone signaling at the larval-puparium transition mediates a switch from proliferation to cell cycle arrest and terminal differentiation for lymph gland hemocytes during metamorphosis. Without ecdysone signaling, hemocytes may continue to proliferate and fail to undergo terminal differentiation leading to the hypertrophic lymph gland phenotype observed. Further studies will be needed to examine whether the ecdysone induced cell cycle arrest in larval hemocytes occurs in the G2 phase, or whether their cell cycle arrest proceeds via a similar pathway to that shown here for the wing.

The Ecdysone Receptor is a repressive complex in the wing

Multiple lines of evidence suggest that the Ecdysone Receptor complex in the larval wing acts as a repressor for certain early pupa targets and that the binding of ecdysone to the receptor relieves

this repression (Fig. 3.7). For example loss of EcR by RNAi or loss of the EcR dimerization partner, USP, de-represses ecdysone target genes that are high in the early pupal wing such as BroadZ1 and bFtz-F1 (Ghbeish et al., 2001; Schubiger and Truman, 2000). The EcR/USP heterodimer also cooperates with the SMRTR co-repressor in the wing to prevent precocious expression of ecdysone target genes such as BrZ1 (Heck et al., 2012). Consistent with our hypothesis that a repressive EcR/USP complex prevents precocious expression of Broad and thereby a precocious G2 arrest, inhibition of SMRTR can also cause a G2 arrest (Pile et al., 2002). Thus, in the context of the early pupal wing, we propose that the significant pulse of ecdysone at the larval to puparium transition relieves the inhibition of a repressive receptor complex, leading to Broad-Z1 activation (Fig. 3.7). Consistent with this model, high levels of Broad-Z1 in the larval wing lead to precocious neural differentiation at the margin (Schubiger et al., 2005), and in our hands precocious inhibition of *stg* expression in the wing pouch (Fig. 3.5). Interestingly, a switch in Broad isoform expression also occurs during the final cell cycle in the larval eye, such that BrZ1 becomes high in cells undergoing their final cell cycle and entering into terminal differentiation (Brennan et al., 2001). However in this case, BrZ1 expression is not associated with a G2 arrest and occurs in an area of high Stg expression, suggesting the downstream BrZ1 targets in the eye may be distinct from those in the wing.

The Ecdysone Receptor has also been shown to down regulate Wg expression via the transcription factor Crol at the wing margin, to indirectly promote CycB expression (Mitchell et al., 2013). While a loss of EcR at the margin decreased CycB protein levels, effects of EcR loss on CycB levels in the wing blade outside of the margin were not obvious (Mitchell et al., 2013). We suggest that in the wing, the role for EcR outside of the margin acts on the cell cycle via a different mechanism through *stg*. Consistent with a distinct mechanism acting in the wing blade,

over-expression of Cyclin B in the early prepupal wing could not promote increased G2 progression or bypass the prepupal G2 arrest (Fig. 3.5). Instead our results on the prepupal G2 arrest are consistent with previous findings that Stg is the rate-limiting component for G2-M cell cycle progression in the fly wing pouch and blade (Neufeld et al., 1998).

Gene expression changes during metamorphosis in the wing.

In order to identify the gene expression changes in the wing that occur in response to the major peaks of eccdysone during metamorphosis, we performed RNA-seq on a timecourse of pupal wings. We observed major changes in gene expression in this tissue during metamorphosis (Fig. 3.3, Fig. 3.3a.). In addition, we identified known ecdysone targets that are affected differently in the wing during the first larval-to-pupal ecdysone pulse and the second larger pulse at 24h APF (Fig. 3.4). Ecdysone signaling induces different direct targets with distinct kinetics (King-Jones and Thummel, 2005). Furthermore specific targets, for example Ftz-F1 can modulate the expression of other ecdysone targets, to shape the response to the hormone (King-Jones et al., 2005). Thus, we expect that a pulse of ecdysone leads to sustained effects on gene expression and the cell cycle, even after the ecdysone titer returns to its initial state. These factors together with the differences in the magnitude of the ecdysone pulse may contribute to the differences in the response to the early vs. later pulses in the wing.

Ecdysone signaling can also affect the cell cycle and cell cycle exit via indirect mechanisms such as altering cellular metabolism. This is used to promote cell cycle exit and terminal differentiation in neuroblasts, where a switch toward oxidative phosphorylation leads to progressive reductive divisions, (divisions in the absence of growth) leading to reduced neuroblast cell size and eventually terminal differentiation (Homem et al., 2014). Although

reductive divisions do occur in the final cell cycle of the pupa wing (Aigouy et al., 2010, our unpublished results), this type of mechanism does not provide a temporary arrest to synchronize the final cell cycle in neuroblasts as we see in wings. Importantly, we do see a striking reduction in the expression of genes involved in protein synthesis and ribosome biogenesis in the wing during metamorphosis, consistent with the lack of cellular growth (Fig. 3.3, O'Keefe et al., 2012). Instead the increased surface area of the pupal wing comes from a flattening, elongation and apical expansion of the cells due to interactions with the extracellular matrix creating tension and influencing cell shape changes (Etournay et al., 2015). This is also consistent with our findings that a significant number of genes associated with protein targeting to the membrane are increased as the wing begins elongation in the early pupa (Fig. 3). Further studies will be needed to determine whether the changes in expression of genes involved in ribosome biogenesis and protein targeting to the membrane are controlled by ecdysone signaling, or some other downstream event during early wing metamorphosis.

Tissue specific responses to ecdysone can mediate opposite effects on the cell cycle through the same target

Perhaps the most interesting and least understood aspect of steroid hormone signaling is how a diversity of cell-type and tissue-specific responses are generated to an individual hormone. Cell cycle responses to ecdysone signaling are also highly cell type specific. For example, progenitors of the adult abdominal epidermis termed histoblasts become specified during embryogenesis and remain quiescent in G2 phase during larval stages. During pupal development, the abdominal histoblasts are triggered to proliferate by a pulse of ecdysone to replace the larval abdominal epidermis. This is in contrast to the behavior of the wing imaginal disc, where epithelial cells

undergo asynchronous rapid proliferation during larval stages, but during metamorphosis the cell cycle dynamics become restructured to include a G2 arrest followed by a final cell cycle and entry into a permanently postmitotic state.

How do the same system-wide pulses of ecdysone at the larval to puparium transition lead to such divergent effects on the cell cycle? Surprisingly it seems to be through divergent effects on tissue specific pathways that act on the same cell cycle targets. In the abdominal histoblasts the larval to puparium pulse of ecdysone triggers cell cycle re-entry and proliferation via indirect activation of Stg (Ninov et al., 2009), by modulating the expression of a microRNA that targets Stg (Verma and Cohen, 2015) (Fig. 3.4 C). This tissue-specific addition of the microRNA essentially opposes Broad's repressive effects on *stg* expression. Thus, tissue specific programs of gene regulatory networks can create divergent outcomes from the same system-wide hormonal signal, even when they ultimately act on the same target.

Materials and Methods

Cell culture: Clone-8 (Cl-8) and S2R+ cells were obtained from the DGRC. A strongly ecdysone responsive Kc167 subclone was obtain from Dr. K. Cadigan (University of Michigan, Ann Arbor). All cells were cultured at 25°C in Schneider's media (Invitrogen) supplemented with penicillin-streptomycin (Gibco) and 10% heat-inactivated "Optima" fetal bovine serum (Atlanta Biologicals). For Cl-8 cells, the media was supplemented with 5 µg mL^{-1} insulin (Sigma) and 2.5% fly extract. Fly extract was prepared and stored as described (https://dgrc.bio.indiana.edu/include/file/additions_to_medium.pdf). Cell counting/viability was performed manually using a hemocytometer and trypan blue staining. 20-Hydroxyecdysone (Sigma) was dissolved at 1mg mL^{-1} in DMSO or water. RNAi experiments were performed in 6-well dishes, with 1-3X10^6 cells mL^{-1}. Cells were seeded for 12-24h in complete media. Media was removed, cells were washed with 1mL 1XPBS and replaced with 0.5mL serum free medium containing 10-20µg mL^{-1} dsRNA overnight. 0.5mL of complete medium was added and cells were incubated for 3 days prior to flow cytometry or treatment with 20-HE.

Primers used for dsRNA synthesis using T7 Polymerase as described (Rogers and Rogers, 2008):

T7-Wee-fwd: TAATACGACTCACTATAGGGATGACTTTGACAAGGACAC
T7-Wee-rev: TAATACGACTCACTATAGGATCTAGTCGATTGACGCATT

T7-Myt1-fwd: TAATACGACTCACTATAGGAATTGCACGACGACAAACAC
T7-Myt1-rev: TAATACGACTCACTATAGGTGTCCAGATGGATGAGATTC

T7-Myt1-fwd2: TAATACGACTCACTATAGGACAACAATCTGAACCGAAGC
T7-Myt1-rev2: TAATACGACTCACTATAGGTGGAGCCATATACCTCGAAT

T7-EcR-fwd: TAATACGACTCACTATAGGTGCGAAATGGACATGTACAT
T7-EcR-rev: TAATACGACTCACTATAGGTCCCGCGTATATGATCTATT

T7-Br-fwd: TAATACGACTCACTATAGGCTGCAGGATGTCAACTTCAT
T7-Br-rev: TAATACGACTCACTATAGGGTGCTTGATCGTACTGAAGT

Flow cytometry- Flow cytometry analysis for DNA content in Figs 3.1, 3.2 and Fig. 3.1 C was performed on live cells in 1X PBS with DyeCycleViolet (Life Technologies) at a 1:2,000 dilution for 30 minutes at room temperature. Cells were run on an Attune Cytometer (Life Technologies) under standard settings using the Violet laser with the 450/40 filter. Flow cytometry analysis for DNA content in Fig. 3.1a. A was performed on Ethanol fixed cells, treated with RNaseA (Sigma) and stained with propidium iodide (Sigma) as described (Bettencourt-Dias et al., 2004) and analyzed on a FACSCalibur (BD). For EdU incorporation assays, cells were cultured in complete medium with 10 μM EdU for the indicated timepoints, and either chased with complete media lacking EdU for the indicated timepoints prior to fixation (Fig. 3.2 F) or fixed immediately and stained (Figs. 3.1 G and 3.2 A) using the protocol of the Click-IT EdU AlexaFluor-488 Flow Cytometry kit (Life Technologies). For all EdU treated samples DNA was stained with FX CycleViolet (Life Technologies) for 30 min. at room temperature and samples were analyzed on an Attune cytometer. Results from multiple replicates were graphed and analyzed by one-way ANOVA (for comparing groups) or paired t-tests (for individual comparisons) using Prism. P-values are indicated as follows; from $p<0.05$ *, $p<0.01$ **, $p<0.001$ ***, n.s. = $p>0.05$.

Western blots: Western blots were performed using BioRad TGX precast 4-20% gels, and HRP conjugated secondary antibodies with high sensitivity ECL detection reagents (Thermo) as described (Sun and Buttitta, 2015). We used the following antibodies; anti-Tyr15-P-cdc2 (Cell

Signaling Technologies, #9111), anti-EcR common (DSHB, Ag10.2 and DDA2.7), anti-Wee (kindly provided by Dr. S. Campbell), rabbit anti-GFP (1:1000 Invitrogen) anti Broad Z1 and Broad-Core (DSHB, 1:100, #Z1.3C11.OA1 and #25E9.D7), rabbit anti phospho-histone H3 Ser10 (Upstate, 1:4,000), mouse anti-a-tubulin (DSHB, AA4.3 1:1,000) and anti-total cdc2 (Millipore, #06-923). For Fig. 3.1, western blot signal was quantified using Image J and presented as the ratio of pCdc2 to total Cdc2.

Fly stocks: The *w*;*engrailed-Gal4*,*UAS-GFP*; *tub-Gal80TS* and *w*;*apterous-Gal4*,*UAS-GFP*; *tub-Gal80TS* stocks have been described (Buttitta et al., 2007). The *w*;+,*act>CD2,stop>Gal4*,*UAS-dsRed* (BL# 30558) was recombined with the Stg-GFP protein trap (YD0685) kindly provided by Dr. Y. Yamashita (University of Michigan). EcR RNAi (Schubiger and Truman, 2000), Broad TRiP RNAi lines (BL #27272 and #33641) and UAS-BrZ1 (BL#51379) were crossed to y,w,*hsflp*^{122} and are available in the Bloomington Stock Center. The *broad* null allele *npr3* was also used (BL#5964).

Immunofluorescence: For EdU labeling, cells were cultured with 10 µM EdU for 45 min. in complete medium and fixed and stained using the protocol of the Click-IT EdU AlexaFluor-555 Imaging kit (Life Technologies). DNA was stained for 10 min. with 1µg ml^{-1} Hoechst 33258. For *Drosophila* tissues, pupa were collected and staged at 25°C, using the immobile white-prepupa stage as 0h APF. Tissues were dissected and fixed in paraformaldehyde, followed by washed in 1XPBS-0.1%Triton-X100 and blocking and staining as described (Buttitta et al., 2007). For Figs. 3.4-6 all samples within each figure were scanned with the same gain and laser intensity settings as the control genotypes. For Fig. 3.6 GFP signal in the wing pouch (pouch boundary defined by folding at hinge) was quantified (pixels*area) using Image J.

RNAseq Gene expression analysis: Animals were staged at 25°C as described (O'Keefe et al., 2012). Forty wings for each stage were manually dissected and RNA was isolated using Trizol as previously described (McKay and Lieb, 2013). Two independent replicates for each timepoint were performed. Libraries for RNA seq were generated using the stranded mRNA sequencing kit from KAPA Biosystems (catalog # KK8421). Reads were mapped to the genome (dm3) using Tophat2 (Kim et al., 2013) using a transcript annotation file for the alignment. The Htseq-count

tool (Anders et al., 2015) was used to count reads mapping to genes, and the EdgeR package in Bioconductor (Robinson et al., 2010) was used to calculate RPKMs. For heatmaps of core cell cycle gene expression across the time series, the percent maximum of TMM normalized read counts was used for hierarchical clustering analysis based on average linkage. For gene ontology analysis, we defined differentially expressed genes as those having a logCPM greater than 2 in at least one sample and changing by at least 2-fold between pairwise time points. The resulting gene lists were submitted to DAVID (Huang da et al., 2009) gene ontology analysis, and subsequently filtered using REViGO (Supek et al., 2011) to remove redundant terms.

Acknowledgements

We thank Dr. S. Campbell, Dr. M. Schubiger as well as Dr. K. Cadigan and Dr. Y. Yamashita (University of Michigan) for providing reagents. We thank the TRiP at Harvard Medical School (NIH/NIGMS R01-GM084947) for providing transgenic RNAi fly stocks. Stocks obtained from the Bloomington *Drosophila* Stock Center (NIH P40OD018537) were also used in this study. Antibodies were obtained from the Developmental Studies Hybridoma Bank (DSHB), created by the NICHD of the NIH and maintained at The University of Iowa. Cell lines were obtained from the *Drosophila* Genomics Resource Center (DGRC), supported by NIH grant 2P40OD010949-10A1. We thank the members of the Buttitta Lab for helpful discussions and assistance with dissections for RNA-seq experiments.

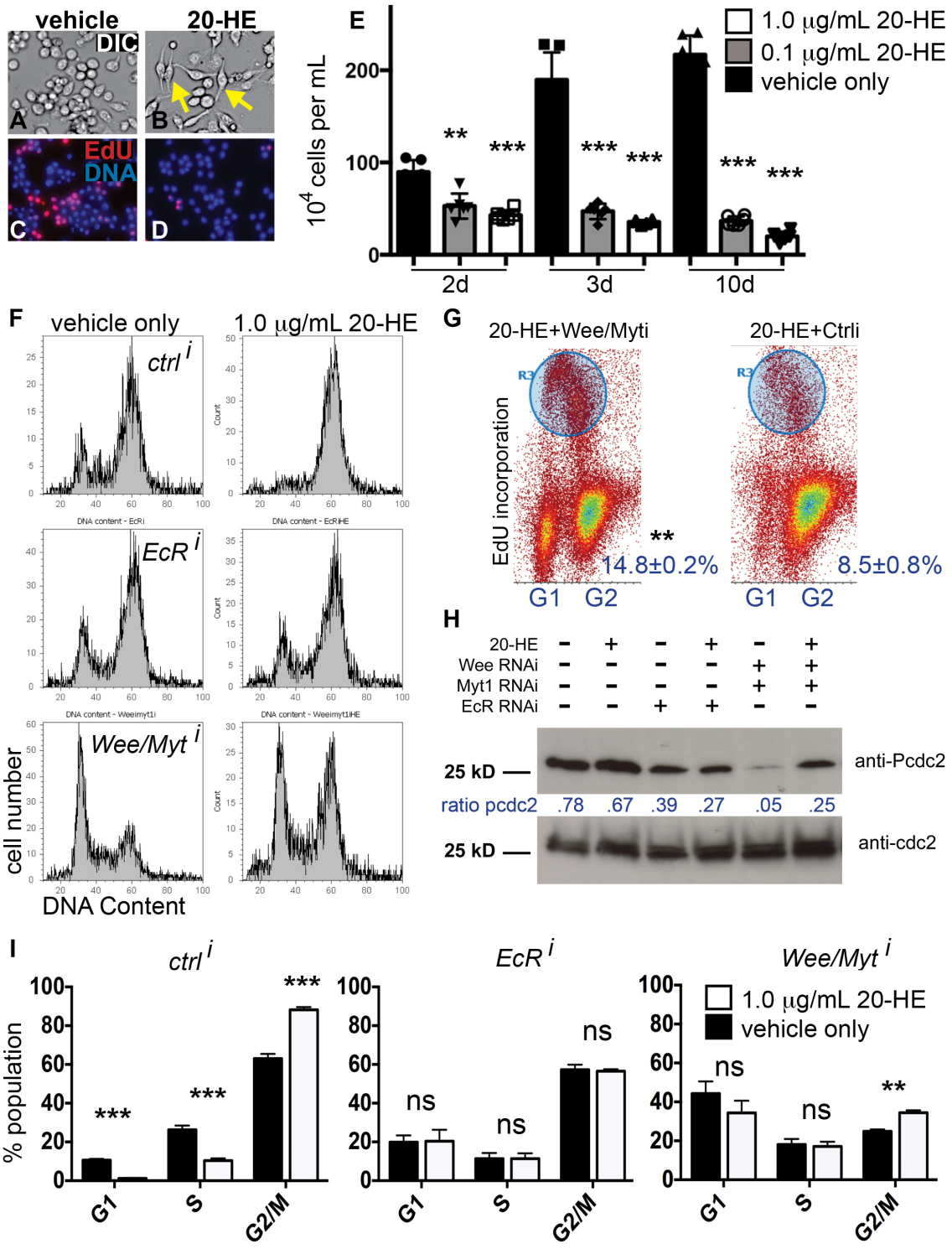

Fig. 3.1 Kc cell response to 20-HE involves a Wee/Myt-dependent cell cycle arrest in G2. Cells were treated with vehicle only (DMSO) or 1μg mL^{-1} 20-Hydroxyecdysone (20-HE) in DMSO for 48 hours (A-I) or the indicated number of days (E). Cells treated with 20-HE exhibit an altered cell shape and reduce EdU incorporation indicating cell cycle arrest (A-D). Sustained

treatment with 20-HE for 2-10 days results in fewer cells from a sustained cell cycle arrest and increased apoptosis (E, see also Fig. 3.1a.) Error bars indicate the s.e.m. of four replicates, p-values were determined by paired t-tests with vehicle treated controls and range from $p<0.01$** to $p<0.001$***. (F) Flow cytometry confirmed that 20-HE induced cell cycle arrest occurs in G2, which can be blocked by treatment with RNAi (i) to the *Ecdysone Receptor* (*EcRi*) or partially blocked by RNAi to the Cdc2 kinases *wee* and *myt1 (wee/myti)*. Control (ctrl) dsRNA matches a region of Bluescript SK vector (Rogers and Rogers, 2008) and does not alter cell growth or proliferation. (G) Treatment with *wee/myt1* RNAi partially restores proliferation as shown by EdU incorporation increasing from 8% to 15% in the presence of 1μg mL^{-1} 20-HE. (H) Levels of tyrosine-15-phosphorylated Cdc2 (pCdc2) are reduced by *EcR* RNAi and *wee/myt1* RNAis. (I) The cell cycle distribution as determined by FACS is altered in the presence of 20-HE. This effect is suppressed by knockdown of EcR. Knockdown of Wee/Myt kinases partially suppresses the increase in the G2 population in response to 20-HE. Error bars indicate the s.e.m. of four replicates, p-values were determined by paired t-tests with vehicle treated controls and range from not significant (ns=$p>0.05$) to $p<0.01$** or $p<0.001$***.

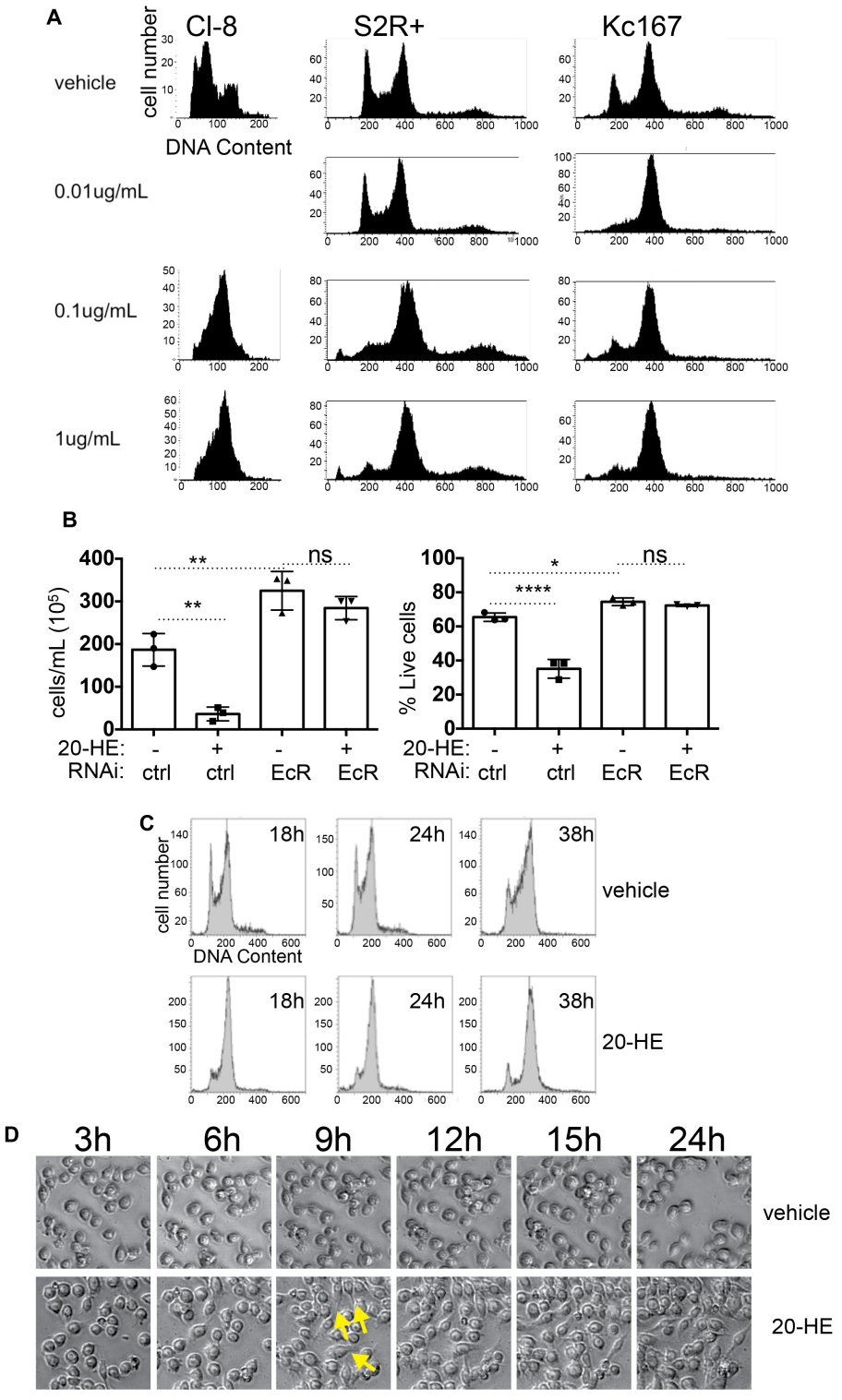

Fig. 3.1a. (A) Cells were treated with vehicle only (DMSO) or the indicated concentration of 20-Hydroxyecdysone (20-HE) in DMSO for 24 hours. DNA content was examined by flow cytometry. (B) Cells were treated with the indicated RNAi for 48h and then exposed to vehicle or 1μg mL^{-1} 20-HE for 48 hours. Cell numbers were counted (left) and trypan blue staining was

used to assay for live/dead cells (right). Knockdown of the Ecdysone Receptor (EcR) prevents cell cycle arrest and apoptosis induced by 20-HE. It also increases cell proliferation and survival in the absence of 20-HE for Kc cells. Error bars indicate s.e.m. t-tests were used to determine significance ($p<0.05$*, $p<0.01$**, $p<0.001$***, ns= $p>0.05$) (C) Kc cells were treated with vehicle or 1μg mL^{-1} 20-HE for the indicated number of hours. 20-HE induces a stable G2 cell cycle arrest after 18h. (D) Kc cells were treated with vehicle (mock) or 1μg mL^{-1} 20-HE monitored by live imaging for 24h. Cell shape changes occur within 9h of 20-HE exposure and precede the G2 arrest that occurs at 18h of exposure. We did not observe any increase or decrease in cell motility associated with the cell shape change.

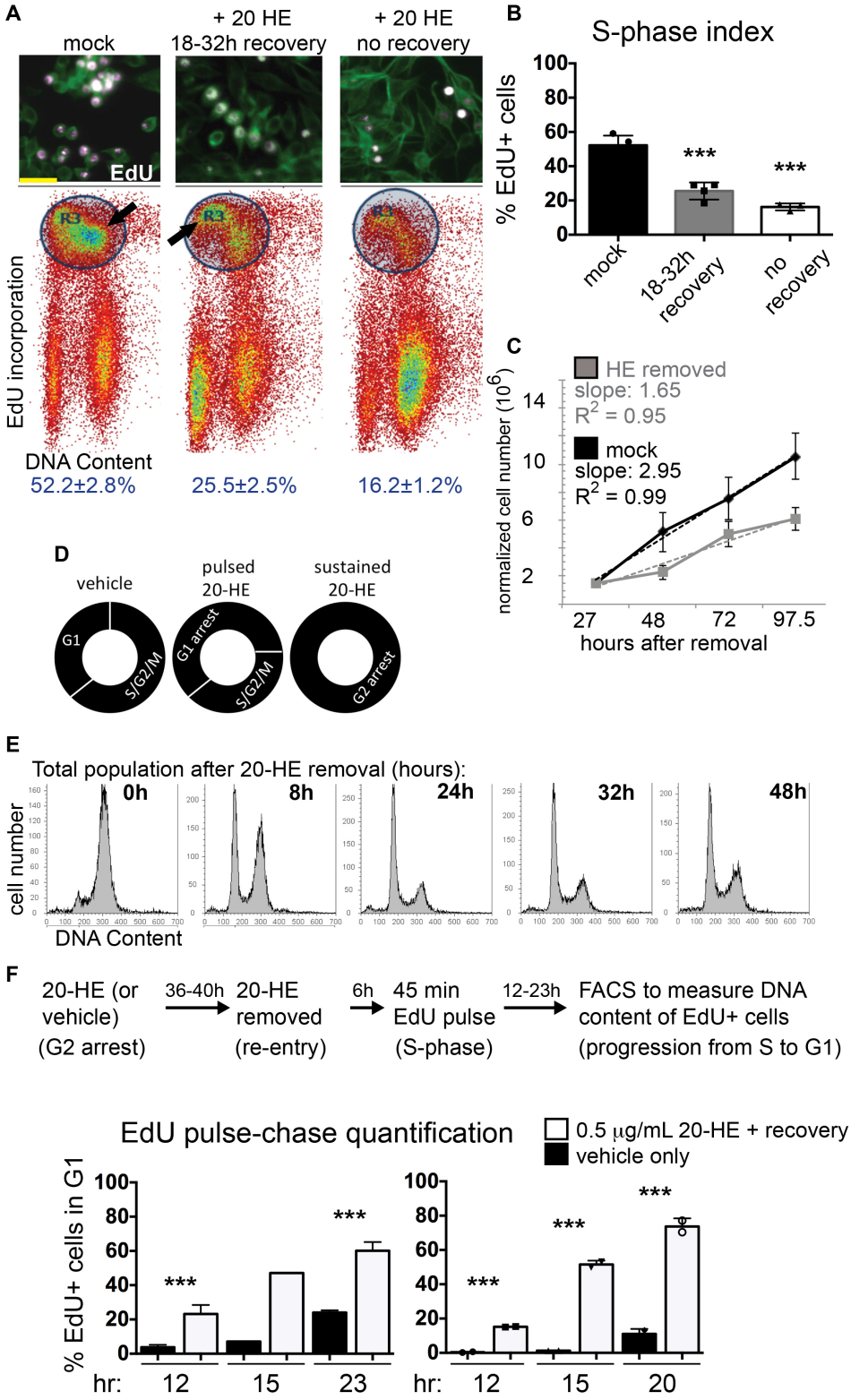

Fig. 3.2 20-HE induced arrest is reversible and leads to prolonged alterations in cell cycle dynamics.

(A) Cells were treated with vehicle (mock) or 1μg mL^{-1} 20-HE for 48h followed by removal and replacement with fresh media for the indicated number of hours. "No recovery" indicates

continued incubation with 20-HE. EdU incorporation for 45 minutes was used to examine cell cycle re-entry after 20-HE removal. Gating (blue circle) was used to identify early and late S-phase cells (indicated by arrows). (B) Quantification of EdU positive cells, error bars indicate s.e.m. of four replicates, p-values were determined by t-test compared to mock treated controls. Removal of HE for 18-32h only partially restores EdU incorporation. (C) Normalized cell counts after mock treatment or removal of 20-HE for the indicated hours. Cells treated with 20-HE fail to recover normal proliferation even several days after hormone removal. Error bars indicate s.e.m. of four replicates. (D) A diagram depicting the relative cell cycle phasing of Kc cells with the indicated treatments. (E) Cells were treated with 0.5 μg mL^{-1} 20-HE for 36h followed by removal, washing and media replacement for the indicated number of hours. One to two days after 20-HE removal the majority of cells exhibit a G1 DNA content, suggesting a rapid cell cycle re-entry followed by a G1 arrest. For quantification see. Fig. 3.2a. A. (F) An EdU pulse-chase experiment was performed to track the cell cycle progression of cells after 20-HE removal. Cells that re-enter the cell cycle 6h after 20-HE removal were pulsed with EdU and followed for the indicated number of hours. The percentage of EdU positive cells that progress from S-phase through the cell cycle to G1 after 20-HE removal is shown. S to G1 progression proceeds more rapidly after 20-HE exposure. Two independent pulse-chase experiments with 2 replicates are shown. Paired t-tests indicate significant differences ($p<0.001$ ***) between mock treated controls and 20-HE removal.

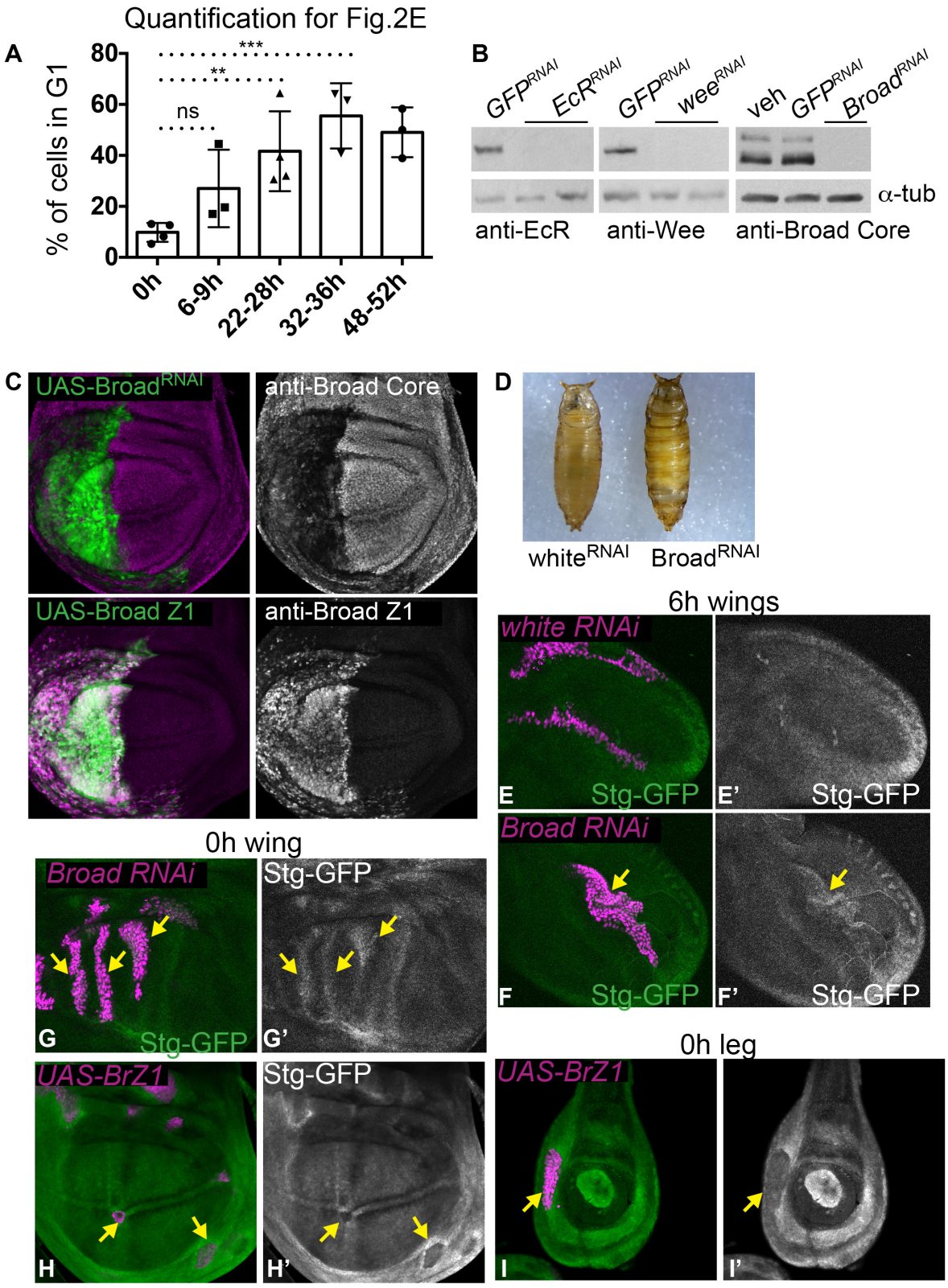

Fig. 3.2a. (A) Quantification of cells in G1 for the experiment shown in Fig. 3.2E. Error bars indicate std. dev. p-values were determined by t-tests. (B) Kc cells were cultured with 10mg mL^{-1} of the indicated dsRNAs for RNAi mediated knockdown for 3 days. Western blots for EcR,

Wee and Broad indicated highly effective knockdown. Tubulin serves as a protein loading control. (C) Knockdown of *Broad* using *engrailed-Gal4, Gal80^{TS}* with two independent UAS-RNAi lines driven by *engrailed-gal4* (*en-Gal4*) generated identical phenotypes, effectively reducing total Broad levels in the wing, and (D) disrupting pupa development and pupa cuticle tanning in each posterior segment . (C) UAS-BrZ1 effectively induced ectopic precocious expression of BrZ1 in the larval wing. (E-I) A Stg-GFP protein trap was recombined with an *actin-"flipout stop"-Gal4* transgene (*act>Gal4*) to generate heat-shock induced *flp/FRT, UAS-RFP* labeled clones expressing the indicated UAS transgenes. (F,G) Knockdown of *broad* increased Stg-GFP expression at the indicated timepoints. (H-I) Overexpression of BrZ1 reduced Stg-GFP in the wing margin and hinge area as well as the proximal leg at 0h APF (arrows).

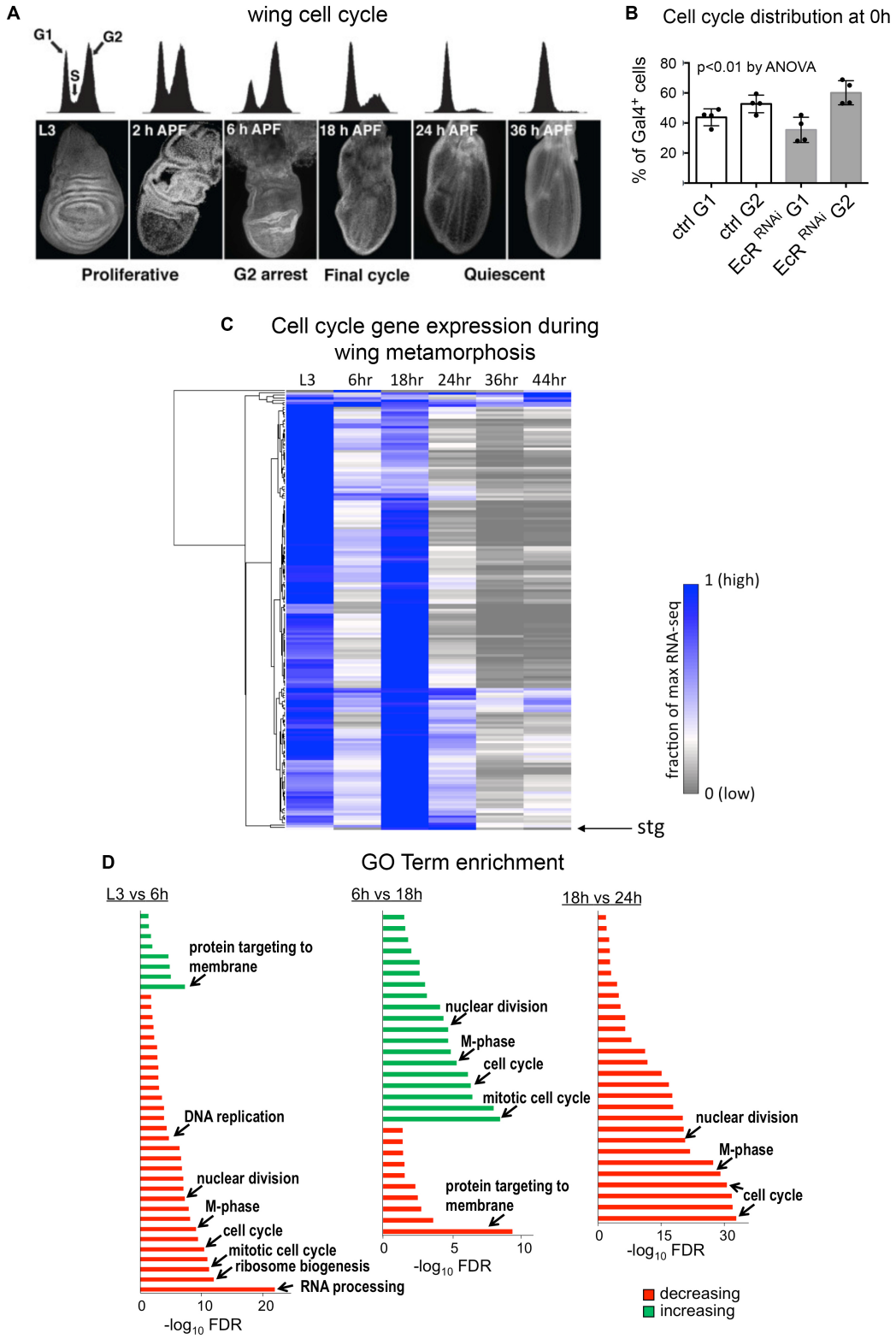

Fig. 3.3 Cell cycle changes during wing metamorphosis.
(A) *Drosophila* wings undergo a temporary G2 arrest at 6h after puparium formation (APF) followed by one additional cell cycle and a subsequent G1 arrest as indicated by flow cytometry

on staged, dissected wing tissues. This figure is reproduced from (O'Keefe et al., 2012). (B) RNAi to all isoforms of EcR was expressed in the dorsal compartment of larval wings using *apterous-Gal4*, *UAS-GFP*, *Gal80^{TS}* (*Gal4+*). EcR RNAi + GFP or GFP alone (ctrl) was expressed for 24-96h prior to dissection, dissociation and analysis by FACS at 0hAPF for cell cycle distribution in G1 and G2. Inhibition of EcR resulted in a significant fraction of cells at 0h APF exhibiting a G2 arrest. (C) RNA-seq was performed on dissected wings at the indicated timepoints to monitor changes in gene expression. A core cluster of 183 cell cycle genes exhibit dynamic regulation during wing metamorphosis, with high expression during the proliferative L3 stage and the final cell cycle, followed by very low expression after cell cycle exit at 24h. Most cell cycle genes also decrease expression during the G2 arrest at 6h, although *string* (*stg*) behaves as an outlier in this cluster, showing the most dramatic decrease at 6h. (D) Analysis of GO term enrichment revealed that genes involved in cell cycle and cell growth (ribosome biogenesis) decrease during the G2 arrest at 6h. During cell cycle re-entry (18h) cell cycle genes are upregulated to promote progression through a rapid final cell cycle. Cell cycle genes are again strongly downregulated at 24h to promote cell cycle exit.

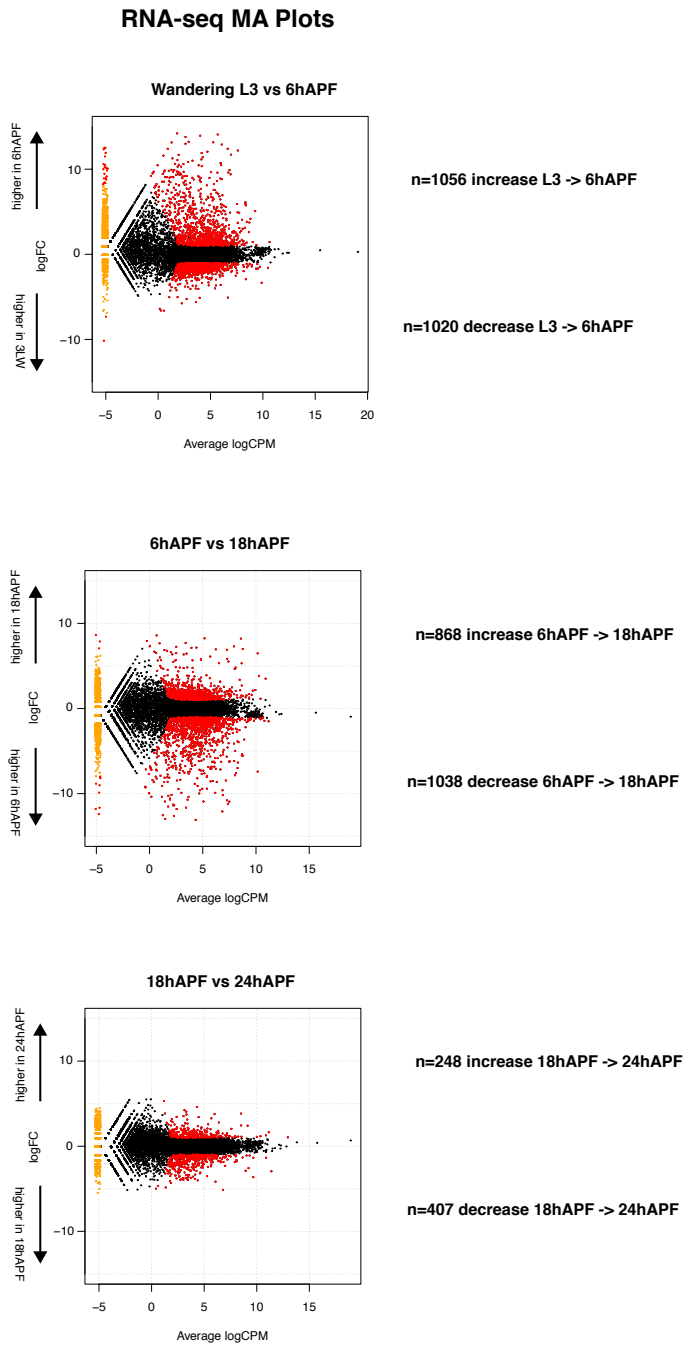

Fig. 3.3a.
Comparative MA expression plots (log Fold Change vs. average log counts per million) are shown for RNAseq on pupal wings at the indicated timepoints along with the numbers of differentially expressed genes for each comparison. FDR= false discovery rate, CPM=counts per million reads.

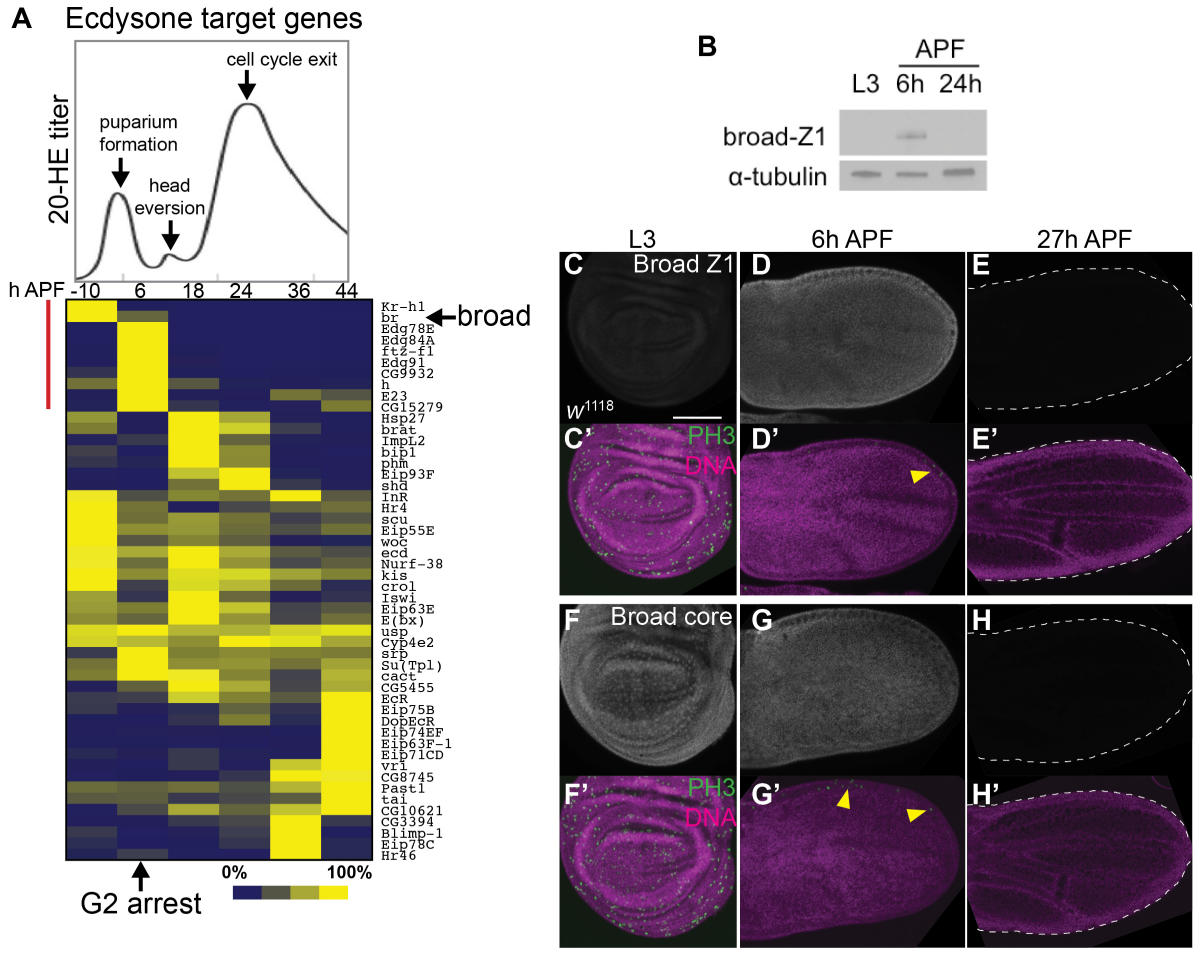

Fig. 3.4 G2 arrest in the prepupal wing coincides with a peak of Broad Z1 expression. (A) The titer of ecdysone in animals from -10h APF to 44h APF (at 25°C) is shown. This graph is adapted from (Ashburner, 1989). Known ecdysone targets were clustered using Pearson correlation coefficients according to their expression changes during metamorphosis in the wing by RNA-seq. Each gene is represented as a fraction of its maximum expression across the time course. The top cluster (indicated by a red line) contains targets induced specifically prior to or during the G2 arrest. The RNA-seq heatmap signal for the direct ecdysone target *broad* encompasses all isoforms. (B) Endogenous BroadZ1 (BrZ1) protein levels were assayed in dissected wings of the indicated stages by western blot. BrZ1 peaks at 6h. Alpha-tubulin from the same blot serves as a protein loading control. (C-H) Wings of the indicated stages were dissected, fixed and immunostained for all Broad isoforms (Broad core) or BrZ1. Broad isoforms are expressed at L3 stage prior to puparium formation, while BrZ1 is specific to the early prepupa wing. All images were taken with identical gain and laser intensities for comparison.

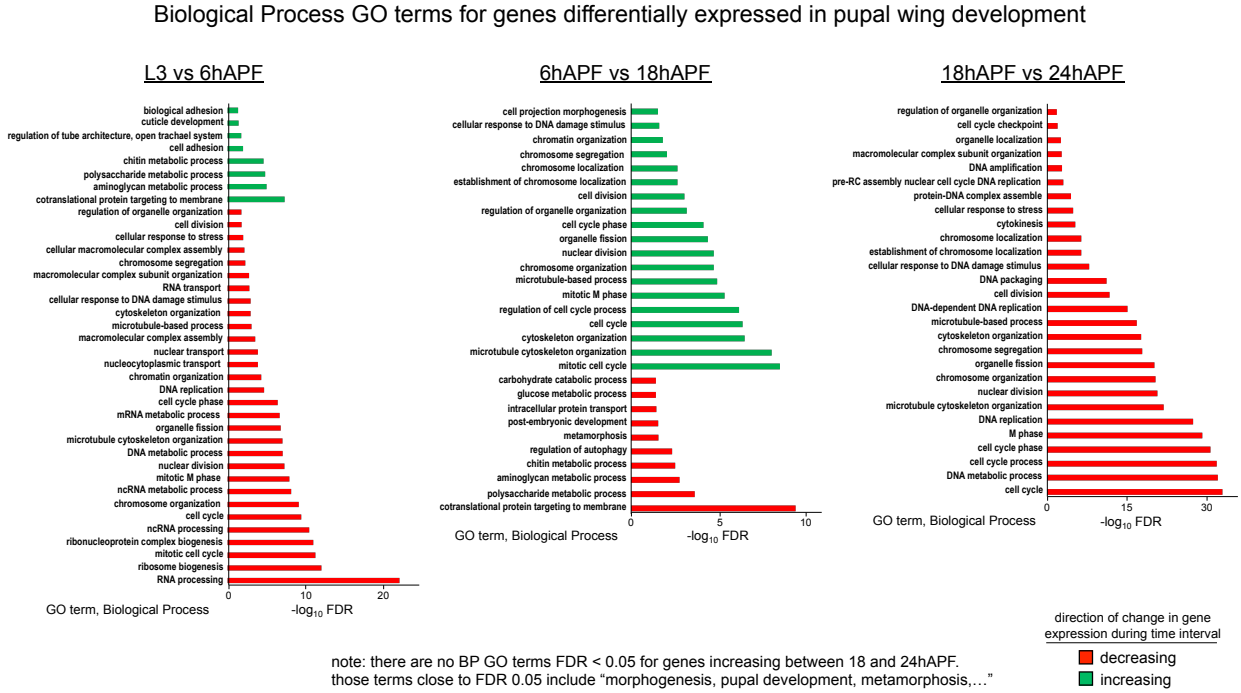

Fig. 3.4a. Complete GO term analysis for the RNA-seq timecourse data shown in Fig. 3.3 B.

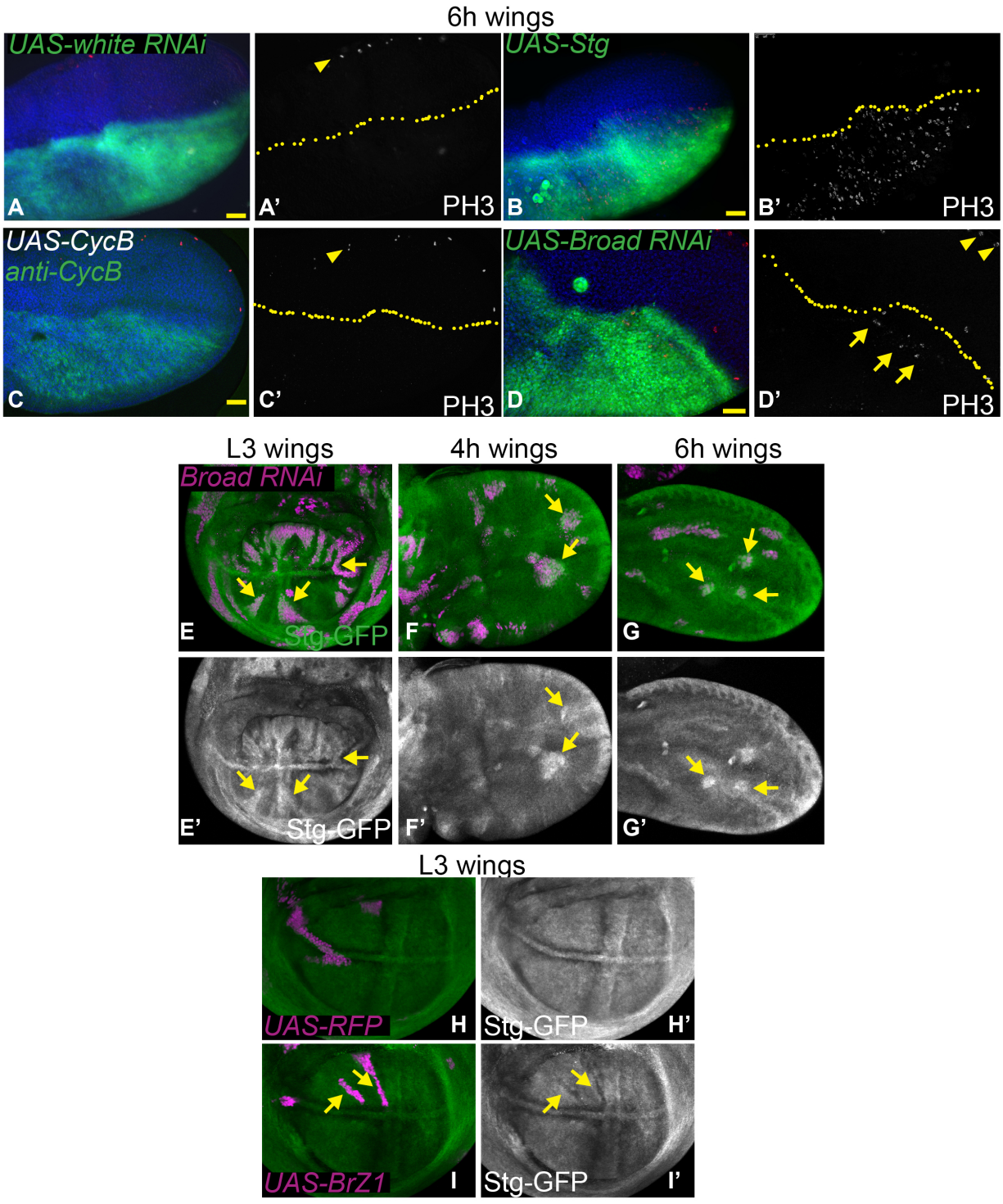

Fig. 3.5 The prepupal wing G2 arrest is partially dependent upon Broad regulation of String.

(A-D) *en-gal4* coupled with a temperature-sensitive *tubulin-Gal80 (TS)* was used to drive UAS-driven expression from mid-L3 to avoid defects in pupariation. Wings were dissected at 6h APF and stained for mitoses using anti-phosphohistone H3 (PH3)(Su et al., 1998). (A) A UAS

transgene driving expression of RNAi to the eye pigment gene *white* was used as a negative control. At 6h APF mitoses are normally restricted to the anterior margin (arrowhead) but are absent from the wing blade (n=6/6). (B) Expression of *string* in the posterior wing bypasses the G2 arrest and drives cells of the posterior wing into an early mitosis (n=7/7), (C) while overexpression of CycB does not (n=8/8). (D) Knockdown of *Broad* leads to ectopic mitoses in the posterior wing (arrows, n=9/14). (E-I) A Stg-GFP protein trap was recombined with an *actin-"flipout stop"-Gal4* transgene (*act>Gal4*) to generate heat-shock induced *flp/FRT, UAS-RFP* labeled clones expressing the indicated UAS transgenes. (E-G) *Broad* RNAi increases Stg-GFP at L3, 4 and 6h APF (H-I) while BrZ1 overexpression decreases Stg-GFP levels. Representative experiments are shown, which were independently replicated 2-3 times.

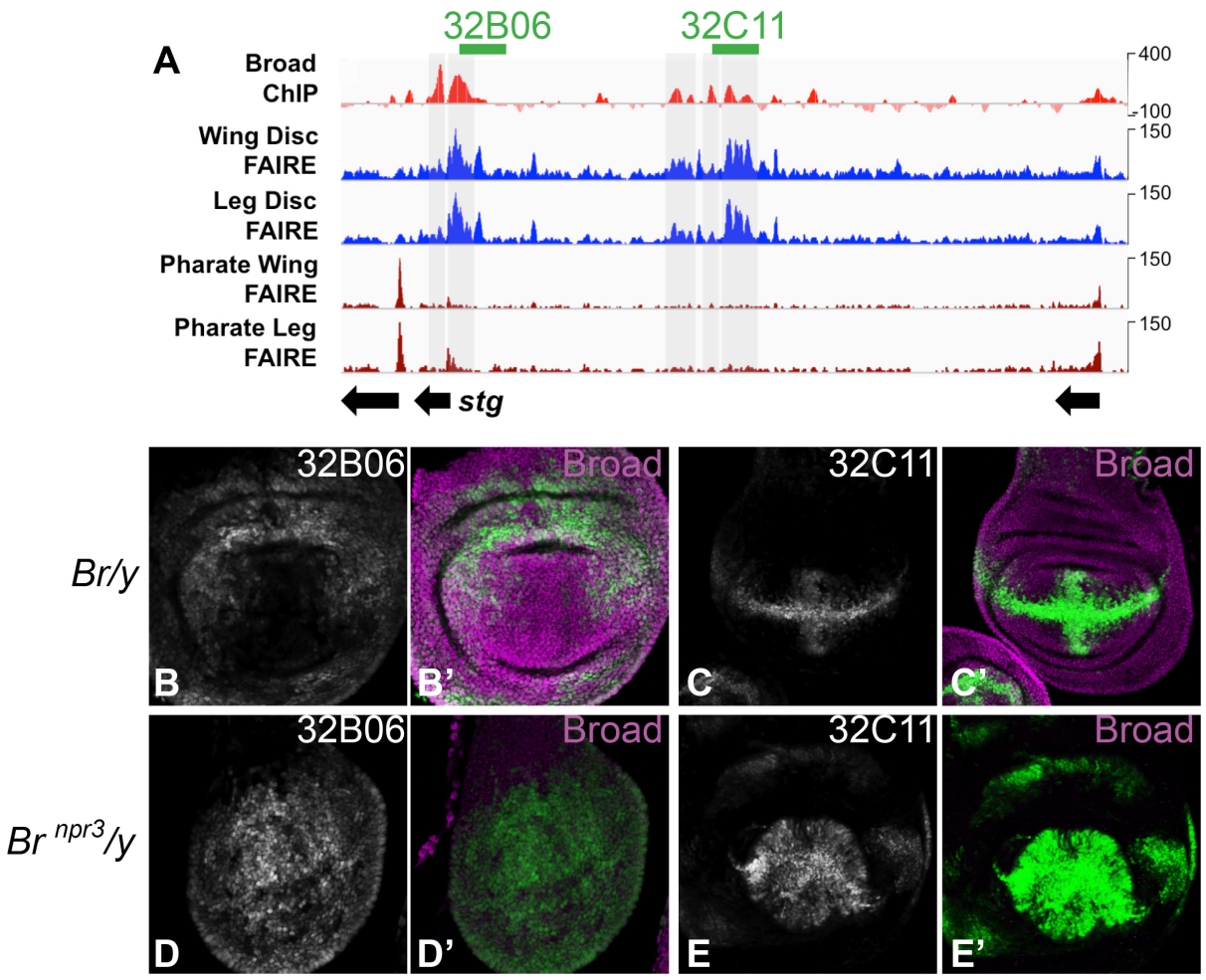

Fig. 3.6 Broad binds to the *stg* regulatory locus and overlaps with wing enhancers. (A) An 80kb window of the *stg* locus is shown including Broad ChIP-seq signal at 0h APF (modencode dataset #3806, www.modencode.org), and potential regulatory elements revealed by FAIRE that are accessible during larval stages in the wing and leg disc, but become inaccessible after cell cycle exit in the pharate tissues (McKay and Lieb, 2013). Two regions are shown that overlap with reporters from the Janelia Gal4 collection previously shown to drive expression in the wing (Andrade-Zapata and Baonza, 2014). (B-C) Male animals hemizygous for *broad* show expression of these reporters in the wing. (D-E) Animals hemizygous for the *broad npr3* null allele show loss of Broad expression and ectopic reporter expression in the central wing pouch (for 32B06) and additional expression outside of the anterior-posterior and dorsal-ventral boundary regions (for 32C11). GFP expression is shown in green, and Broad protein expression is shown in magenta.

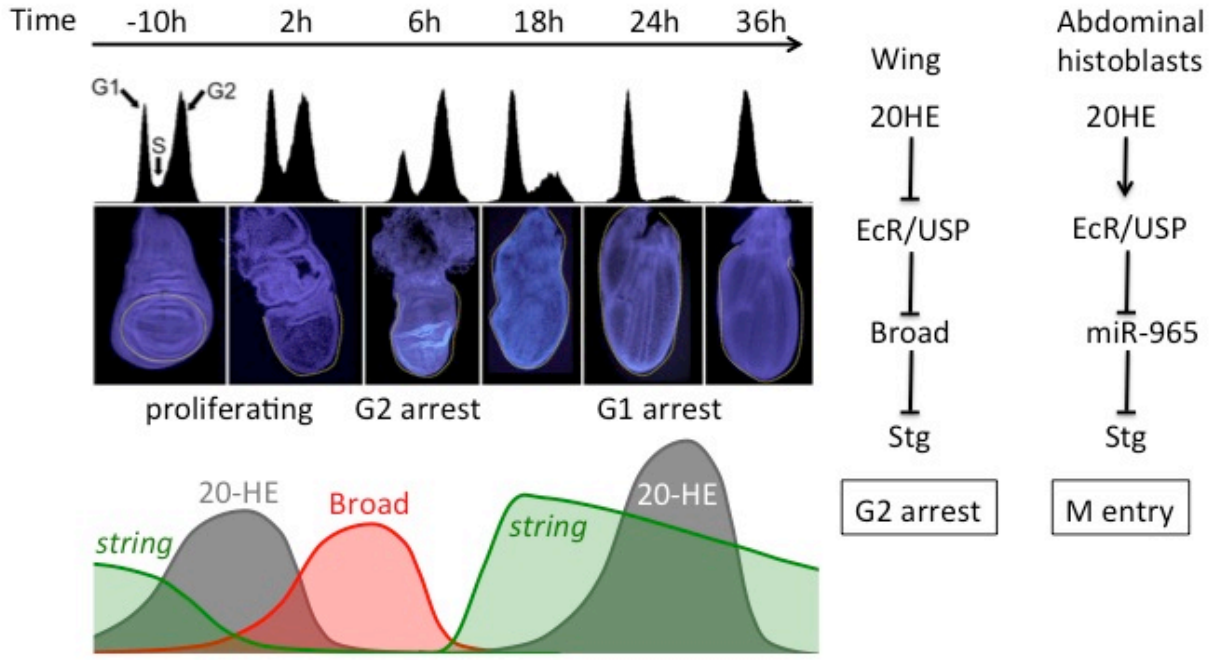

Fig. 3.7 A model for how the temporal dynamics of Ecdysone signaling induce two phases of cell cycle arrest in *Drosophila* wings

Pulses of Ecdysone signaling, Broad expression and String expression are temporally regulated during wing metamorphosis to coordinate cell cycle changes with differentiation and morphogenesis. In the wing, ecdysone relieves EcR/USP repression of Broad, which in turn regulates Stg. The outcome is opposite to that of the recently worked out molecular pathway for G2 progression in the abdominal histoblasts (Verma and Cohen, 2015).

References

Aigouy, B., Farhadifar, R., Staple, D. B., Sagner, A., Roper, J. C., Julicher, F. and Eaton, S. (2010). Cell flow reorients the axis of planar polarity in the wing epithelium of Drosophila. *Cell* **142**, 773-786.

Anders, S., Pyl, P. T. and Huber, W. (2015). HTSeq--a Python framework to work with high-throughput sequencing data. *Bioinformatics* **31**, 166-169.

Andrade-Zapata, I. and Baonza, A. (2014). The bHLH factors extramacrochaetae and daughterless control cell cycle in Drosophila imaginal discs through the transcriptional regulation of the Cdc25 phosphatase string. *PLoS Genet* **10**, e1004233.

Ashburner, M. (1989). *Drosophila; A laboratory handbook*: Cold Spring Harbor Press.

Beckstead, R. B., Lam, G. and Thummel, C. S. (2005). The genomic response to 20-hydroxyecdysone at the onset of Drosophila metamorphosis. *Genome Biol* **6**, R99.

Besson, M. T., Cordier, G., Quennedey, B., Quennedey, A. and Delachambre, J. (1987). Variability of ecdysteroid-induced cell cycle alterations in Drosophila Kc sublines. *Cell Tissue Kinet* **20**, 413-425.

Bettencourt-Dias, M., Giet, R., Sinka, R., Mazumdar, A., Lock, W. G., Balloux, F., Zafiropoulos, P. J., Yamaguchi, S., Winter, S., Carthew, R. W., et al. (2004). Genome-wide survey of protein kinases required for cell cycle progression. *Nature* **432**, 980-987.

Breitman, T. R., Selonick, S. E. and Collins, S. J. (1980). Induction of differentiation of the human promyelocytic leukemia cell line (HL-60) by retinoic acid. *Proc Natl Acad Sci U S A* **77**, 2936-2940.

Brennan, C. A., Ashburner, M. and Moses, K. (1998). Ecdysone pathway is required for furrow progression in the developing Drosophila eye. *Development* **125**, 2653-2664.

Brennan, C. A., Li, T. R., Bender, M., Hsiung, F. and Moses, K. (2001). Broad-complex, but not ecdysone receptor, is required for progression of the morphogenetic furrow in the Drosophila eye. *Development* **128**, 1-11.

Buttitta, L. A., Katzaroff, A. J., Perez, C. L., de la Cruz, A. and Edgar, B. A. (2007). A double-assurance mechanism controls cell cycle exit upon terminal differentiation in Drosophila. *Dev Cell* **12**, 631-643.

Cherbas, L., Hu, X., Zhimulev, I., Belyaeva, E. and Cherbas, P. (2003). EcR isoforms in Drosophila: testing tissue-specific requirements by targeted blockade and rescue. *Development* **130**, 271-284.

Cherbas, L., Willingham, A., Zhang, D., Yang, L., Zou, Y., Eads, B. D., Carlson, J. W., Landolin, J. M., Kapranov, P., Dumais, J., et al. (2011). The transcriptional diversity of 25 Drosophila cell lines. *Genome Res* **21**, 301-314.

Cottam, D. M. and Milner, M. J. (1997a). Effect of age on the growth and response of a Drosophila cell line to moulting hormone. *Tissue Cell* **29**, 727-732.

---- (1997b). The effects of several ecdysteroids and ecdysteroid agonists on two Drosophila imaginal disc cell lines. *Cell Mol Life Sci* **53**, 600-603.

Courgeon, A. M. (1972). Action of insect hormones at the cellular level. Morphological changes of a diploid cell line of Drosophila melanogaster, treated with ecdysone and several analogues in vitro. *Exp Cell Res* **74**, 327-336.

Davis, M. B., Carney, G. E., Robertson, A. E. and Bender, M. (2005). Phenotypic analysis of EcR-A mutants suggests that EcR isoforms have unique functions during Drosophila development. *Dev Biol* **282**, 385-396.

Djabrayan, N. J., Cruz, J., de Miguel, C., Franch-Marro, X. and Casanova, J. (2014). Specification of differentiated adult progenitors via inhibition of endocycle entry in the Drosophila trachea. *Cell Rep* **9**, 859-865.

Echalier, G. (1997). *Drosophila: Cells in Culture*: Academic Press.

Etournay, R., Popovic, M., Merkel, M., Nandi, A., Blasse, C., Aigouy, B., Brandl, H., Myers, G., Salbreux, G., Julicher, F., et al. (2015). Interplay of cell dynamics and epithelial tension during morphogenesis of the Drosophila pupal wing. *Elife* **4**, e07090.

Fain, M. J. and Stevens, B. (1982). Alterations in the cell cycle of Drosophila imaginal disc cells precede metamorphosis. *Dev Biol* **92**, 247-258.

Gauhar, Z., Sun, L. V., Hua, S., Mason, C. E., Fuchs, F., Li, T. R., Boutros, M. and White, K. P. (2009). Genomic mapping of binding regions for the Ecdysone receptor protein complex. *Genome Res* **19**, 1006-1013.

Gautam, N. K., Verma, P. and Tapadia, M. G. (2015). Ecdysone regulates morphogenesis and function of Malpighian tubules in Drosophila melanogaster through EcR-B2 isoform. *Dev Biol* **398**, 163-176.

Ghbeish, N., Tsai, C. C., Schubiger, M., Zhou, J. Y., Evans, R. M. and McKeown, M. (2001). The dual role of ultraspiracle, the Drosophila retinoid X receptor, in the ecdysone response. *Proc Natl Acad Sci U S A* **98**, 3867-3872.

Graves, B. J. and Schubiger, G. (1982). Cell cycle changes during growth and differentiation of imaginal leg discs in Drosophila melanogaster. *Dev Biol* **93**, 104-110.

Grigorian, M., Mandal, L. and Hartenstein, V. (2011). Hematopoiesis at the onset of metamorphosis: terminal differentiation and dissociation of the Drosophila lymph gland. *Dev Genes Evol* **221**, 121-131.

Heck, B. W., Zhang, B., Tong, X., Pan, Z., Deng, W. M. and Tsai, C. C. (2012). The transcriptional corepressor SMRTER influences both Notch and ecdysone signaling during Drosophila development. *Biol Open* **1**, 182-196.

Herboso, L., Oliveira, M. M., Talamillo, A., Perez, C., Gonzalez, M., Martin, D., Sutherland, J. D., Shingleton, A. W., Mirth, C. K. and Barrio, R. (2015). Ecdysone promotes growth of imaginal discs through the regulation of Thor in D. melanogaster. *Sci Rep* **5**, 12383.

Homem, C. C., Steinmann, V., Burkard, T. R., Jais, A., Esterbauer, H. and Knoblich, J. A. (2014). Ecdysone and mediator change energy metabolism to terminate proliferation in Drosophila neural stem cells. *Cell* **158**, 874-888.

Huang da, W., Sherman, B. T. and Lempicki, R. A. (2009). Systematic and integrative analysis of large gene lists using DAVID bioinformatics resources. *Nat Protoc* **4**, 44-57.

Inaba, M., Yuan, H. and Yamashita, Y. M. (2011). String (Cdc25) regulates stem cell maintenance, proliferation and aging in Drosophila testis. *Development* **138**, 5079-5086.

Jia, D., Bryant, J., Jevitt, A., Calvin, G. and Deng, W. M. (2016). The Ecdysone and Notch Pathways Synergistically Regulate Cut at the Dorsal-Ventral Boundary in Drosophila Wing Discs. *J Genet Genomics* **43**, 179-186.

Jiang, C., Baehrecke, E. H. and Thummel, C. S. (1997). Steroid regulated programmed cell death during Drosophila metamorphosis. *Development* **124**, 4673-4683.

Jiang, C., Lamblin, A. F., Steller, H. and Thummel, C. S. (2000). A steroid-triggered transcriptional hierarchy controls salivary gland cell death during Drosophila metamorphosis. *Mol Cell* **5**, 445-455.

Kim, D., Pertea, G., Trapnell, C., Pimentel, H., Kelley, R. and Salzberg, S. L. (2013). TopHat2: accurate alignment of transcriptomes in the presence of insertions, deletions and gene fusions. *Genome Biol* **14**, R36.

King-Jones, K., Charles, J. P., Lam, G. and Thummel, C. S. (2005). The ecdysone-induced DHR4 orphan nuclear receptor coordinates growth and maturation in Drosophila. *Cell* **121**, 773-784.

King-Jones, K. and Thummel, C. S. (2005). Nuclear receptors--a perspective from Drosophila. *Nat Rev Genet* **6**, 311-323.

Lee, C. Y., Simon, C. R., Woodard, C. T. and Baehrecke, E. H. (2002). Genetic mechanism for the stage- and tissue-specific regulation of steroid triggered programmed cell death in Drosophila. *Dev Biol* **252**, 138-148.

Lehman, D. A., Patterson, B., Johnston, L. A., Balzer, T., Britton, J. S., Saint, R. and Edgar, B. A. (1999). Cis-regulatory elements of the mitotic regulator, string/Cdc25. *Development* **126**, 1793-1803.

Lopes, C. S. and Casares, F. (2015). Eye selector logic for a coordinated cell cycle exit. *PLoS Genet* **11**, e1004981.

MacAlpine, D. M., Rodriguez, H. K. and Bell, S. P. (2004). Coordination of replication and transcription along a Drosophila chromosome. *Genes Dev* **18**, 3094-3105.

McKay, D. J. and Lieb, J. D. (2013). A common set of DNA regulatory elements shapes Drosophila appendages. *Dev Cell* **27**, 306-318.

Milan, M., Campuzano, S. and Garcia-Bellido, A. (1996). Cell cycling and patterned cell proliferation in the Drosophila wing during metamorphosis. *Proc Natl Acad Sci U S A* **93**, 11687-11692.

Mitchell, N., Cranna, N., Richardson, H. and Quinn, L. (2008). The Ecdysone-inducible zinc-finger transcription factor Crol regulates Wg transcription and cell cycle progression in Drosophila. *Development* **135**, 2707-2716.

Mitchell, N. C., Lin, J. I., Zaytseva, O., Cranna, N., Lee, A. and Quinn, L. M. (2013). The Ecdysone receptor constrains wingless expression to pattern cell cycle across the Drosophila wing margin in a Cyclin B-dependent manner. *BMC Dev Biol* **13**, 28.

Neufeld, T. P., de la Cruz, A. F., Johnston, L. A. and Edgar, B. A. (1998). Coordination of growth and cell division in the Drosophila wing. *Cell* **93**, 1183-1193.

Ninov, N., Chiarelli, D. A. and Martin-Blanco, E. (2007). Extrinsic and intrinsic mechanisms directing epithelial cell sheet replacement during Drosophila metamorphosis. *Development* **134**, 367-379.

Ninov, N., Manjon, C. and Martin-Blanco, E. (2009). Dynamic control of cell cycle and growth coupling by ecdysone, EGFR, and PI3K signaling in Drosophila histoblasts. *PLoS Biol* **7**, e1000079.

O'Keefe, D. D., Thomas, S. R., Bolin, K., Griggs, E., Edgar, B. A. and Buttitta, L. A. (2012). Combinatorial control of temporal gene expression in the Drosophila wing by enhancers and core promoters. *BMC Genomics* **13**, 498.

Peel, D. J. and Milner, M. J. (1990). The Diversity of Cell Morphology in Cloned Cell-Lines Derived from Drosophila Imaginal Disks. *Roux Arch Dev Biol* **198**, 479-482.

Pile, L. A., Schlag, E. M. and Wassarman, D. A. (2002). The SIN3/RPD3 deacetylase complex is essential for G(2) phase cell cycle progression and regulation of SMRTER corepressor levels. *Mol Cell Biol* **22**, 4965-4976.

Robinson, M. D., McCarthy, D. J. and Smyth, G. K. (2010). edgeR: a Bioconductor package for differential expression analysis of digital gene expression data. *Bioinformatics* **26**, 139-140.

Rogers, S. L. and Rogers, G. C. (2008). Culture of Drosophila S2 cells and their use for RNAi-mediated loss-of-function studies and immunofluorescence microscopy. *Nat Protoc* **3**, 606-611.

Saucedo, L. J. and Edgar, B. A. (2007). Filling out the Hippo pathway. *Nat Rev Mol Cell Biol* **8**, 613-621.

Schubiger, M., Carre, C., Antoniewski, C. and Truman, J. W. (2005). Ligand-dependent de-repression via EcR/USP acts as a gate to coordinate the differentiation of sensory neurons in the Drosophila wing. *Development* **132**, 5239-5248.

Schubiger, M. and Palka, J. (1987). Changing spatial patterns of DNA replication in the developing wing of Drosophila. *Dev Biol* **123**, 145-153.

Schubiger, M., Tomita, S., Sung, C., Robinow, S. and Truman, J. W. (2003). Isoform specific control of gene activity in vivo by the Drosophila ecdysone receptor. *Mech Dev* **120**, 909-918.

Schubiger, M. and Truman, J. W. (2000). The RXR ortholog USP suppresses early metamorphic processes in Drosophila in the absence of ecdysteroids. *Development* **127**, 1151-1159.

Shlyueva, D., Stelzer, C., Gerlach, D., Yanez-Cuna, J. O., Rath, M., Boryn, L. M., Arnold, C. D. and Stark, A. (2014). Hormone-responsive enhancer-activity maps reveal predictive motifs, indirect repression, and targeting of closed chromatin. *Mol Cell* **54**, 180-192.

Sopko, R., Lin, Y. B., Makhijani, K., Alexander, B., Perrimon, N. and Bruckner, K. (2015). A systems-level interrogation identifies regulators of Drosophila blood cell number and survival. *PLoS Genet* **11**, e1005056.

Sorrentino, R. P., Carton, Y. and Govind, S. (2002). Cellular immune response to parasite infection in the Drosophila lymph gland is developmentally regulated. *Dev Biol* **243**, 65-80.

Stevens, B., Alvarez, C. M., Bohman, R. and O'Connor, J. D. (1980). An ecdysteroid-induced alteration in the cell cycle of cultured Drosophila cells. *Cell* **22**, 675-682.

Stoiber, M., Celniker, S., Cherbas, L., Brown, B. and Cherbas, P. (2016). Diverse Hormone Response Networks in 41 Independent Drosophila Cell Lines. *G3 (Bethesda)*.

Su, T. T., Sprenger, F., DiGregorio, P. J., Campbell, S. D. and O'Farrell, P. H. (1998). Exit from mitosis in Drosophila syncytial embryos requires proteolysis and cyclin degradation, and is associated with localized dephosphorylation. *Genes Dev* **12**, 1495-1503.

Sun, D. and Buttitta, L. (2015). Protein phosphatase 2A promotes the transition to G0 during terminal differentiation in Drosophila. *Development* **142**, 3033-3045.

Supek, F., Bosnjak, M., Skunca, N. and Smuc, T. (2011). REVIGO summarizes and visualizes long lists of gene ontology terms. *PLoS One* **6**, e21800.

Talbot, W. S., Swyryd, E. A. and Hogness, D. S. (1993). Drosophila tissues with different metamorphic responses to ecdysone express different ecdysone receptor isoforms. *Cell* **73**, 1323-1337.

Verma, P. and Cohen, S. M. (2015). miR-965 controls cell proliferation and migration during tissue morphogenesis in the Drosophila abdomen. *Elife* **4**.

Wu, M. Y., Cully, M., Andersen, D. and Leevers, S. J. (2007). Insulin delays the progression of Drosophila cells through G2/M by activating the dTOR/dRaptor complex. *EMBO J* **26**, 371-379.

Yamanaka, N., Rewitz, K. F. and O'Connor, M. B. (2013). Ecdysone control of developmental transitions: lessons from Drosophila research. *Annu Rev Entomol* **58**, 497-516.

Yin, V. P. and Thummel, C. S. (2004). A balance between the diap1 death inhibitor and reaper and hid death inducers controls steroid-triggered cell death in Drosophila. *Proc Natl Acad Sci U S A* **101**, 8022-8027.

Zelhof, A. C., Ghbeish, N., Tsai, C., Evans, R. M. and McKeown, M. (1997). A role for ultraspiracle, the Drosophila RXR, in morphogenetic furrow movement and photoreceptor cluster formation. *Development* **124**, 2499-2506.

Zhang, C., Robinson, B. S., Xu, W., Yang, L., Yao, B., Zhao, H., Byun, P. K., Jin, P., Veraksa, A. and Moberg, K. H. (2015). The ecdysone receptor coactivator Taiman links Yorkie to transcriptional control of germline stem cell factors in somatic tissue. *Dev Cell* **34**, 168-180.

Zirin, J., Cheng, D., Dhanyasi, N., Cho, J., Dura, J. M., Vijayraghavan, K. and Perrimon, N. (2013). Ecdysone signaling at metamorphosis triggers apoptosis of Drosophila abdominal muscles. *Dev Biol* **383**, 275-284.

CHAPTER IV

GENERAL DISCUSSION

Adult tissues are mostly composed of cells that have undergone a developmentally regulated exit from the cell cycle and have differentiated into their final cell fate. It is not fully understood how environmental cues and changes in hormone levels impinge upon the cell cycle regulatory machinery to stop proliferation and promote the transition to a non-cycling, terminally differentiated state. Though the transition to a post-mitotic state is associated with cell cycle gene repression via activity of the major cell cycle repressor (DREAM), fly tissues that have lost DREAM activity will still exit the cell cycle, indicating that there are still unknown factors involved in this process. This work demonstrates that the NuA4 complex and steroid hormone ecdysone are part of two essential separate signaling pathways that can impact cell cycle gene expression and cell cycle progression to properly coordinate the differentiation-associated cell cycle exit and development.

NuA4

Our research helped clarify previous data pertaining to Tip60/NuA4's role in cell cycle regulation. As mentioned in chapter I, E2F/DP master cell cycle transcription factor complexes drive cell cycle progression by oscillating between functioning as transcriptional activators (E2F1/DP) and repressors (E2F/DP/Rb and DREAM) of cell cycle gene expression (Fig. 1.3). Our data suggest that the changes in E2F/DP activity that we and others have found (Lu et al.,

2007) may be an indirect effect of NuA4 inhibition slowing progression through late S/G2, which causes a concomitant increase in E2F1 activity through the mechanism of cell cycle compensation (Reis & Edgar, 2004, Flegel et al., 2016). Alternatively, NuA4 knockdown may also induce E2F1 activity as a result of the cell perceiving DNA damage (Moon et al., 2008). Though certain E2F1 activities were increased, Tip60/NuA4 inhibition actually decreased E2F1 protein levels and slowed the overall cell cycle, suggesting that Tip60/NuA4 is also required for the accumulation of E2F1 that would have otherwise accompanied the temporary cell cycle arrest to promote proper cell cycle compensation (Reis & Edgar, 2004). Since endogenous E2F1 activity is highest during S phase when E2F1 protein is naturally degraded, Tip60/NuA4 inhibited cells are likely temporarily arrested in late S phase or early G2 before E2F1 protein levels accumulate. This is consistent with our assays using the Drosophila FUCCI cell cycle reporters.

An increase in the percentage of cells in G2 phase was also found when NuA4 was inhibited in mouse embryonic stem cells (mESCs) (Fazzio et al., 2008). Contrary to NuA4's ability to promote gene transcription via acetylation of histone H4 (H4Ac), Fazzio et al. (2008) found that NuA4 represses differentiation-specific genes to maintain mESC pluripotency. It was suggested that a pluripotency transcription factor (Nanog) and NuA4 function together to regulate the expression of a common set of differentiation genes. Although it is important to note that NuA4 was actually found at 55% of all mESC promoters (Fazzio et al., 2008). Fazzio et al. (2008) speculated that NuA4 acetylated histone H4, H2A variants, or non-histone targets to achieve this context-dependent regulation of gene expression. In light of our findings in chapter II where we revealed an unappreciated role for NuA4 in resolving endogenous DNA damage during every cell cycle, we wonder whether knockdown of NuA4 could instead activate a DNA

damage response (DDR) that may indirectly promote mESC differentiation. This would be consistent with recent work that suggests cell cycle arrest or slowing promotes ESC differentiation (Hardwick et al., 2015). Although we have not distinguished whether NuA4 inhibition affects the amount of DNA damage occurring or just the perception of damage, knockdown of NuA4 activates a DNA damage response which attempts to preserve the integrity of the tissue by repairing the damage or eliminating the cell (Wells & Johnston, 2012).

Activation of a DDR in differentiated cells results in apoptosis or cell cycle arrest and DNA repair, whereas the effects upon pluripotent (such as mESCs) or multipotent cells are context-dependent (Sherman et al., 2011). For example, a DDR in mESCs can induce differentiation by activating p53 that then directly suppresses the expression of *nanog* (Lin et al., 2005). Since Nanog protein levels were not affected by NuA4 inhibition (Fazzio et al. 2008), if NuA4 knockdown in mESCs did trigger a DDR it may be p53-independent such as we found in chapter II (Flegel et al., 2016). Alternatively, premature differentiation of ES cells could also result if NuA4 inhibition in mESCs reduced H2A variant expression or the variant's ability to associate with and protect Nanog from ubiquitin-proteosome degradation (Wang et al., 2015).

NuA4 could also impact mESC pluripotency without invoking NuA4's involvement in the DDR. ESC identity is determined by the separable regulatory Polycomb, Myc, and Core networks (Kim et al., 2010). The Core network contains Nanog, whose activity is needed at least in part for NuA4's repression of differentiation genes in mESCs (Fazzio et al., 2008). However, NuA4 can also interact with the oncogenic transcription factor Myc in both ESCs and non-ESCs to drive the efficient acetylation of histone H4 and transcription of Myc targets (McMahon et al., 1998, Frank et al., 2003, Doyon et al., 2004, Kim et al., 2010). Similar to NuA4 knockdown, Myc inhibition in mESCs induces a flattened morphology indicative of differentiation,

suggesting that NuA4's role in promoting mESC pluripotency could potentially occur at least in part through its interaction with Myc (Kim et al., 2010).

We found that just 24 hours of *in vivo* Tip60/NuA4 inhibition decreased levels of the G2/M-promoting protein, CycB, and that Tip60 can bind the *cycB* promoter in *Drosophila* cell culture. Although we do not have direct evidence, NuA4 may modify the chromatin at the *cycB* promoter to make it accessible to the transcriptional machinery and drive proper G2/M progression. This hypothesis is supported by over-expression of the *cdc25c/string* phosphatase of CycB/Cdk1 rescuing the slowed progression through late S/G2. Despite the ability of *string* expression to rescue the late S/ G2 defect, the timing of cell cycle exit was still delayed by Tip60/NuA4 inhibition. Closer inspection revealed that many of these mitotic cells after normal cell cycle exit had chromosome segregation errors that were not caused by Tip60/NuA4 inhibited alone. This suggests that *string* overexpression is sufficient to promote the activity of the low levels of CycB/Cdk2 complexes in NuA4 inhibited tissues, but does not fix what caused the reduction of CycB in the first place.

We are not the first to find an interaction between Tip60/NuA4 and CycB/Cdk1. Phosphorylation of mammalian Tip60 at Ser86 and Ser90 has been shown *in vitro* to promote Tip60's acetyltransferase activity (Lemercier et al., 2003, Charvet et al., 2011). Ser90 of Tip60 lies within a canonical CycB/Cdk1 binding site that is targeted by Cdk1 (Lemercier et al., 2003, Mo et al., 2016). Furthermore, high levels of phosphorylated Tip60 are evident when ~90% of human cells are forcibly arrested in G2/M, when CycB/Cdk1 activity is normally high (Mo et al., 2016). In combination with our *in vivo* data that shows Tip60 inhibition reduces both CycB transcript and protein, there may exist an unexpected feed-forward relationship where Tip60 acetyltransferase activity promotes *cycB* expression and CycB/Cdk1 activity in turn promotes

Tip60's activity. A recent mammalian cell culture study indicates that Tip60/NuA4 also functions downstream of CycB to promote the metaphase to anaphase transition. Phosphorylation of Aurora B (AurB) promotes mitotic progression by destabilizing microtubules that have incorrectly attached to chromosomes so as to ultimately allow chromosomes to properly segregate to opposing spindle poles via correct kinetochore-microtubule attachments (Mo et al., 2016). Tip60's acetylation of AurB's activation loop preserves the activity of AurB by protecting it from being dephosphorylated (Mo et al., 2016). If these Tip60 functions are conserved in *Drosophila,* the chromosome segmentation defects we find in Tip60/NuA4 inhibited and *string* or *cycB* overexpression wings could be caused by the persistence of mis-attached microtubules. Whether a result of defects in microtubule attachment or by acquiring DNA damage, cells that persist with chromosomal aberrations have a greater likelihood of oncogenic transformation (Tang et al., 2012). This means that despite NuA4 promoting the expression of targets of the oncogenic Myc and E2F1 transcription factors (Frank et al., 2003, Taubert et al., 2004), NuA4's role in promoting genetic stability also places it as an essential tumor suppressor (Gorrini et al., 2007).

Tip60/NuA4 knockdown in *Drosophila* slowed cell cycle progression to delay the timing of cell cycle exit (Flegel et al., 2016). This change in the rate of proliferation did not affect the timing of differentiation, but it did impact the proper formation and pattern of wing veins. Whether cells in the wing identify as vein or intervein is dependent upon the pattern of differential rates of proliferation that naturally exist in the wing (González-Gaitán et al., 1994, Mao et al., 2013), cell signaling, and expression of cell-fate determinants (De Celis, 2003). Vein formation is also dependent upon the cells being appropriately juxtaposed in the two sheets of epithelial cells that make up the wing (De Celis, 2003). NuA4 inhibition in the wing posterior

likely caused an incorrect number of cells between the layers due to an increase in cell death that was accompanied by improper patterns of proliferation rates to adversely affect the formation of veins that normally convey rigidity and structure to the tissue (De Celis, 2003).

Surprisingly, Tip60/NuA4's impact on cell cycle progression occurred in the absence of factors that it had previously been shown to coactivate (E2F/DP, p53). We therefore looked for answers in its target genes via RNA-seq. We know that Tip60/NuA4 inhibition does not disrupt the ability to initially detect DNA damage (such as unprotected, newly replicated ends of DNA) because pH2Av foci are apparent in Tip60/NuA4 inhibited tissues in the absence of exogenous DNA damaging agents. Upon comparison with a previously reported p53-independent DNA damage response (van Bergeijk et al., 2012), we found a significant amount of the transcriptome of Tip60/NuA4 inhibited proliferating wing discs to correspond with the p53-independent DDR. The precise DDR pathway activated by Tip60/NuA4 inhibition remains to be explored. The p53-independent DDR includes members of the JNK (c-*jun*-NH_2-kinases) pathway, which will be our first candidates to test in the future. Though the JNK pathway has context-dependent roles in morphogenesis, proliferation, and apoptosis (McEwen et al., 2000, McEwen & Peifer, 2005), JNK can also promote DNA repair by phosphorylating sirtuin 6 (Sirt6) (Van Meter et al., 2016). Since NuA4 knockdown in *Drosophila* induces a p53-independent DDR but only a few cells are eliminated, the cells that survived may have repaired their DNA by JNK activation of Sirt6, which has recently been shown to be necessary for the recruitment of poly (ADP-ribose) polymerase 1 (PARP1) to sites of damage to initiate DNA repair in mammals (Ko & Ren, 2012, Van Meter et al., 2016). It remains to be determined if this role of Sirt6 is conserved in flies (Frye, 2000) and whether the survival of NuA4-inhibited cells is dependent upon JNK's activation of Sirt6.

Development and ecdysone

Perturbations to developmentally controlled cell cycle exit and differentiation have historically been used as models for cancer development (Yamanaka et al., 2013). It has long been speculated that the steroid hormone ecdysone in holometabolous insects triggers tissues to complete their development and cells to differentiate into their final fates during metamorphosis. It was previously unknown how pulses of ecdysone impinge upon the cell cycle machinery to make proliferating *Drosophila* cells transition to the non-cycling state called cell cycle exit. We found that a pulse of activated ecdysone (20-HE) induces the expression of the transcription factor, *broad* in the larval wing, which in turn represses the expression of the G2/M-promoting *cdc25c/string.* Cells are arrested in G2 until 20-HE levels drop and cause a decline in *broad* expression. The repression of *string* is therefore released so it can in turn promote CycB/Cdk1 activity for a tissue-wide, rapid cell cycle reentry into the final cell cycle of the wing. Deciphering the components of the signaling cascade induced by ecdysone that impacts proliferation and differentiation in the *Drosophila* wing, may help us understand the signaling cascades involved in the regulation of developmentally controlled cell cycle exit in more complex tissues or organisms (Ollikainen et al., 2006).

Though we now know how the pulse of ecdysone at the larva to pupa transition affects transcription to synchronize the final cell cycle associated with terminal differentiation, we have yet to determine how the later and largest pulse of ecdysone is linked with acquisition of the final cell fate in *Drosophila* pupal wings. Previous studies have focused on the ecdysone-inducible transcription factor Crooked legs (Crol) that downregulates the Wingless (Wg) pathway, which otherwise promotes cell cycle exit and differentiation in the larval wing margin (Quinn et al.,

2012). Since we found in chapter III that a pulse of 20-HE arrested Kc167 cells in G2 phase similar to the arrest found in 6h APF wings, we can find candidate ecdysone responsive factors involved in differentiation by mining a study of ecdysone receptor (EcR) and ultraspiracle (Usp) genomic binding in Kc cells that had been induced to differentiate by exposure to 20-HE (Gauhar et al., 2009). Candidates for further testing *in vivo* could then be chosen by comparing the genes bound by EcR and Usp with those that are differentially expressed over a wing developmental timecourse spanning from the larva to the pupa that includes the 24h APF timepoint that corresponds to the largest pulse of ecdysone (O'Keefe et al., 2012). Though it would be challenging to obtain sufficient knockdown during the critical period without lethally disrupting organismal development (such as we found when inhibiting Broad during our studies in chapter III), we would then need to determine if these ecdysone targets are indeed required for the differentiation of wing cells *in vivo*.

References

Charvet, C., Wissler, M., Brauns-Schubert, P., Wang, S. J., Tang, Y., Sigloch, F. C., … Maurer, U. (2011). Phosphorylation of Tip60 by GSK-3 Determines the Induction of PUMA and Apoptosis by p53. *Molecular Cell*, *42*(5), 584–596.

Dang, C. (1999). c-Myc target genes involved in cell growth, apoptosis, and metabolism. *Molecular and Cellular Biology*, *40*(11), 66–9.

De Celis, J. F. (2003). Pattern formation in the Drosophila wing: The development of the veins. *BioEssays*, *25*(5), 443–451.

Fazzio, T. G., Huff, J. T., & Panning, B. (2008). An RNAi screen of chromatin proteins identifies Tip60-p400 as a regulator of embryonic stem cell identity. *Cell*, *134*(1), 162–74.

Filion, G. J., van Bemmel, J. G., Braunschweig, U., Talhout, W., Kind, J., Ward, L. D., … van Steensel, B. (2010). Systematic Protein Location Mapping Reveals Five Principal Chromatin Types in Drosophila Cells. *Cell*, *143*(2), 212–224.

Flegel, K., Grushko, O., Bolin, K., Griggs, E., & Buttitta, L. (2016). Roles for the histone modifying and exchange complex NuA4 in cell cycle progression in Drosophila melanogaster. *Genetics*, *203*(3), 1265–1281.

Frank, S. R., Parisi, T., Taubert, S., Fernandez, P., Fuchs, M., Chan, H.-M., … Amati, B. (2003). MYC recruits the TIP60 histone acetyltransferase complex to chromatin. *EMBO Reports*, *4*(6), 575–80.

Frye, R. a. (2000). Phylogenetic classification of prokaryotic and eukaryotic Sir2-like proteins. *Biochemical and Biophysical Research Communications*, *273*(2), 793–798.
Gauhar, Z., Sun, L. V, Hua, S., Mason, C. E., Fuchs, F., Li, T., … White, K. P. (2009). Genomic mapping of binding regions for the Ecdysone receptor protein complex. *Genome Research*, *19*, 1006–1013.
González-Gaitán, M., Capdevila, M. P., & García-Bellido, A. (1994). Cell proliferation patterns in the wing imaginal disc of Drosophila. *Mechanisms of Development*, *46*(3), 183–200.
Gorrini, C., Squatrito, M., Luise, C., Syed, N., Perna, D., Wark, L., … Amati, B. (2007). Tip60 is a haplo-insufficient tumour suppressor required for an oncogene-induced DNA damage response. *Nature*, *448*(7157), 1063–1067.
Hardwick, L. J. A., Ali, F. R., Azzarelli, R., & Philpott, A. (2015). Cell cycle regulation of proliferation versus differentiation in the central nervous system. *Cell and Tissue Research*, *359*, 187–200.
Kim, J., Woo, A. J., Chu, J., & Snow, J. W. (2010). A Myc rather than core pluripotency module accounts for the shared signatures of embryonic stem and cancer cells. *Cell*, *143*(2), 313–324.
Ko, H. L., & Ren, E. C. (2012). Functional Aspects of PARP1 in DNA Repair and Transcription. *Biomolecules*, *2*(4), 524–48.
Lemercier, C., Legube, G., Caron, C., Louwagie, M., Garin, J., Trouche, D., & Khochbin, S. (2003). Tip60 acetyltransferase activity is controlled by phosphorylation. *Journal of Biological Chemistry*, *278*(7), 4713–4718.
Lin, T., Chao, C., Saito, S., Mazur, S. J., Murphy, M. E., Appella, E., & Xu, Y. (2005). p53 induces differentiation of mouse embryonic stem cells by suppressing Nanog expression. *Nat Cell Biol*, *7*(2), 165–171.
Lu, J., Ruhf, M.-L., Perrimon, N., & Leder, P. (2007). A genome-wide RNA interference screen identifies putative chromatin regulators essential for E2F repression. *Proceedings of the National Academy of Sciences of the United States of America*, *104*, 9381–9386.
Mao, Y., Tournier, A. L., Hoppe, A., Kester, L., Thompson, B. J., & Tapon, N. (2013). Differential proliferation rates generate patterns of mechanical tension that orient tissue growth. *The EMBO Journal*, *32*(21), 2790–803.
McEwen, D. G., Cox, R. T., & Peifer, M. (2000). The canonical Wg and JNK signaling cascades collaborate to promote both dorsal closure and ventral patterning. *Development (Cambridge, England)*, *127*(16), 3607–17.
McEwen, D. G., & Peifer, M. (2005). Puckered, a Drosophila MAPK phosphatase, ensures cell viability by antagonizing JNK-induced apoptosis. *Development (Cambridge, England)*, *132*(17), 3935–3946.
McMahon, S. B., Van Buskirk, H. a, Dugan, K. a, Copeland, T. D., & Cole, M. D. (1998). The novel ATM-related protein TRRAP is an essential cofactor for the c-Myc and E2F oncoproteins. *Cell*, *94*(3), 363–74. Retrieved from
Mo, F., Zhuang, X., Liu, X., Yao, P. Y., Qin, B., Su, Z., … Yao, X. (2016). Acetylation of Aurora B by TIP60 ensures accurate chromosomal segregation. *Nature Chemical Biology*, (February), 1–9.
Moon, N., Stefano, L. Di, Morris, E. J., Patel, R., White, K., & Nicholas, J. (2008). E2F and p53 Induce Apoptosis Independently during Drosophila Development but Intersect in the Context of DNA Damage. *PLoS Genetics*, *4*(8), 1–10.
O'Keefe, D. D., Thomas, S. R., Bolin, K., Griggs, E., Edgar, B. a, & Buttitta, L. A. (2012).

Combinatorial control of temporal gene expression in the Drosophila wing by enhancers and core promoters. *BMC Genomics*, *13*(1), 498.
Ollikainen, N., Chandsawangbhuwana, C., & Baker, M. E. (2006). Evolution of the thyroid hormone, retinoic acid, ecdysone and liver X receptors. *Integrative and Comparative Biology*, *46*(6), 815–826.
Quinn, L., Lin, J., Cranna, N., Lee, J. E. A., Mitchell, N., & Hannan, R. (2012). Steroid hormones in Drosophila: How ecdysone coordinates developmental signalling with cell growth and division. *Steroid–Basic Science*, 149–168.
Reis, T., & Edgar, B. A. (2004). Negative Regulation of dE2F1 by Cyclin-Dependent Kinases Controls Cell Cycle Timing, *117*, 253–264.
Sherman, M. H., Bassing, C. H., & Teitell, M. A. (2011). DNA damage response regulates cell differentiation. *Trends in Cell Biology*, *21*(5), 312–319.
Tang, H. L., Tang, H. M., Mak, K. H., Hu, S., Wang, S. S., Wong, K. M., … Fung, M. C. (2012). Cell survival, DNA damage, and oncogenic transformation after a transient and reversible apoptotic response. *Mol Biol Cell*, *23*(12), 2240–2252.
Taubert, S., Gorrini, C., Frank, S. R., Parisi, T., Fuchs, M., Chan, H.-M., … Amati, B. (2004). E2F-dependent histone acetylation and recruitment of the Tip60 acetyltransferase complex to chromatin in late G1. *Molecular and Cellular Biology*, *24*(10), 4546–4556.
van Bergeijk, P., Heimiller, J., Uyetake, L., & Su, T. T. (2012). Genome-wide expression analysis identifies a modulator of ionizing radiation-induced p53-independent apoptosis in Drosophila melanogaster. *PloS One*, *7*(5), e36539.
Van Meter, M., Simon, M., Tombline, G., May, A., Morello, T. D., Hubbard, B. P., … Seluanov, A. (2016). JNK Phosphorylates SIRT6 to Stimulate DNA Double-Strand Break Repair in Response to Oxidative Stress by Recruiting PARP1 to DNA Breaks. *Cell Reports*, 2641–2650.
Wang, J., Qiao, M., He, Q., Shi, R., Jia Hui Loh, S., Stanton, L. W., & Wu, M. (2015). Pluripotency Activity of Nanog Requires Biochemical Stabilization by Variant Histone. *Stem Cells*, *33*, 2126–2134.
Wells, B. S., & Johnston, L. A. (2012). Maintenance of imaginal disc plasticity and regenerative potential in Drosophila by p53. *Developmental Biology*, *361*, 263–76.
Yamanaka, N., Rewitz, K. F., & O'Conner, M. B. (2013). Ecdysone Control of Developmental Transitions: Lessons from Drosophila Research. *Ann Rev Entomol*, *58*, 497–516.